SPAIS Scuola Permanente per l'Aggiornamento degli Insegnanti di Scienze Sperimentali

XVI Edizione
Strumenti per la Scienza
Cefalù (Pa)
25-30 luglio 2022

Immagina quel che vedi

Tecniche microscopiche di imaging per la caratterizzazione strutturale e morfologica di aggregati molecolari

venanzi@uniroma2.it

nast
Nanoscience
Nanotechnology
Innovative Instrumentation

Università di Roma
Tor Vergata

Outline

Microscopic imaging has been used as a powerful tool to elucidate structures of individual molecular assemblies with sub-nanometer to millimeter resolution.

- **Using electrons for imaging:**
  Transmission and Scanning Electron Microscopies

- **Using a tip for imaging:**
  Atomic Force Microscopy

- **Using photons for imaging:**
  Super Resolution Fluorescence Microscopy

Spatial resolution of imaging techniques and size of supramolecular assemblies

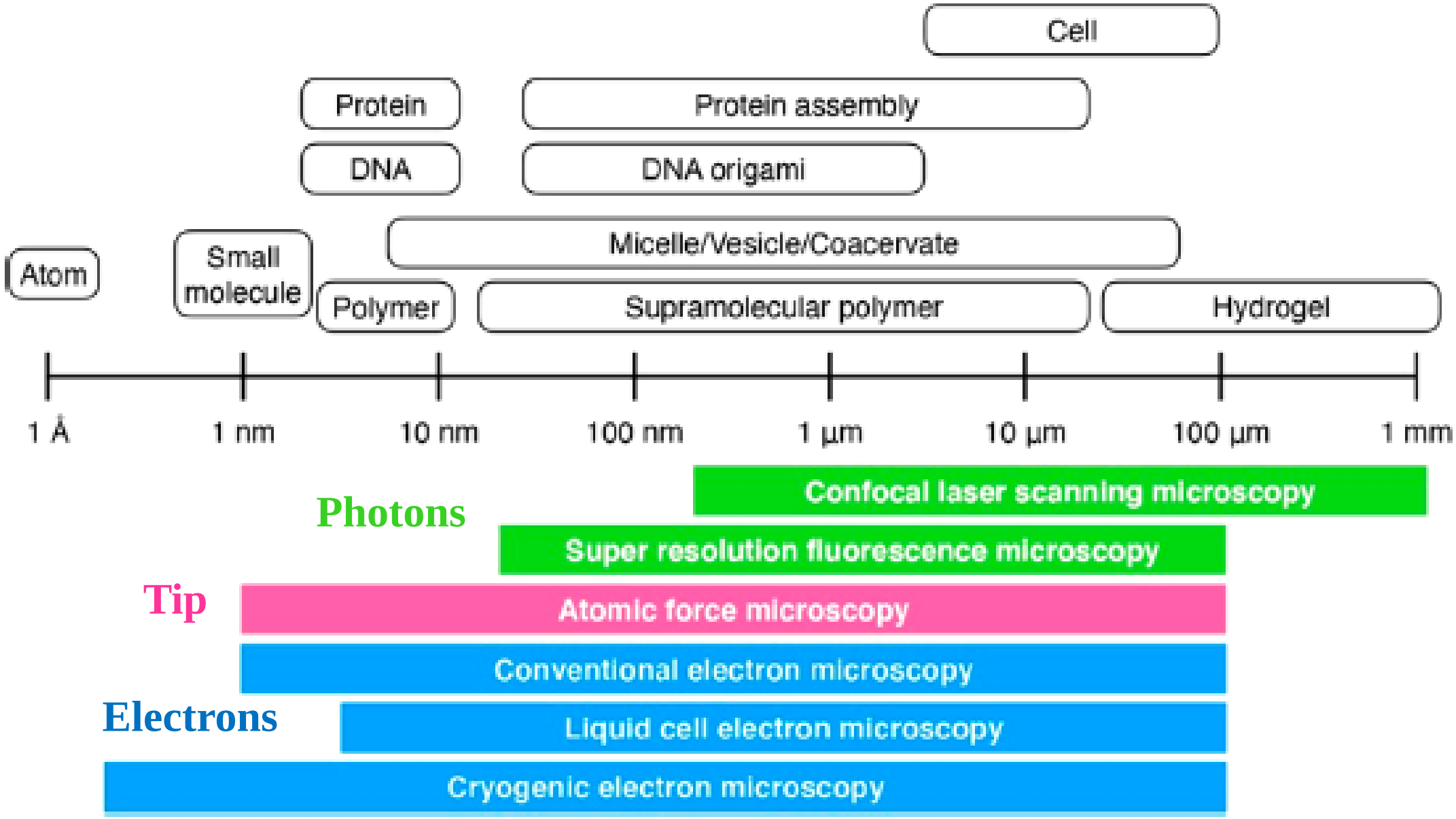

Comparison of high-resolution imaging techniques in molecular and cell biology

Technique/feature	Atomic force microscopy	Super-resolution microscopy (STED, PALM, STORM)	Transmission electron microscopy	Scanning electron microscopy
Resolution	≤1 nm–50 nm*	20–50 nm	0.2–10 nm	2–10 nm
Sample preparation and environment	Sample on support; physiological (buffer solution, temperature, CO_2)	Fluorescence labelling; physiological (buffer solution, temperature, CO_2)	Sample on grid; dehydrated (negative stain); vitrified (cryo-electron microscopy)	Freeze/critical point drying and metal shadowing
Artefacts	Tip, force, scanning	Bleaching, toxicity	Dehydration, ice crystal formation, beam damage	Dehydration, metal shadowing, beam damage
Advantages	Imaging under native conditions; no staining, labelling or fixation necessary; high signal-to-noise ratio; assessment of multiple physical, chemical and biological parameters	Access to three-dimensional cellular structures; high spatiotemporal resolution; monitoring biomolecular processes in life cells	Solves atomic structures of proteins; conformational snapshots of proteins and complexes; molecular-resolution structures within the cell	Imaging surfaces of tissues, cells and interfaces at nanometre-scale resolution
Limitations	Restricted to surfaces	Imaging restricted to fluorescence labels	No life processes	No life processes

CHEMICAL REVIEWS

pubs.acs.org/CR Review

Microscopic Imaging Techniques for Molecular Assemblies: Electron, Atomic Force, and Confocal Microscopies

Ryou Kubota,[§] Wataru Tanaka,[§] and Itaru Hamachi*

Cite This: *Chem. Rev.* 2021, 121, 14281−14347 Read Online

1. ***Molecular self-assembly produced by noncovalent interactions provide a variety of unique 1D/2D/3D structures such as sphere, rod, fiber, tape, grid, sheet, helix, and others with a variety of sizes.***

2. ***Due to the non-covalent nature of the molecular interactions, these structures are dynamic and transform each other. This property may be tightly associated with their functions in many cases.***

3. ***These self-assembled materials are promising soft materials in the next generation where sustainability will be highlighted.***

1. Using electrons for imaging

Electron Microscopies			
	TEM/SEM/STEM	**Cryo EM**	**Liquid cell EM**
Spatial resolution	1-10 nm	0.2-10 nm	3-30 nm
Sample preparation	Dried sample (stained with metal)	Vitrified, sample on grid	solution
Advantage	High resolution	Near-atomic structure	*In situ* imaging
Limitation	No *in situ* imaging	No *in situ*, thin film needed	Lower resolution

TEM: Transmission Electron Microscopy
SEM: Scanning Electron Microscopy
STEM: Scanning Transmission Electron Microscopy

Electrons

De Broglie equation:

$$\lambda = \frac{h}{mv}$$

m=9.1·10^{-31} kg; q=1.6·10^{-19} C

Applying a 50kV potential:

$$E = \frac{1}{2}mv^2 = qV = 1.6\cdot10^{-19}\cdot50000 = 8\cdot10^{-15}\,J$$

$$v = \sqrt{\frac{2E}{m}} = 1.3\cdot10^{8}\,m\cdot s^{-1}$$

$$p = mv = 9.1\cdot10^{-31}\cdot1.3\cdot10^{8} = 1.2\cdot10^{-22}\,m\cdot kg\cdot s^{-1}$$

$$\lambda = \frac{h}{p} = \frac{6.63\cdot10^{-34}}{1.2\cdot10^{-22}} = 5.52\cdot10^{-12}\,m = 5.52\,pm$$

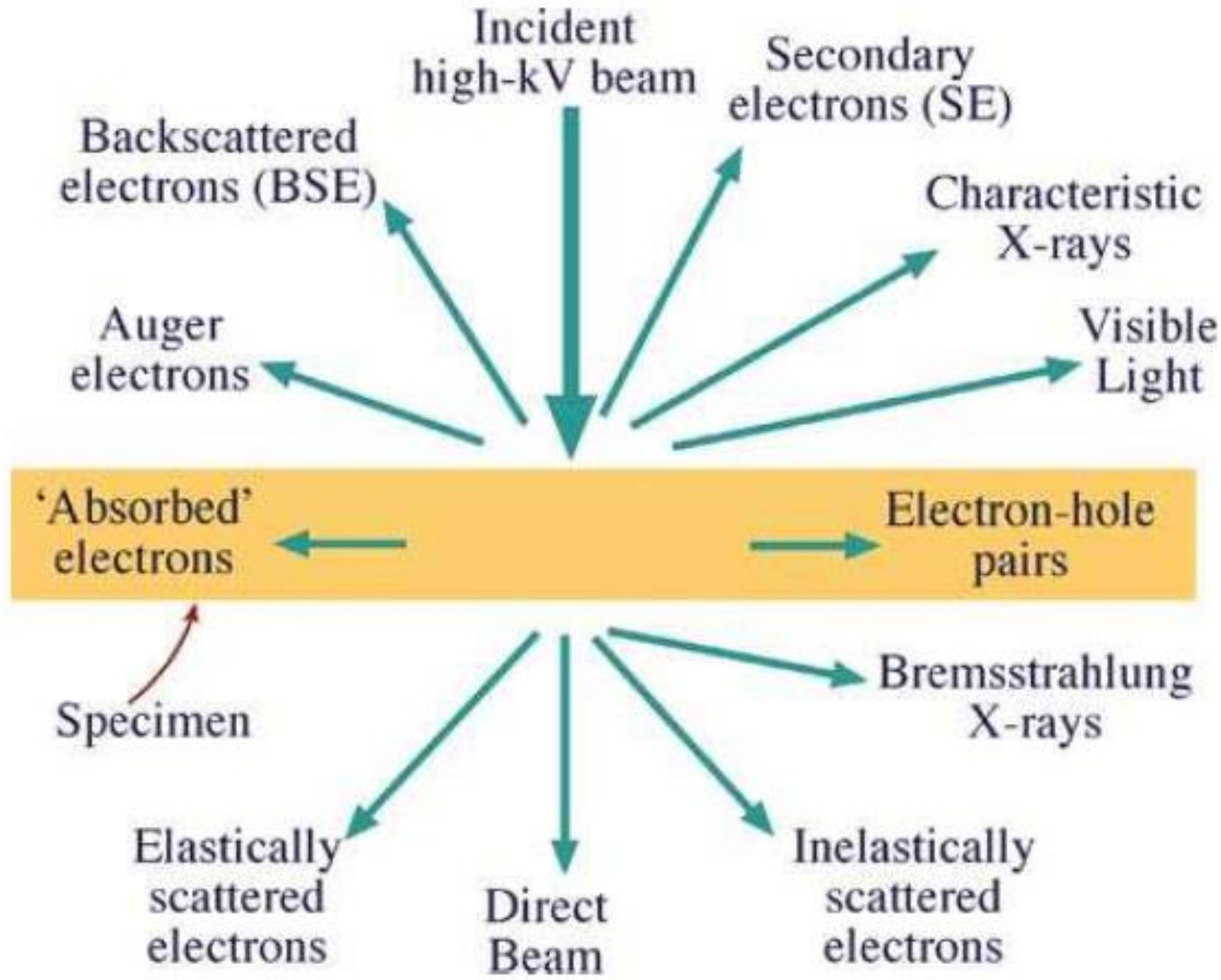
Incident
high-kV beam
Secondary
electrons (SE)
Backscattered
electrons (BSE)
Characteristic
X-rays
Auger
electrons
Visible
Light
'Absorbed'
electrons
Electron-hole
pairs
Specimen
Bremsstrahlung
X-rays
Elastically
scattered
electrons
Direct
Beam
Inelastically
scattered
electrons

TEM

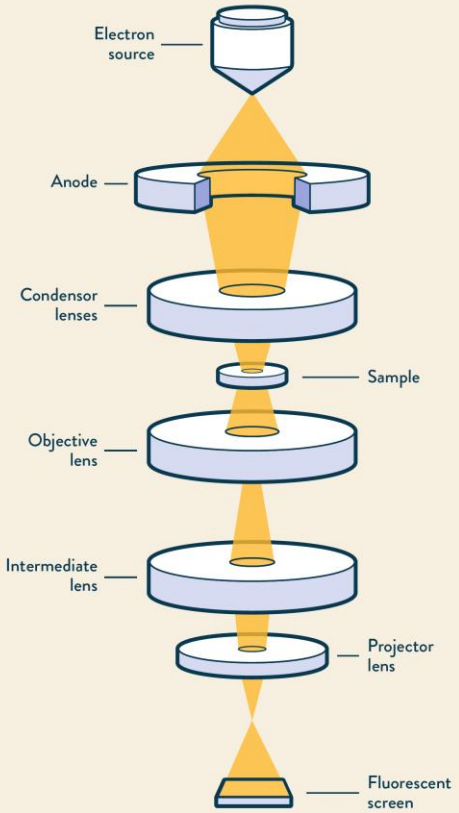

STEM

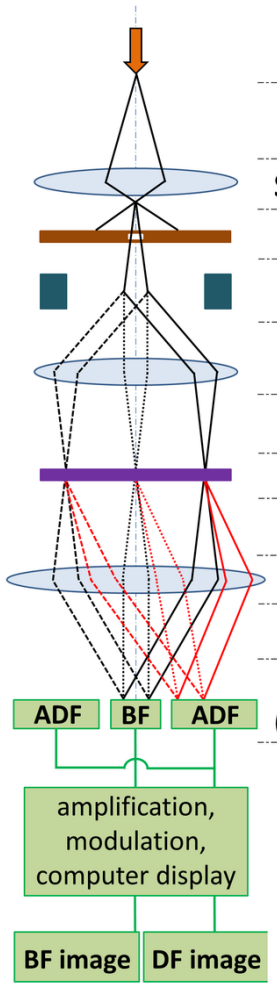

Electron Gun

System of condenser lenses

Condenser aperture

Deflection scan coils

Upper-objective polepiece

Specimen

Lower-objective polepiece

STEM detector
(back focal plane of objective lens)

spot size
0.05 - 0.2 nm

SEM

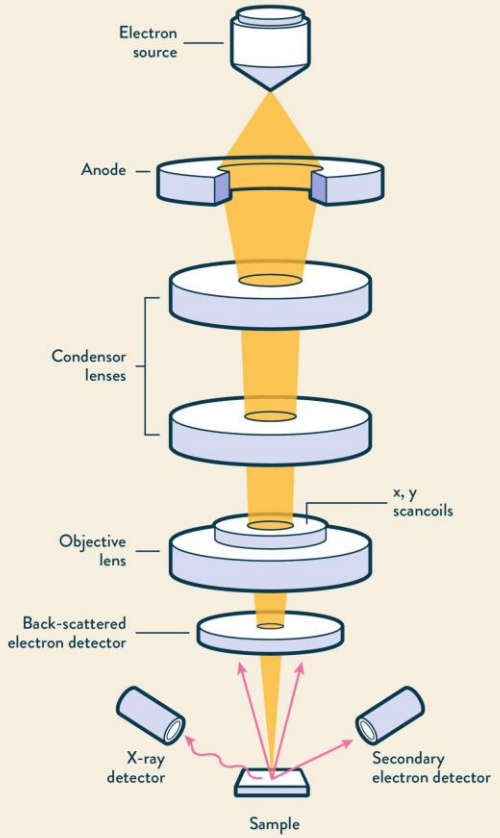

TEM vs cryo-TEM

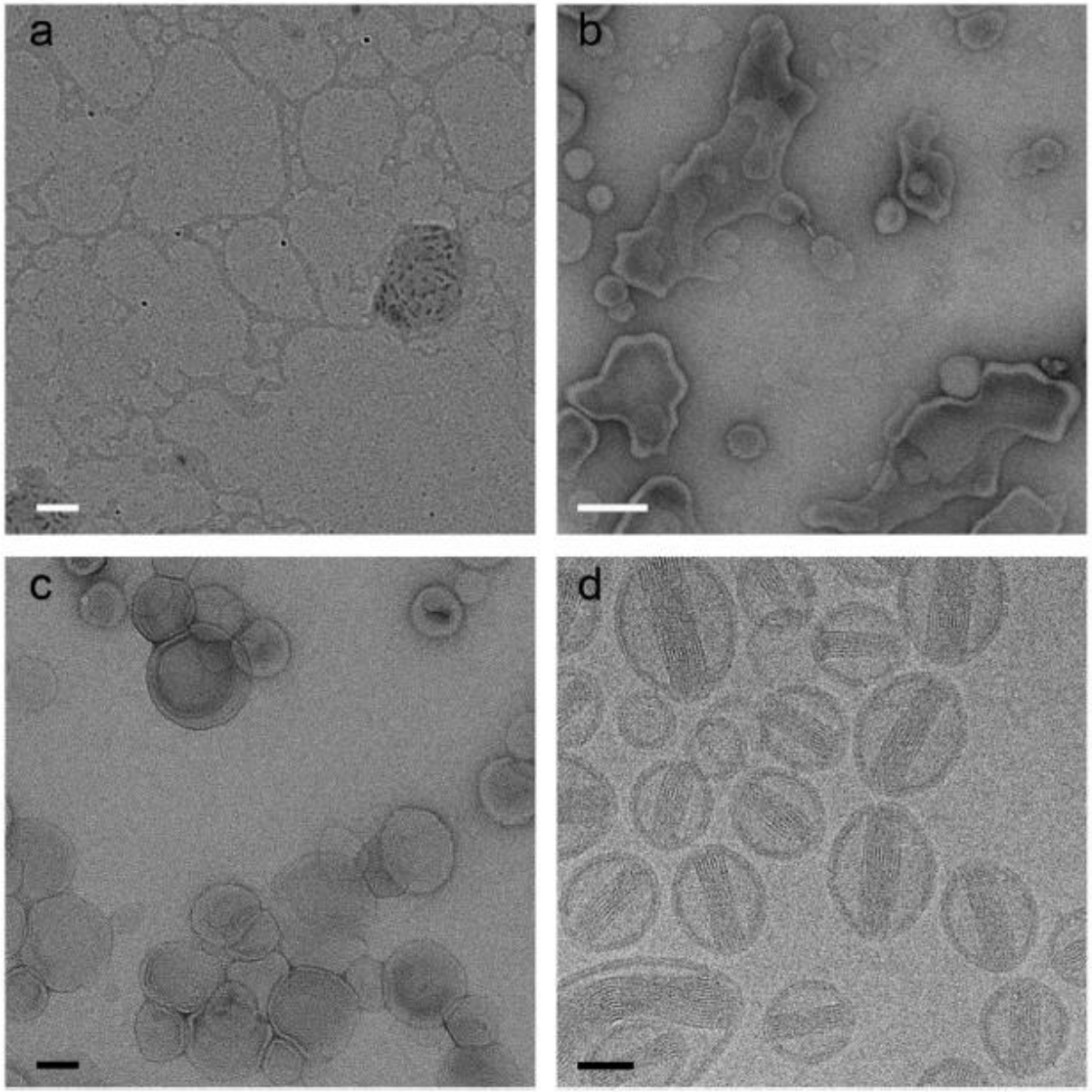

Doxorubicine in liposome

TEM:

a) dried without staining
b) dried before staining
c) negatively stained with 2% Uac

d) Cryo-TEM

white scale bars: 200nm
black bars: 50 nm

2017 Noble Prize in Chemistry
J. Dubochet, J. Franck, R. Henderson
"for developing cryo-electron microscopy for the high-resolution structure determination of biomolecules in solution."

Cryo-TEM: Self-assembly of amphiphilic amino acid derivatives (Fmoc-Ala/His and Z-FF)

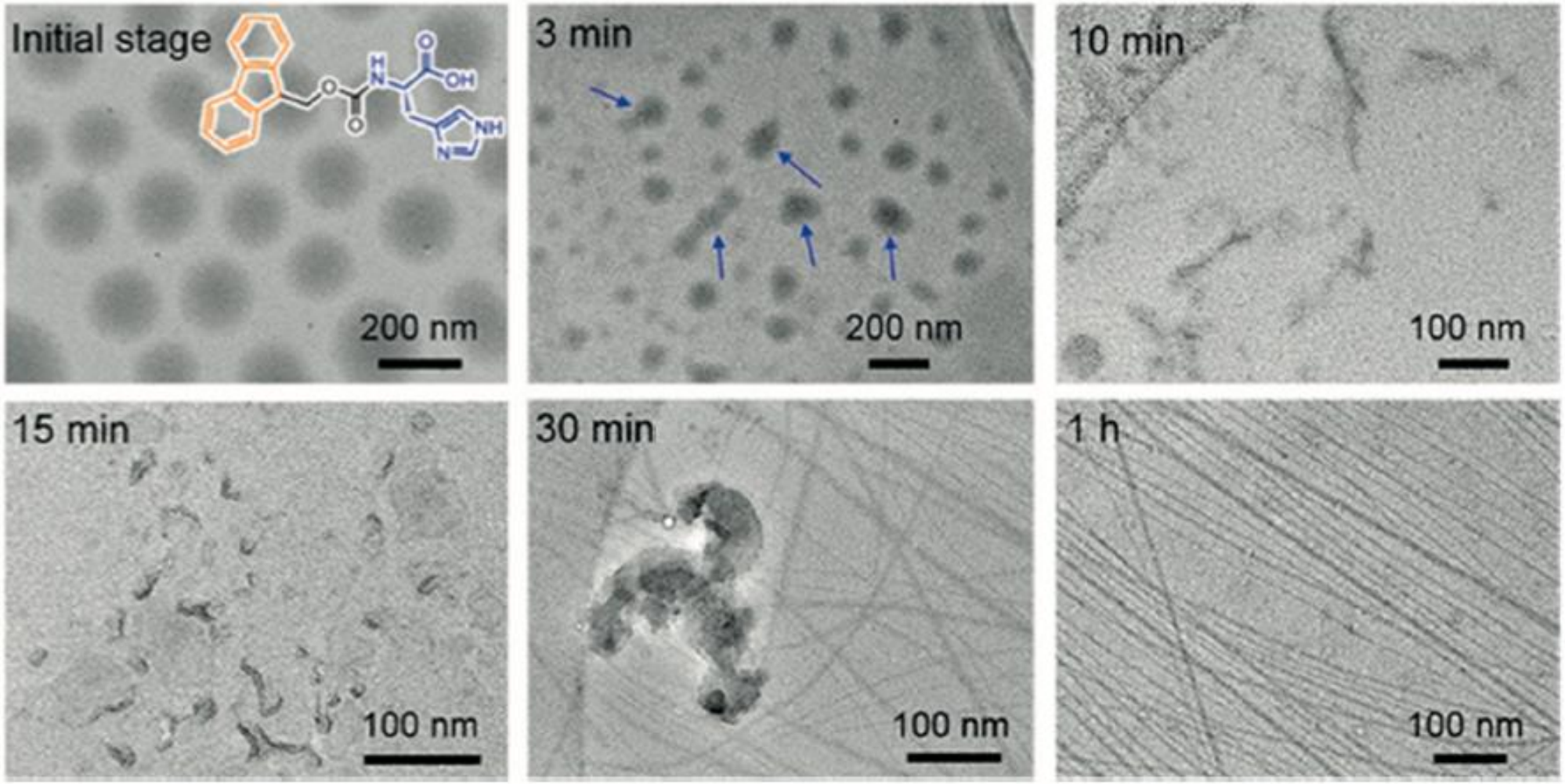

Kinetic liquid−liquid phase separation was observed at the initial stage followed by nucleation and growth of the thermodynamically stable nanofibers from the solute rich droplets after lag-time.

Yuan C. et al. Angew. Chem. Int. Ed. 2019, 58, 18116-18123

Single particle cryo-TEM analysis of a microtubular 3D structure at a resolution of 7.9 Å

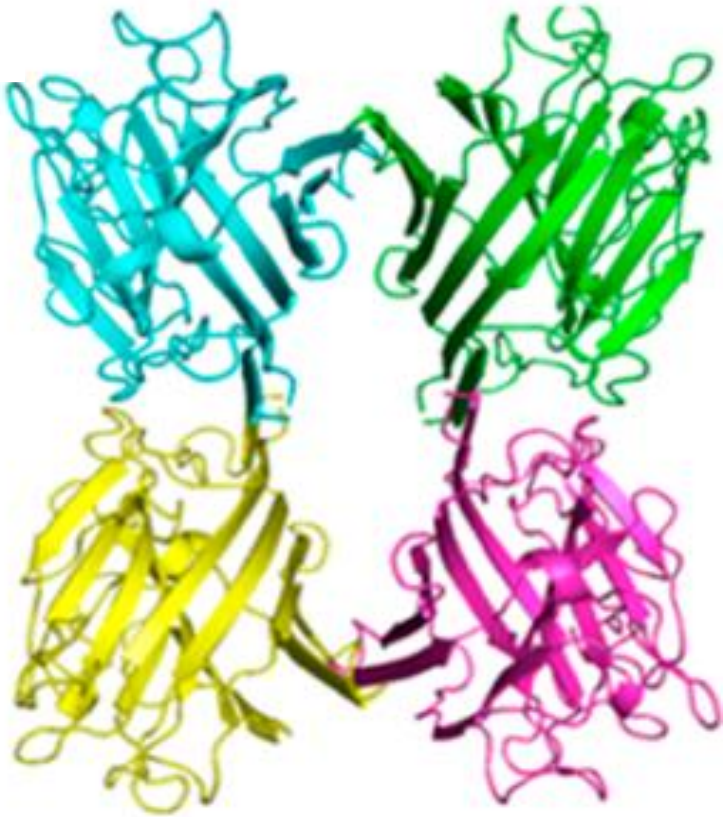

Tetrameric soybean agglutinin

Scale bar: 25 nm

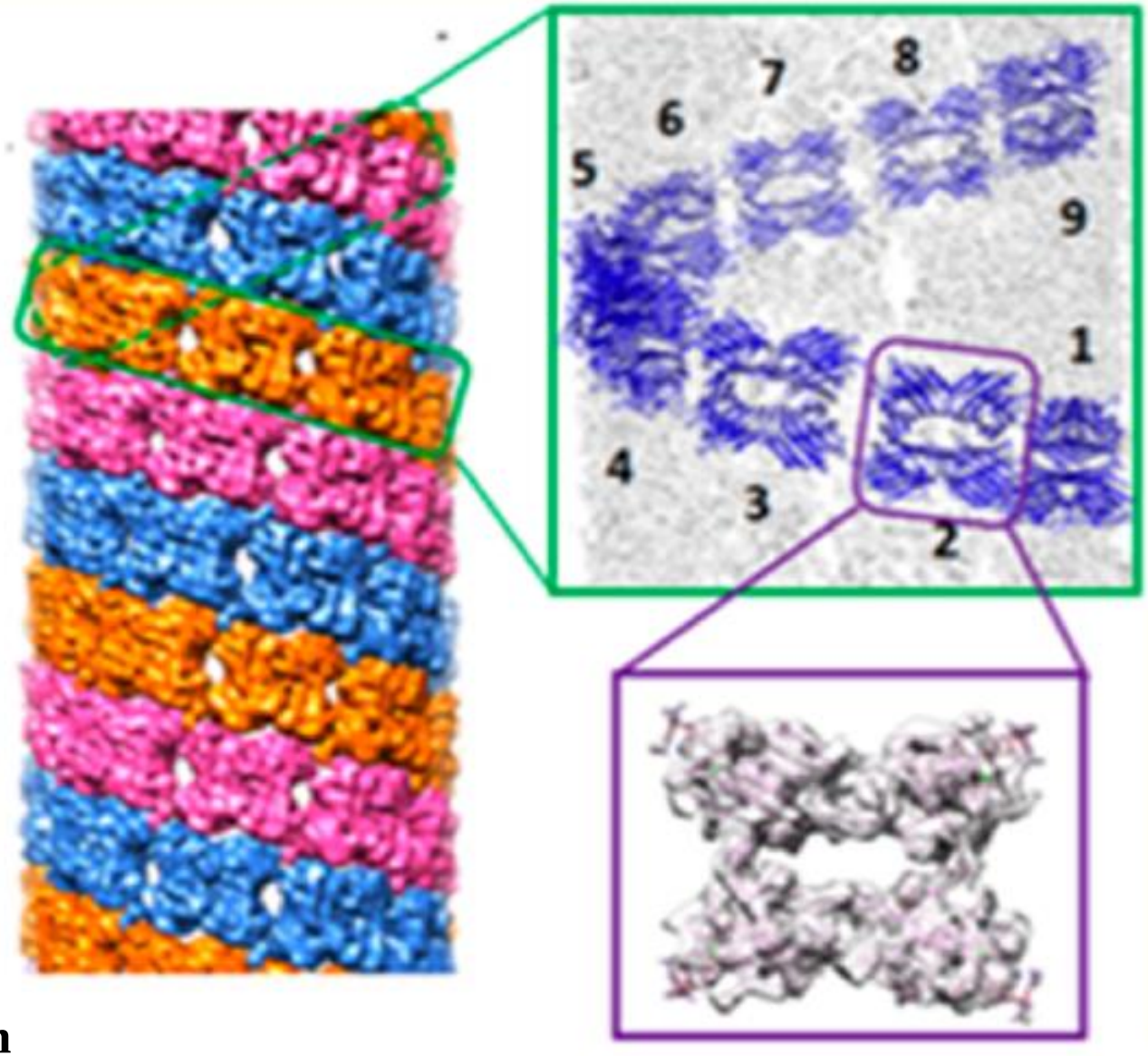

Yang, G et al. J. Am. Chem. Soc. 2016, 138, 1932−1937

Single particle cryo-TEM structure of DLIIKGISVHI fibril

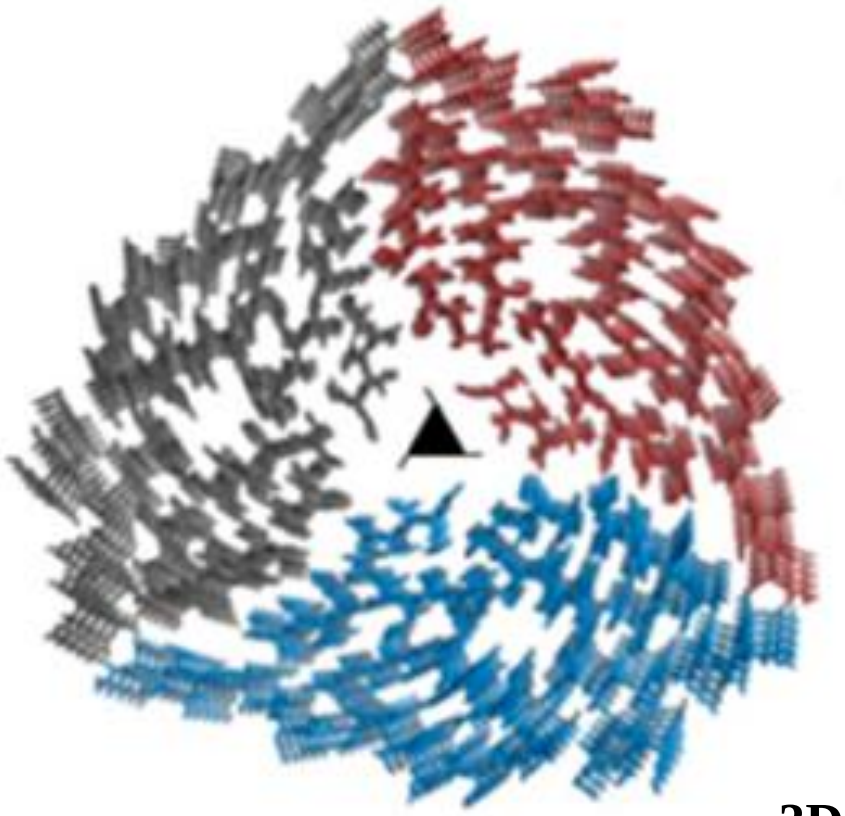

Molecular packing structure of DLIIKGISVHI, derived from an amyloid protein

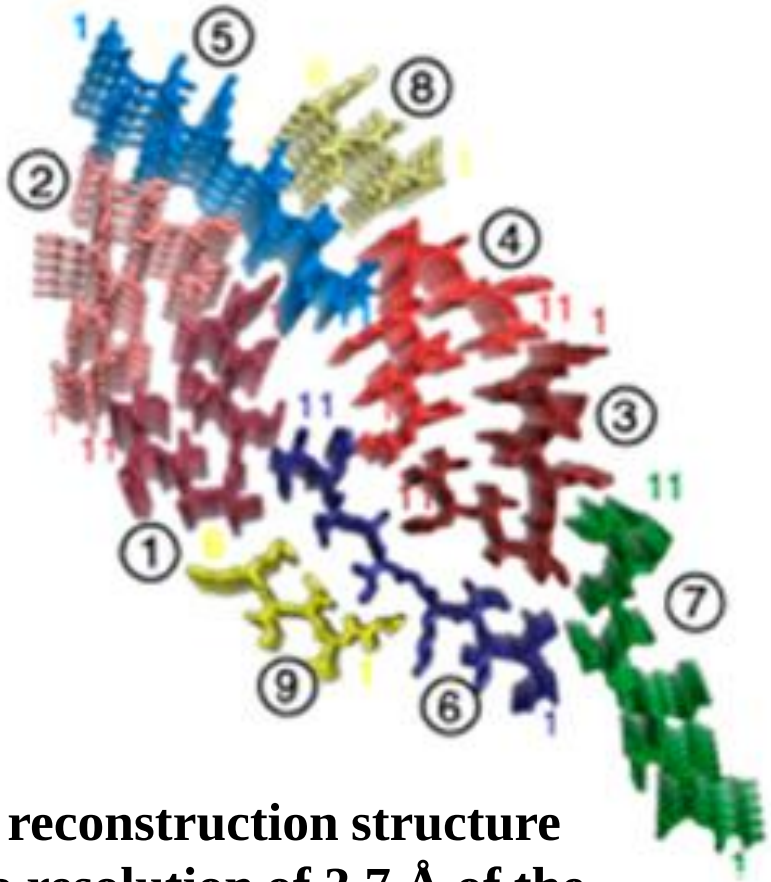

3D reconstruction structure at a resolution of 3.7 Å of the 9 undecapeptides in the amyloid fibril

Guenther, E. L et al. Nat. Struct. Mol. Biol. 2018, 25, 311−319

Liquid Cell Electron Microscopy (LC-EM)

In LC-EM liquid samples are placed in a small space between two thin, tough, and high transmittance membranes, allowing for *in situ* time-lapse imaging of wet samples at nanometer resolution with sub-second time scale.

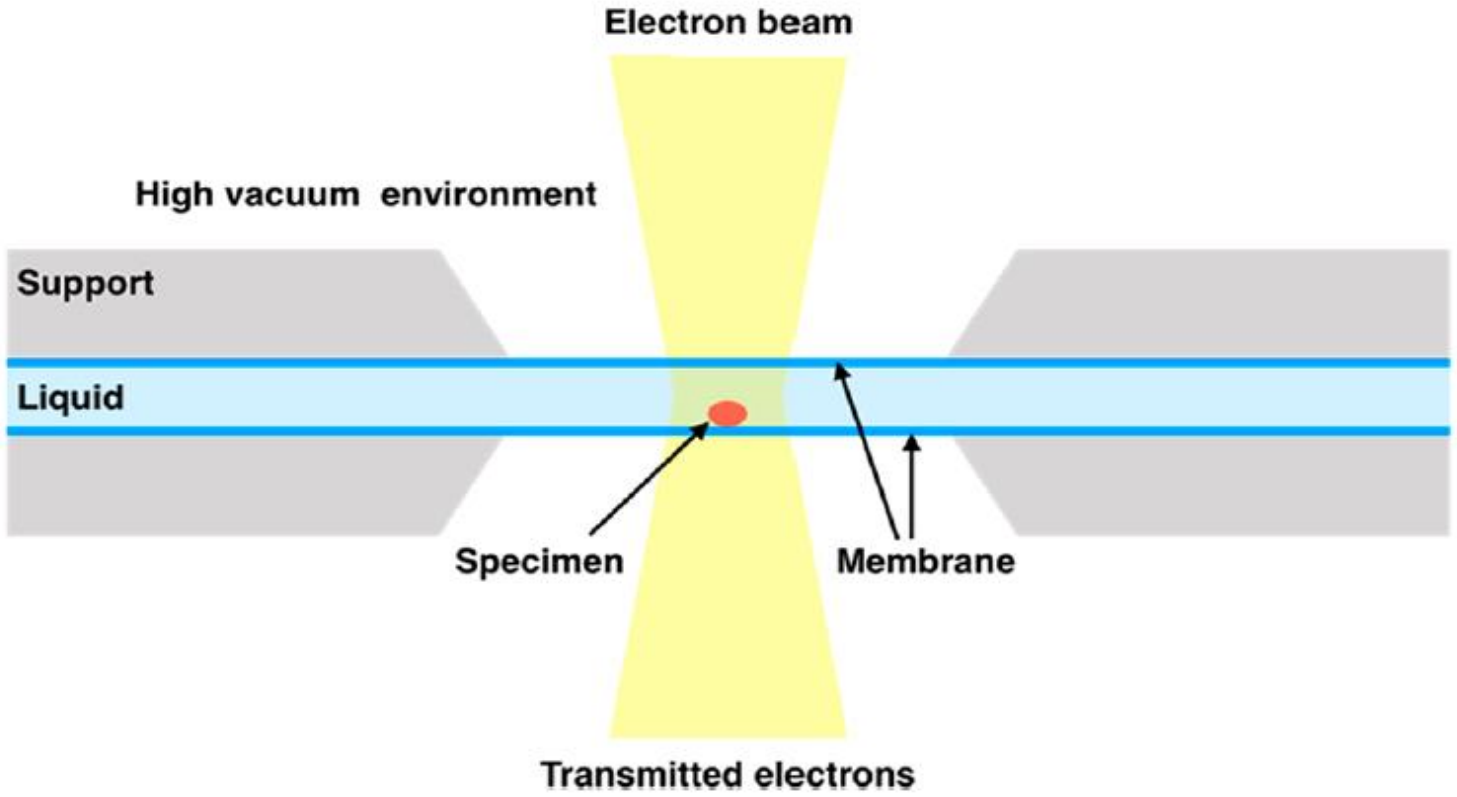

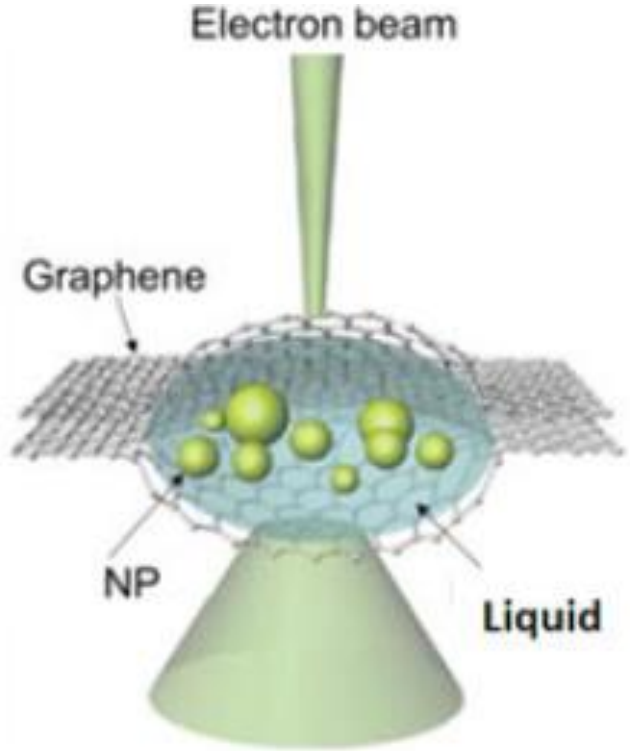

de Jonge, N.; Ross, F. M. Electron Microscopy of Specimens in Liquid. Nat. Nanotechnol. 2011, 6, 695−704.

LC-EM imaging of organic molecular assemblies. (A−G) Evolution of micelles in solution.

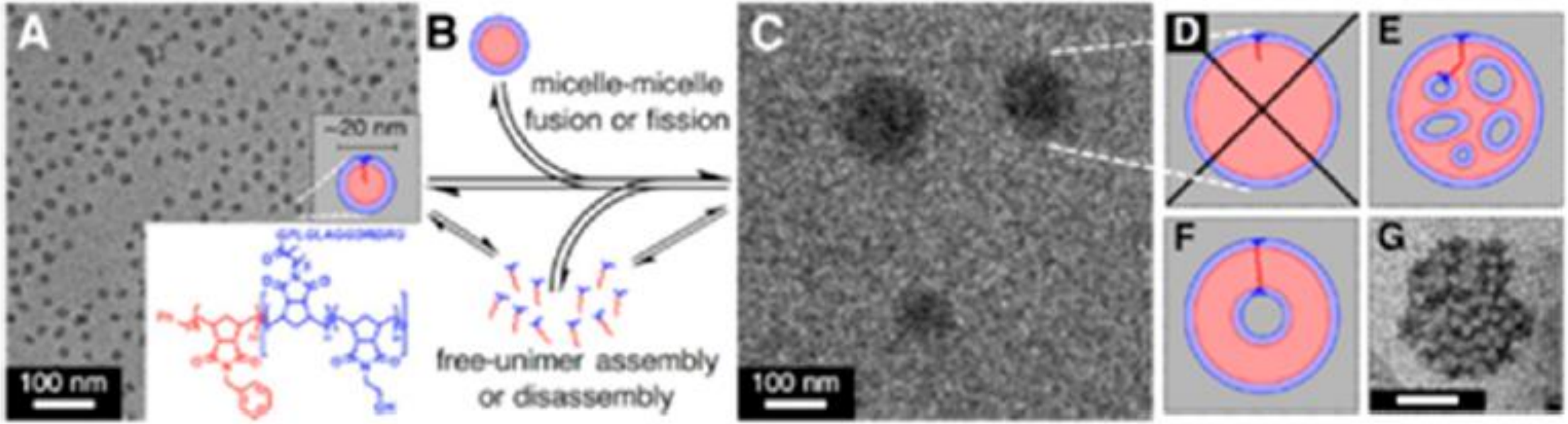

(A) Cryo-TEM image of the initial small micelles.
(B) Schematic illustration of the size evolution process.
(C) LC-TEM image of the large micelles.
(D−F) Potential internal structures supposed by LC-TEM image (D is not possible for the unimer).
(G) Cryo-TEM image of the large micelles.

(H−I) Micelle fusion in solution

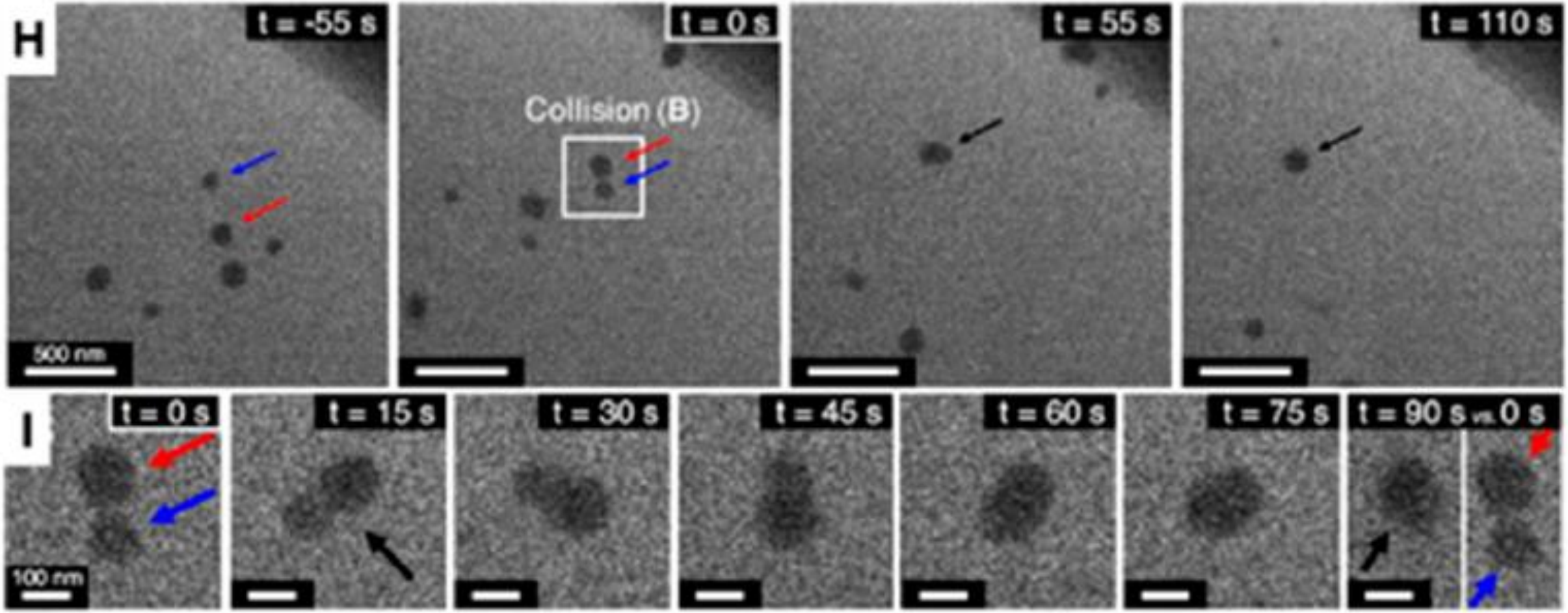

(H) LC-TEM time-lapse images of fusion process of two micelles.
(I) Enlarged images of white square in (H).

Parent, L. R. et al. J. Am. Chem. Soc. 2017, 139, 17140−17151

Coacervate mediated vesicle formation from PEO-b-PCL

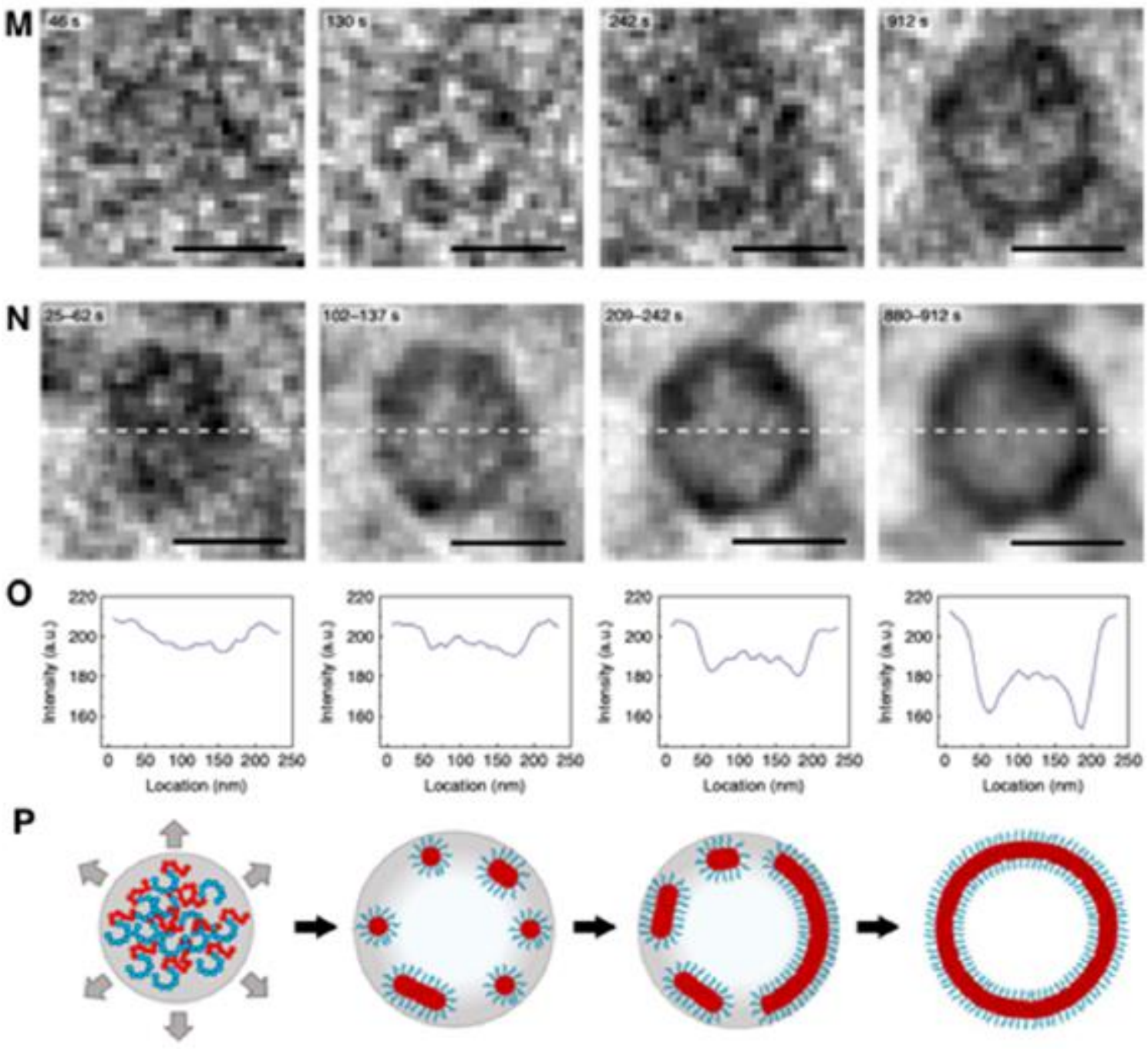

(M) LC-TEM images of the formation process of the vesicle. Scale bars: 100 nm.

(N) 30 frame average time series images of (M).

(O) Line plot intensity profiles along the white dashed line in (N).

(P) Schematic illustration of formation process of the vesicle.

Ianiro, A. et al. Nat. Chem. 2019, 11, 320−328

2. Using a tip for imaging: Atomic Force Microscopy (AFM)

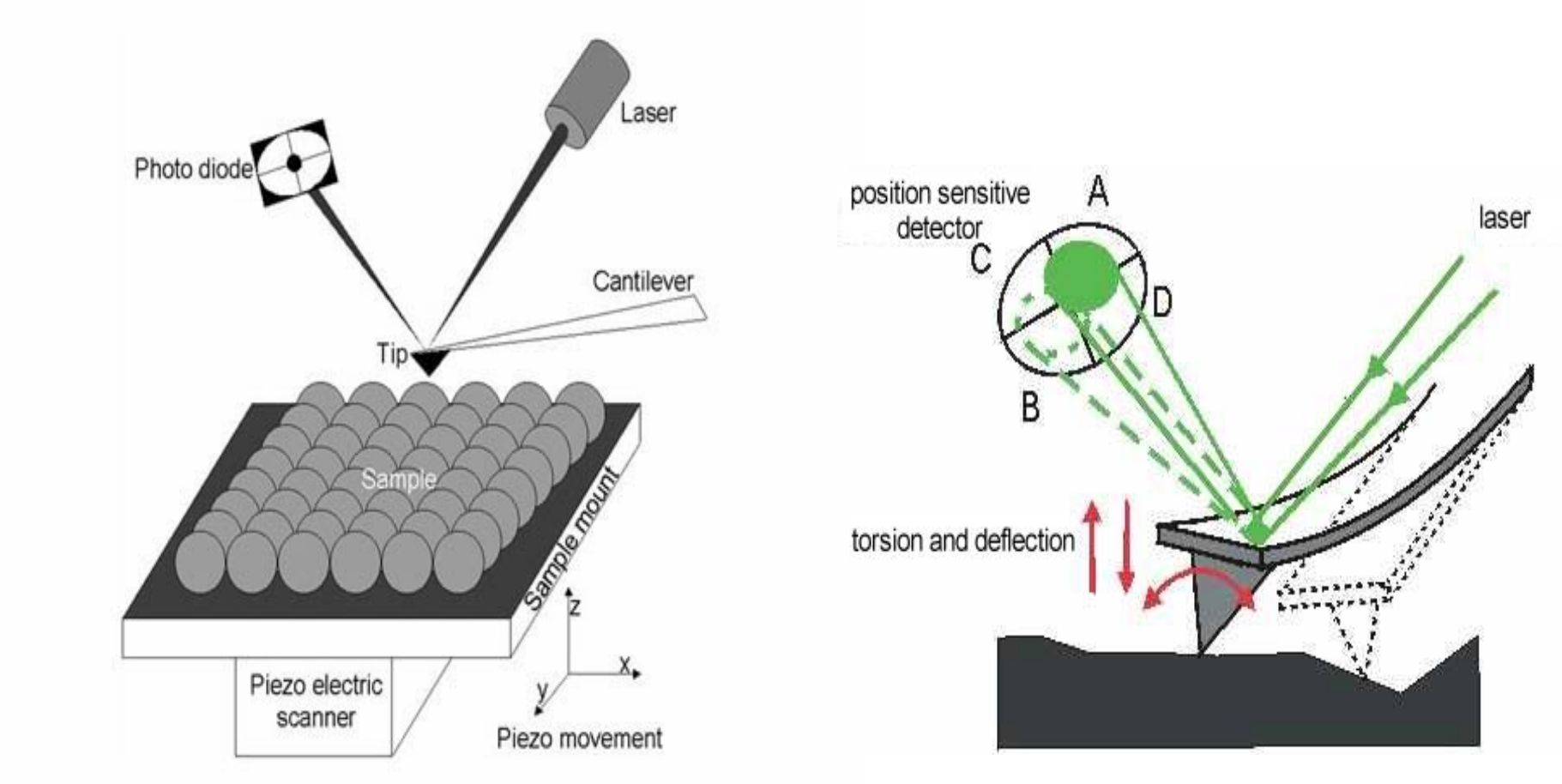

G. Binning, C.F. Quate and C. Berger
Atomic Force Microscopy, Phys. Rev. Lett. 56, 930-933 (1986)

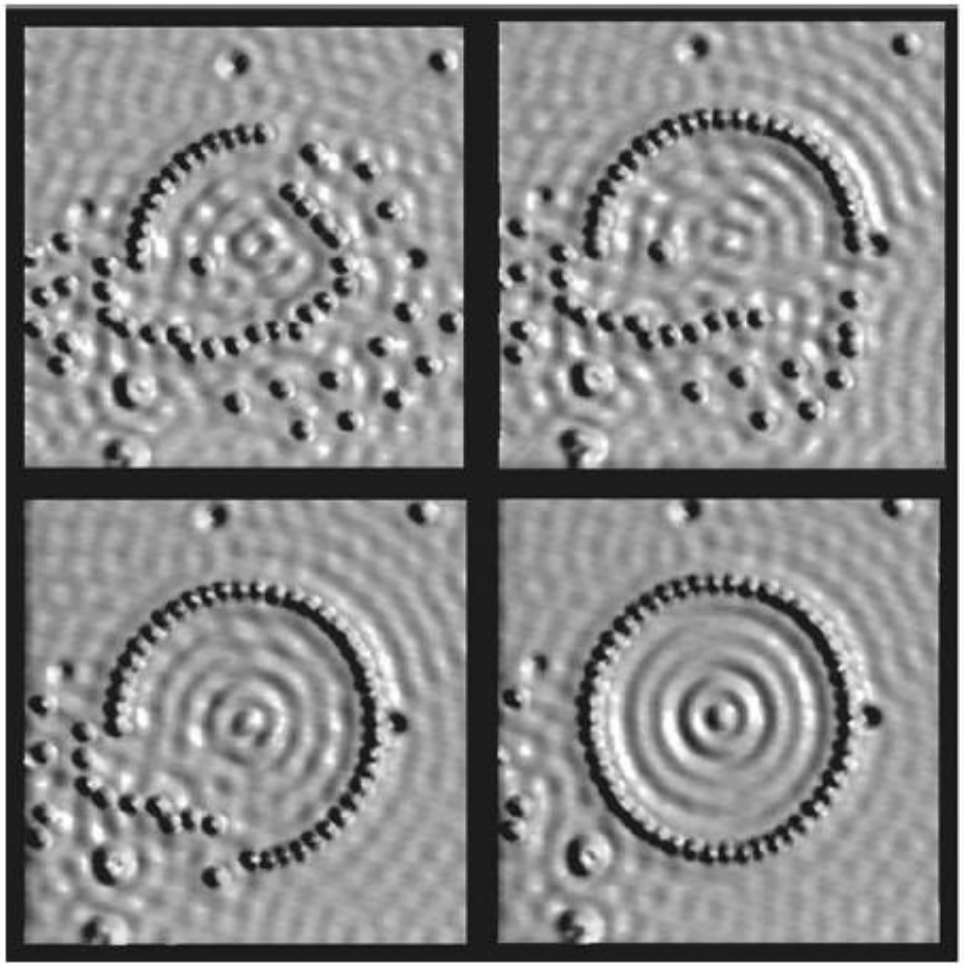

IBM's Quantum Corral. A ring of 48 iron atoms was arranged one at a time (four steps are shown) on a copper surface using the tip of a low-temperature STM. The STM was then used to capture an image of the ring, which measures about 14.3 nm across. The iron atoms confine some of the copper's surface electrons, and this barrier forces the electrons into quantum states, visible as concentric standing waves inside the corral.
Science Vol. 262, No. 5131, October 8, 1993.

Force Distance Atomic Force Microscopy

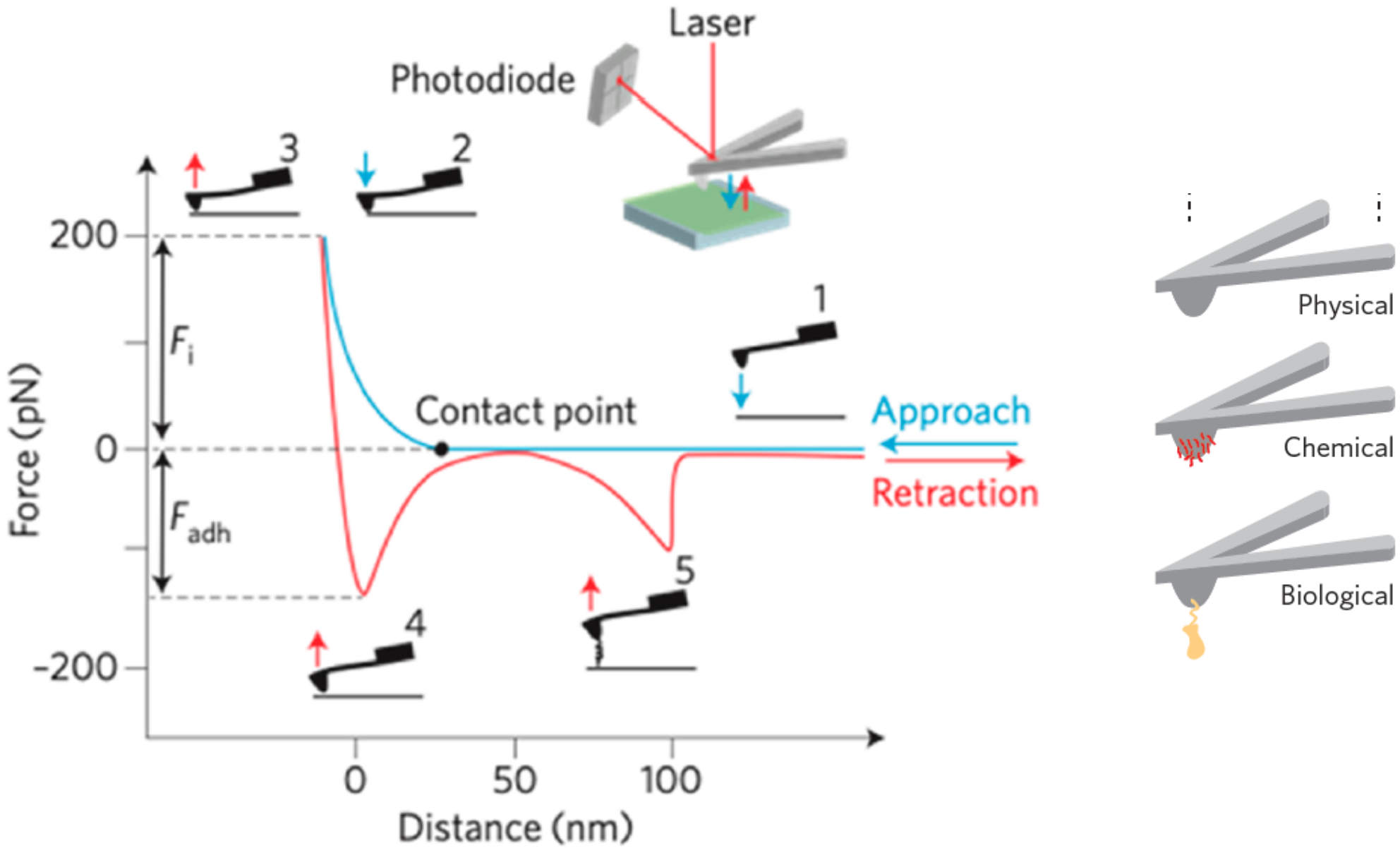

Phe-Phe nanotubes

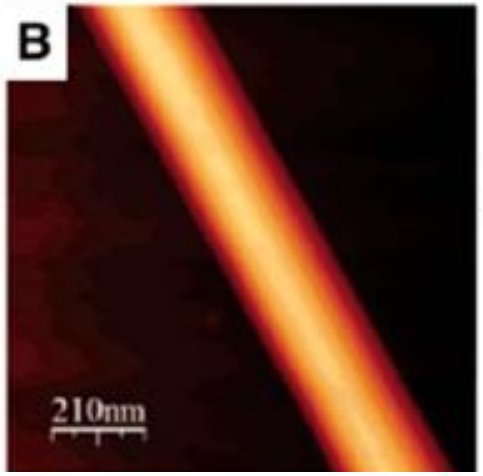

E= 19 GPa

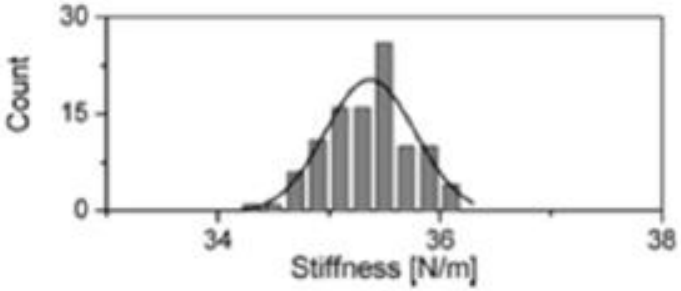

$$\text{E (Young modulus)} = \frac{\sigma\ (stress = force\ per\ unit\ area)}{\varepsilon\ (axial\ strain)}$$

Pro-Phe-Phe

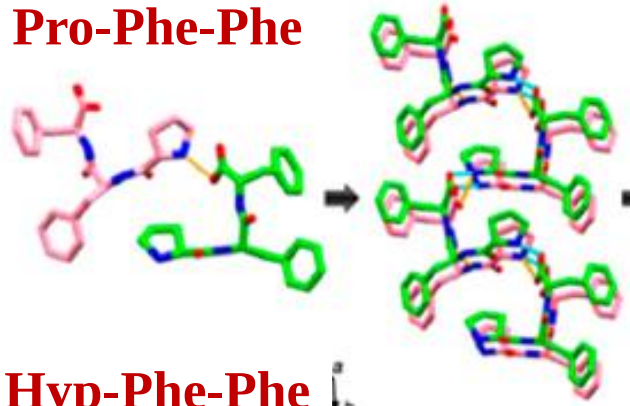

E= 44 GPa

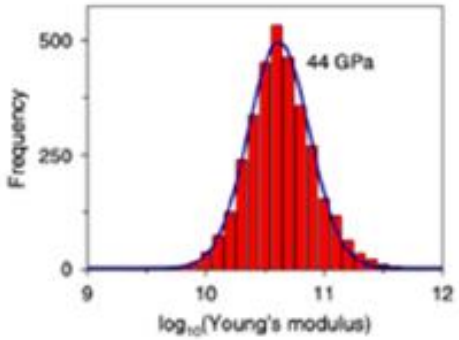

Hyp-Phe-Phe

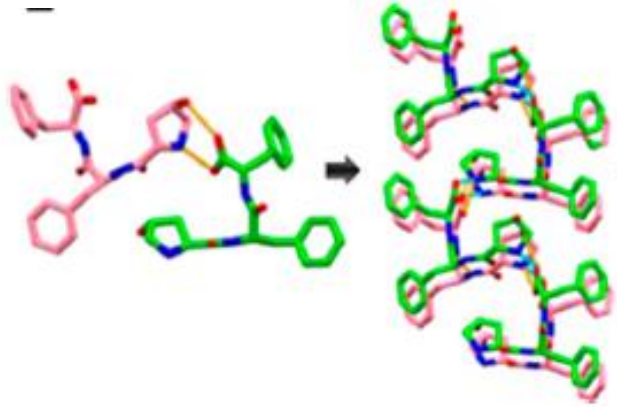

E= 109 GPa

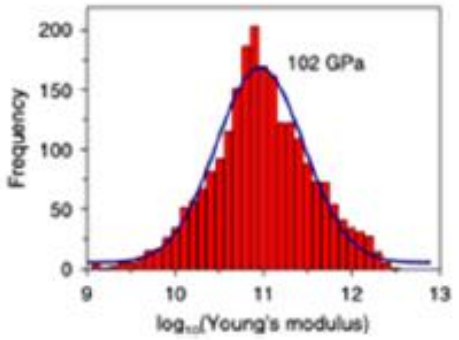

Comparison of Young's moduli of materials

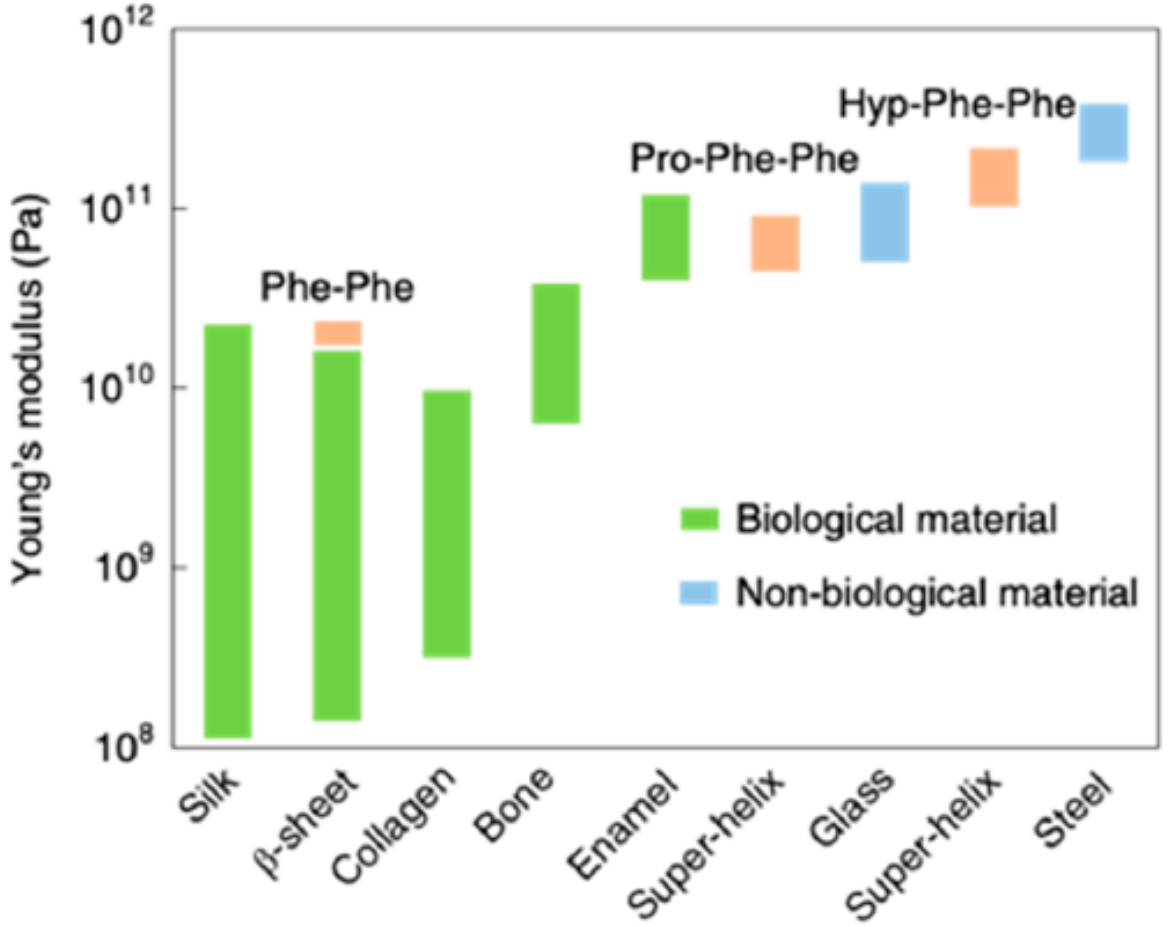

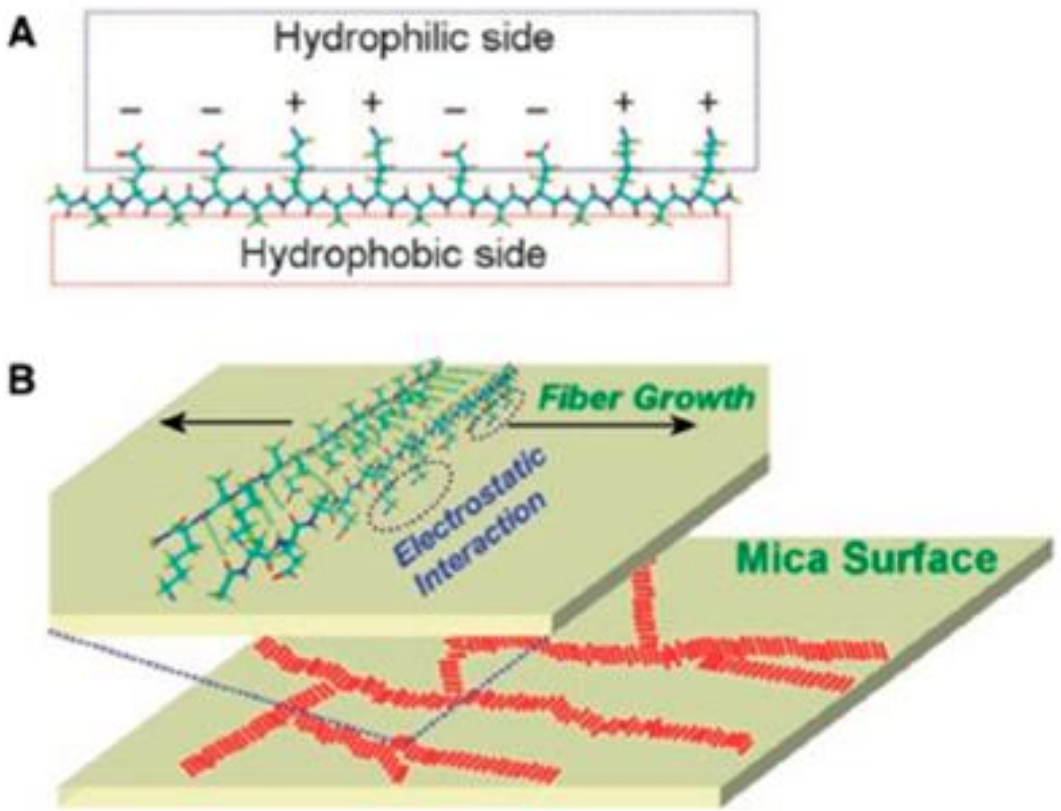

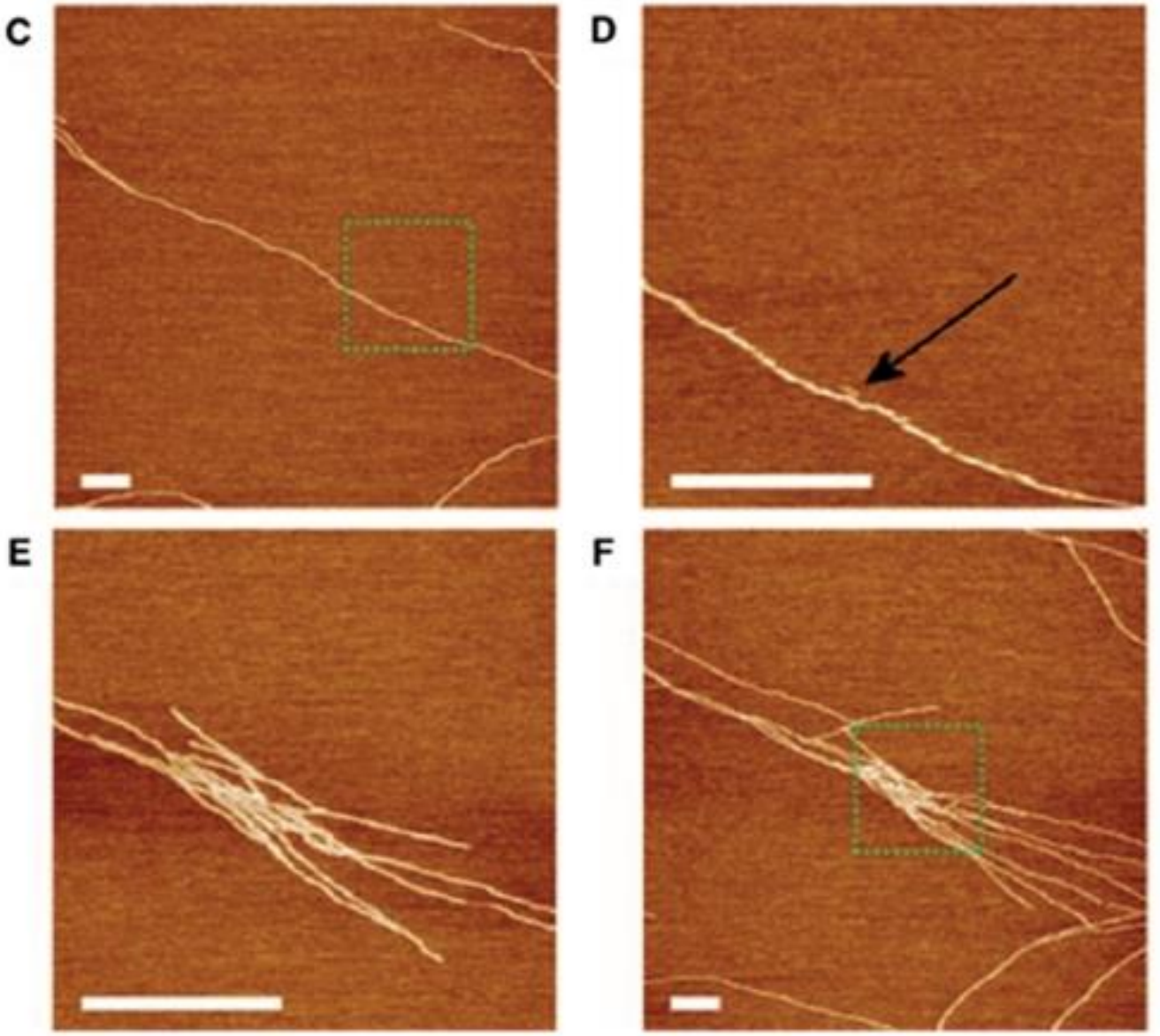

(A) Molecular structure of EAK16-II.
(B) Schematic illustration of interaction between EAK16-II fibers and a mica surface.
(C) AFM image of EAK16-II fibers on mica.
(D) Enlarged image of a green square in (C).
(E) AFM image after three times scan at the same location as (D) showing many growing fibers.
(F) Lower magnification AFM image after the manipulation. Scale bars: 200 nm.

High Speed AFM

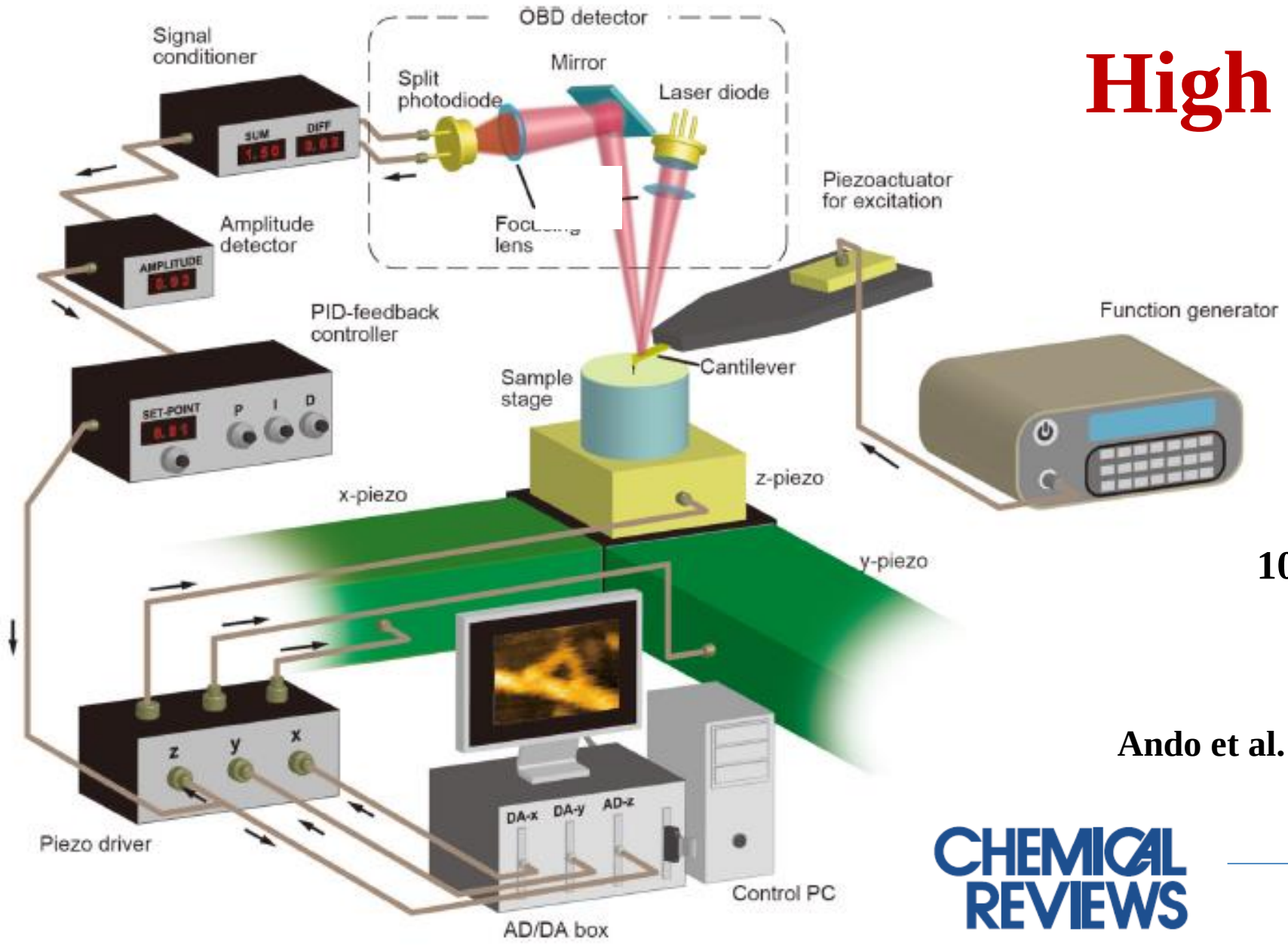

Schematic illustration of HS-AFM

10-20 frames per second

Ando et al. Chem. Rev. 2014, 114, 3120−3188

CHEMICAL REVIEWS
ACS Editors' Choice
Review
pubs.acs.org/CR
Terms of Use

Filming Biomolecular Processes by High-Speed Atomic Force Microscopy

Toshio Ando,*[†,‡,§] Takayuki Uchihashi,[†,‡,§] and Simon Scheuring[∥]

High Speed-AFM images of dynamic assembly/disassembly of annexin-V 2D crystal

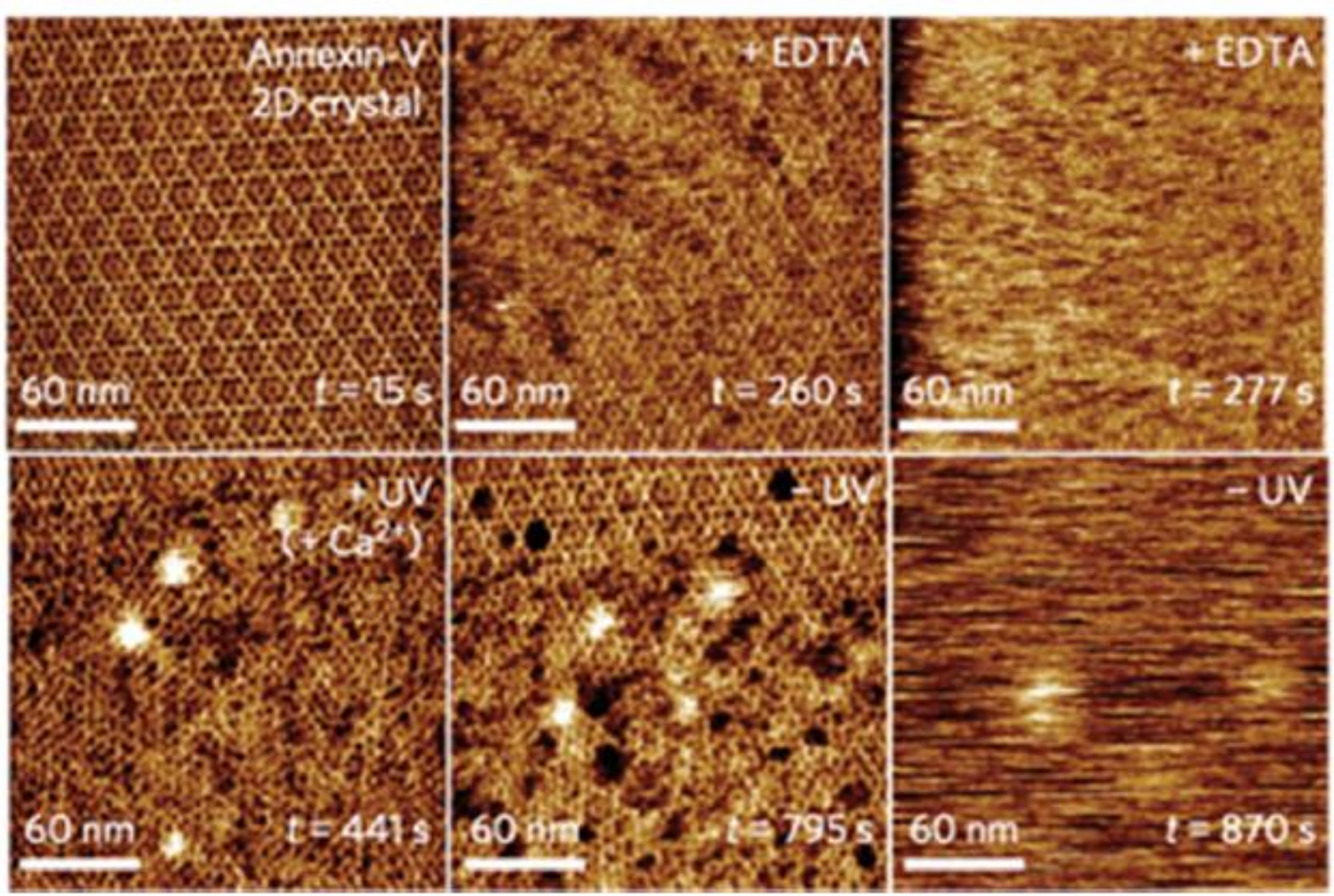

Disassembly by EDTA addition (Ca^{2+} sequestration)

Partial reconstruction by photoassisted release of Ca^{2+}.

Miyagi, A et al. Nat. Nanotechnol. 2016, 11, 783−790

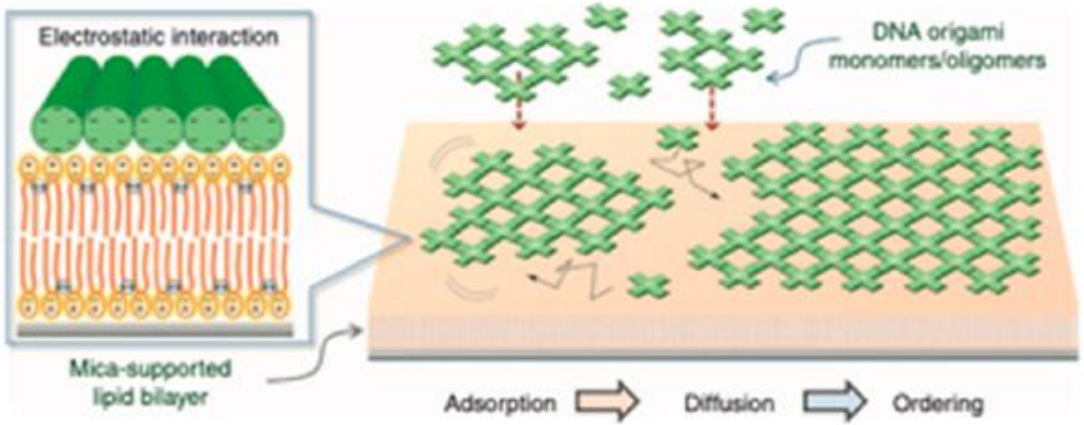

Schematic illustration of DNA origami assembly on lipid-coating mica.

Time-lapse HS-AFM images of large DNA origami lattices formation. Scale bars: 200 nm.

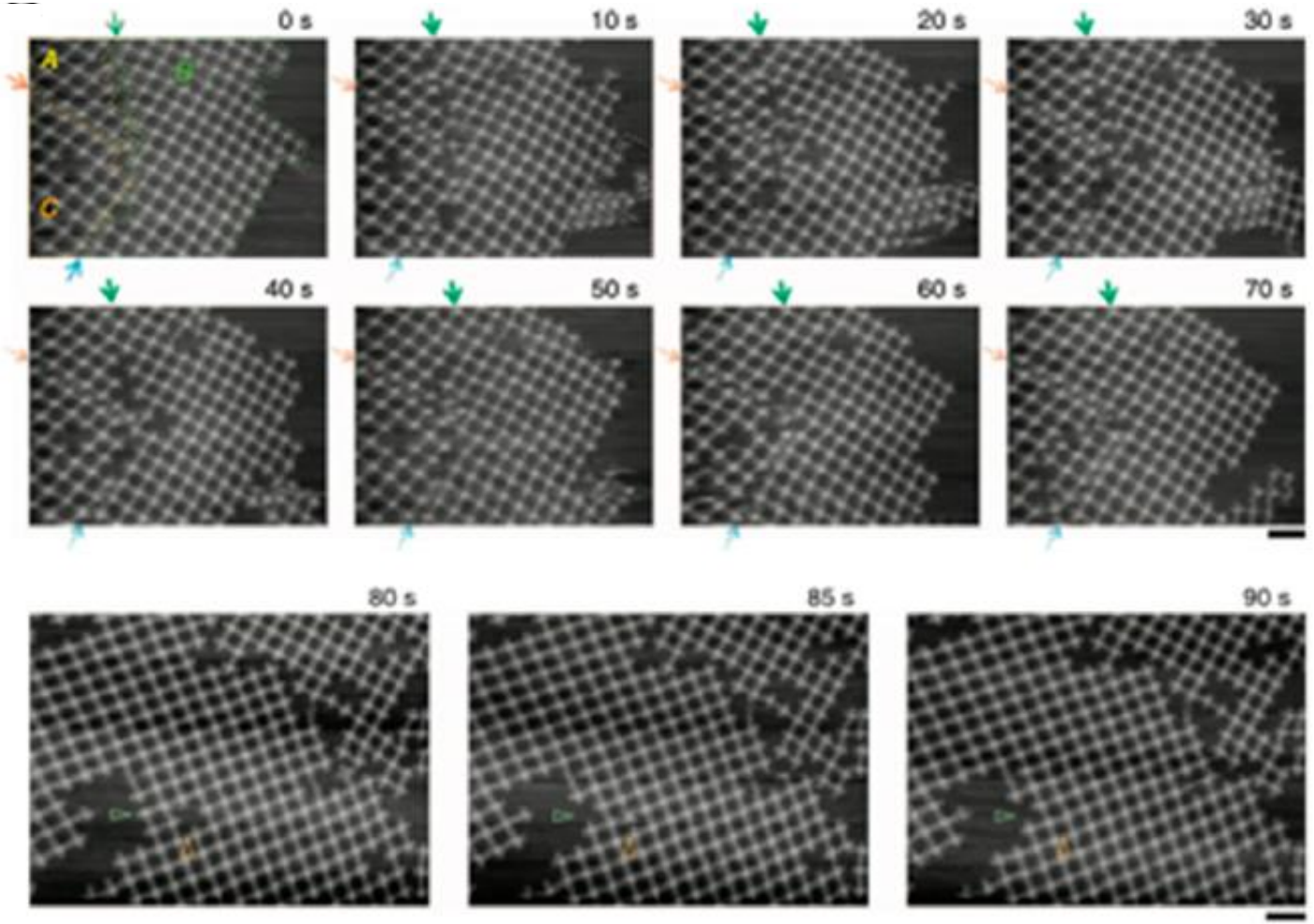

Myosin V (M5-HMM) movement on actin filament captured by HS-AFM

(a,b) Successive AFM images showing processive movement of M5-HMM in 1 μM ATP.

(c) Clips of successive images showing long processive run of M5-HMM in 1 μM ATP (14 steps are recorded).

(d) Schematic explaining structural features of two-headed bound M5-HMM observed in the presence of nucleotides.

(e) Successive AFM images showing stepping process in 1 μM ATP. The swinging lever is highlighted with a thin white line.

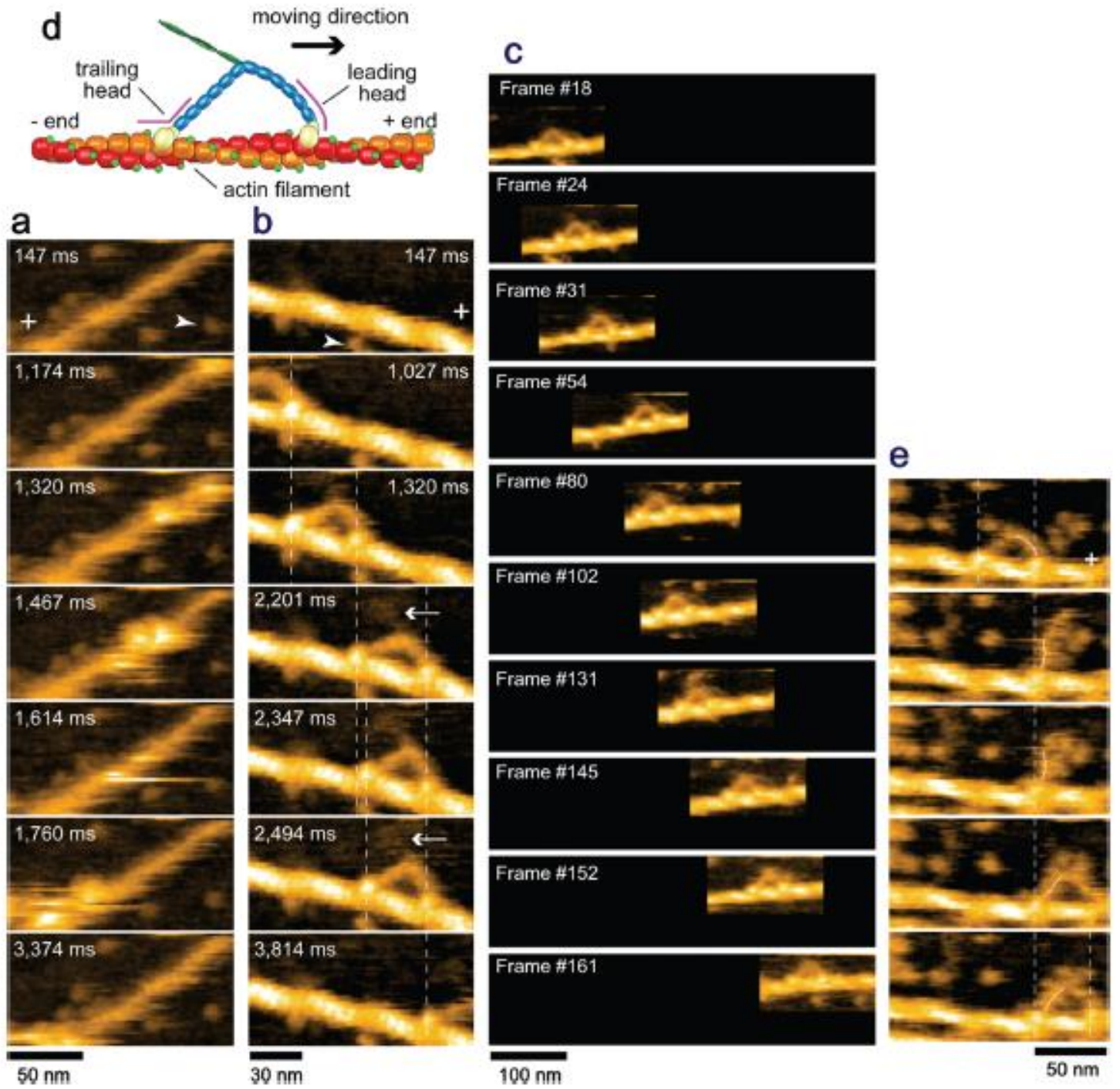

3. Using photons for Imaging: Fluorescence Microscopy

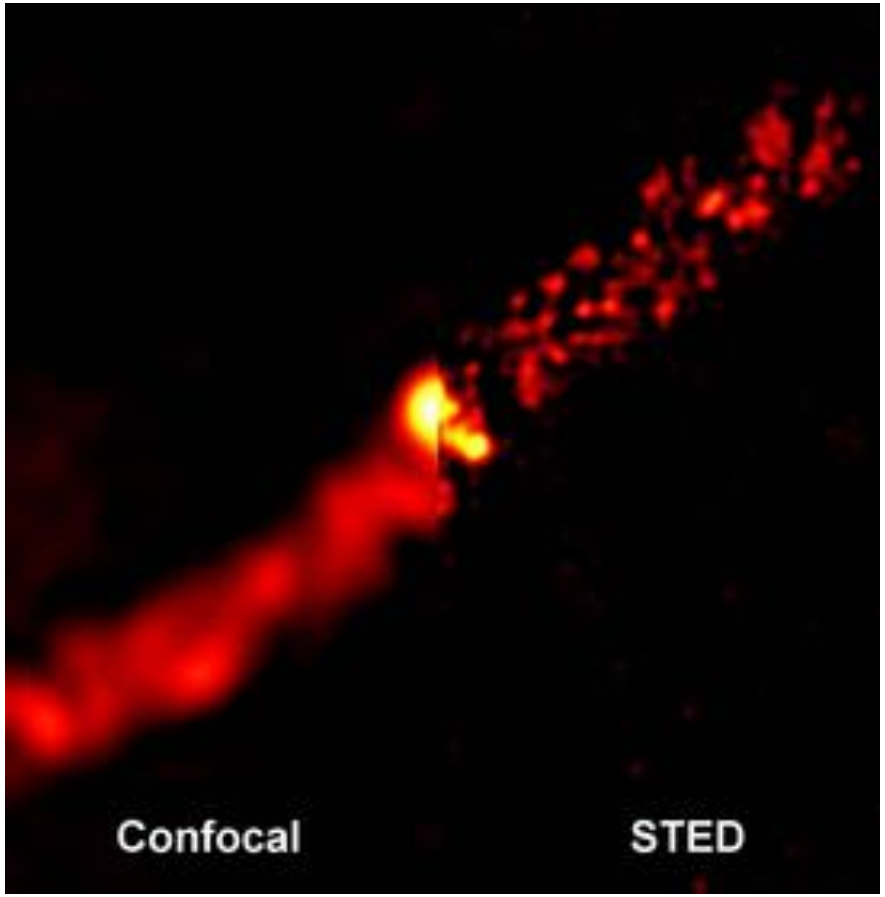

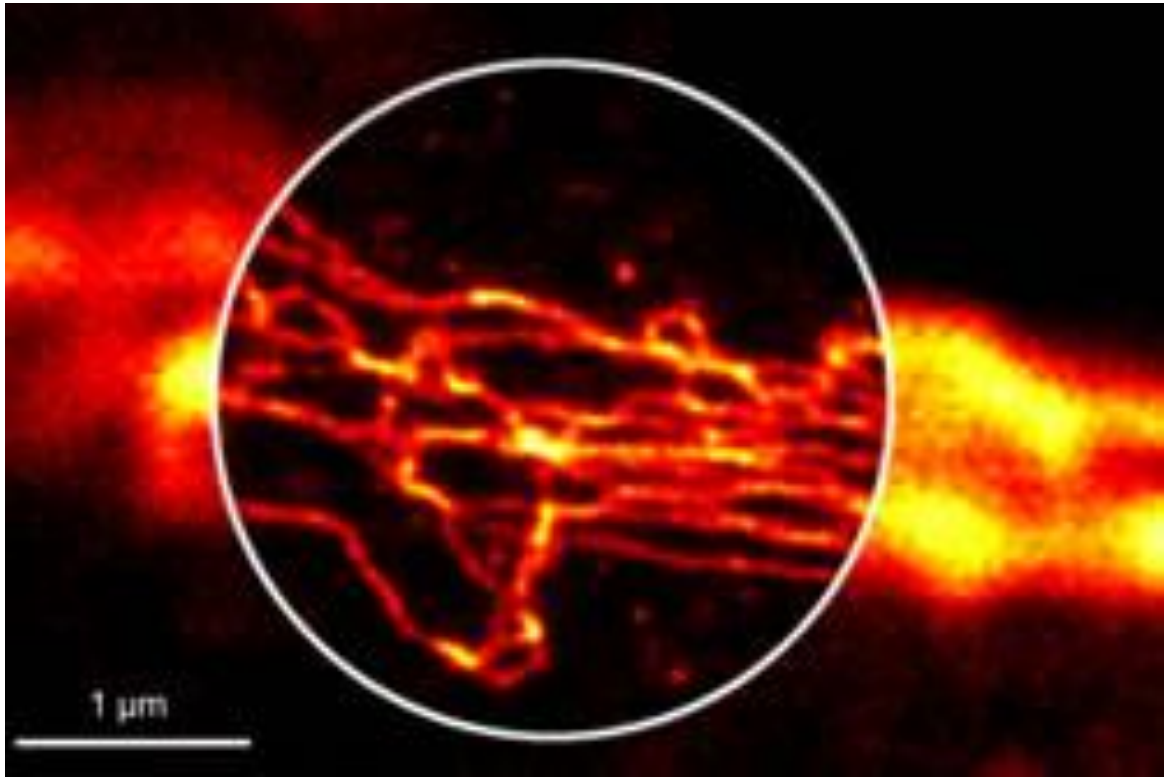

Pujals, S. et al. *Nat. Rev. Chem.* 2019, 3, 68−84
Schermelleh, L. et al. *Nat. Cell Biol.* 2019, 21, 72−84
Sahl, S. J. et al. *Nat. Rev. Mol. Cell Biol.* 2017, 18, 685−701

Using photons for Imaging: History

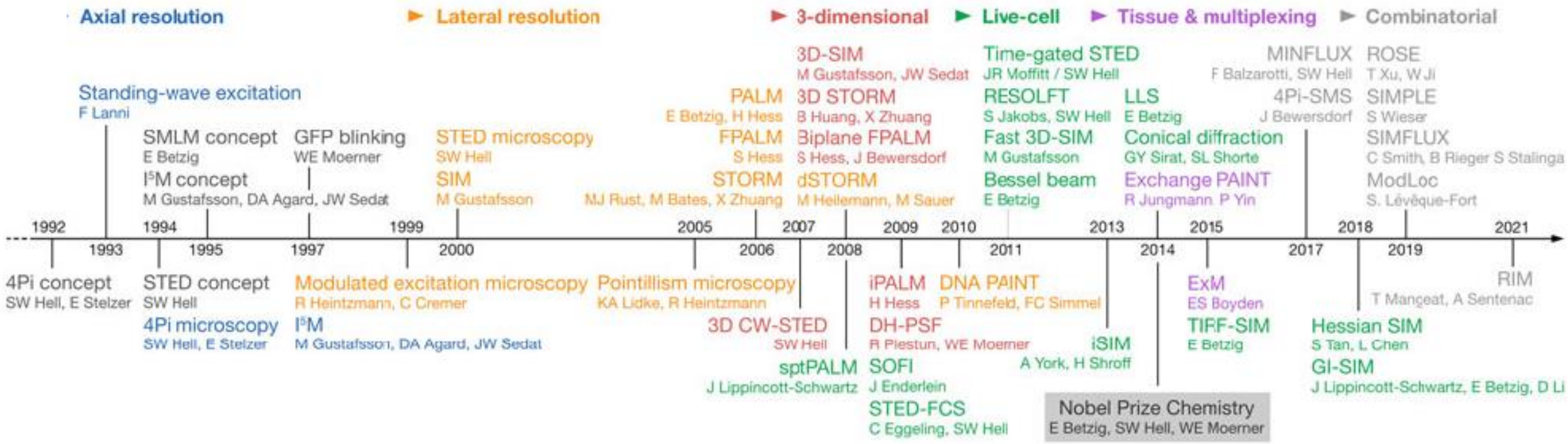

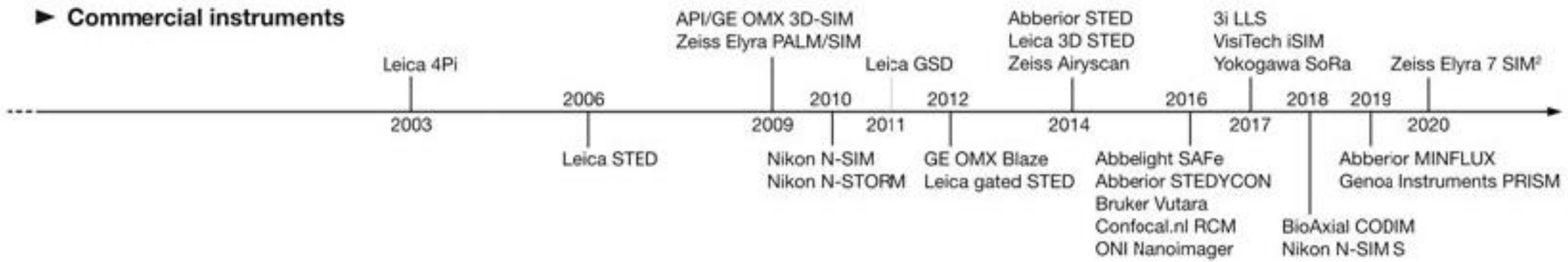

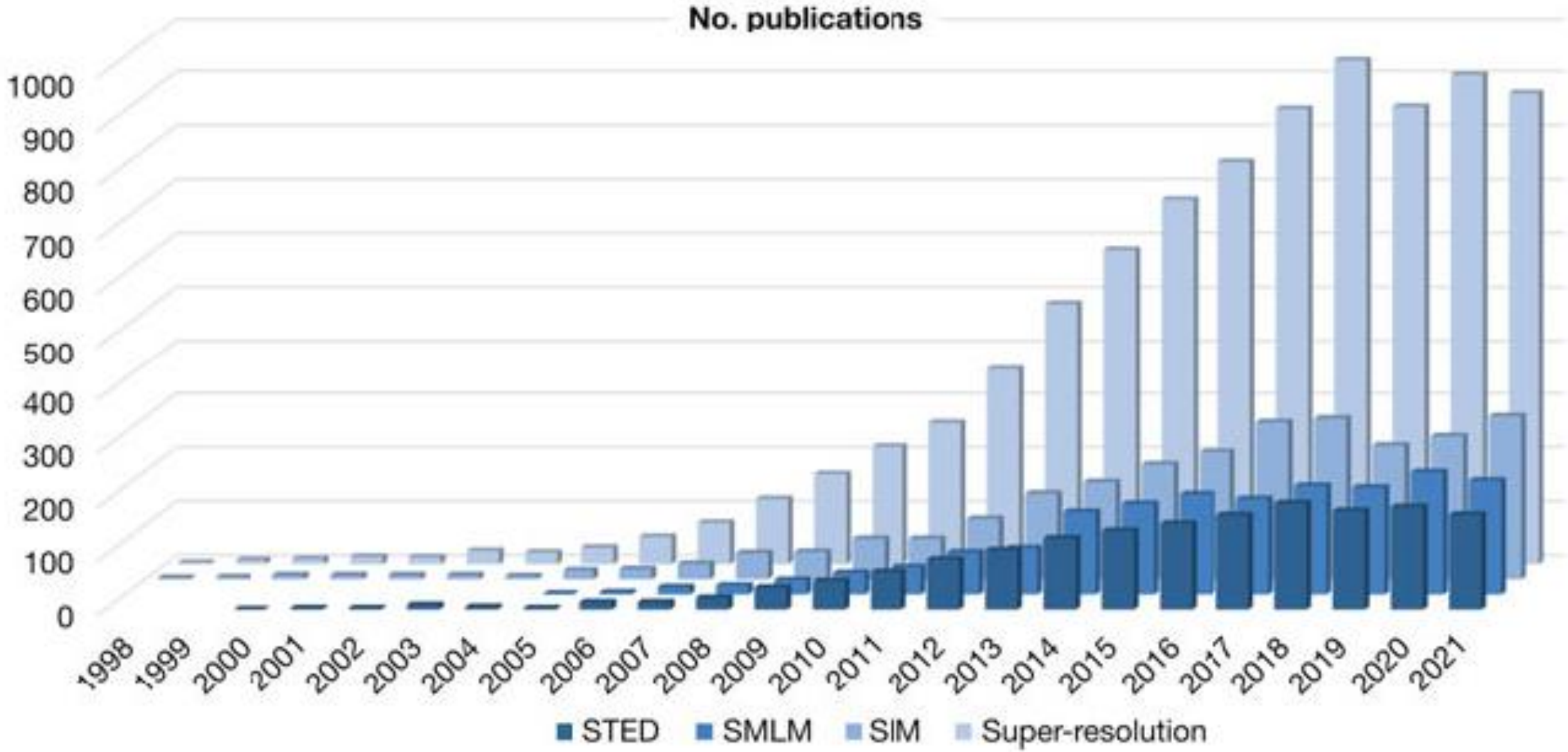
No. publications
1000
900
800
700
600
500
400
300
200
100
0
1998
1999
2000
2001
2002
2003
2004
2005
2006
2007
2008
2009
2010
2011
2012
2013
2014
2015
2016
2017
2018
2019
2020
2021
STED
SMLM
SIM
Super-resolution

Confocal Fluorescence Microscopy Imaging of gels (early 2000)

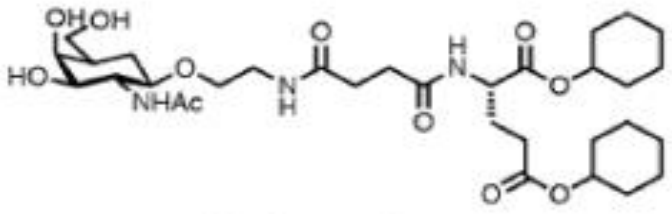

Hydrogelator

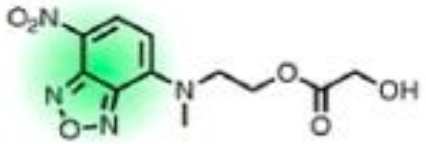

Fluorescent probe (HANBD)

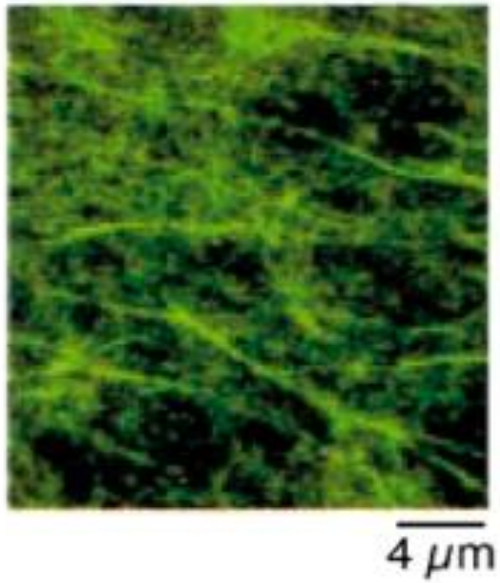

Kiyonaka, S. et al. J. Am. Chem. Soc. 2002, 124, 10954−10955

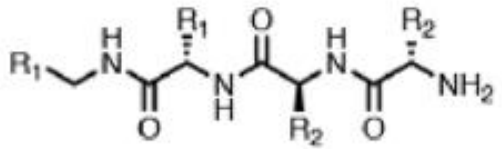

$K_{160}L_{40}$

R_1: 

R_2: 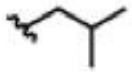

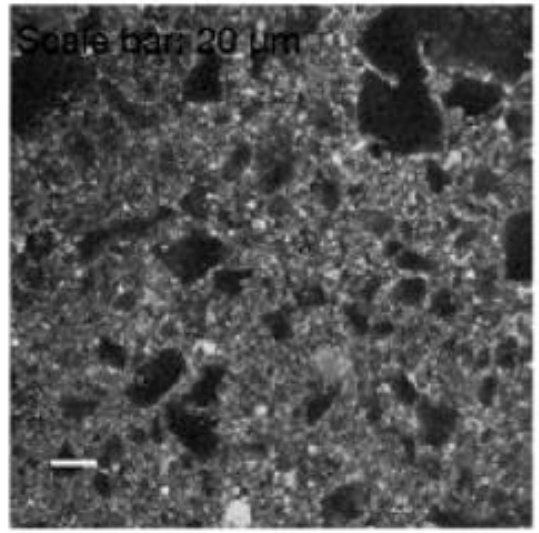

Scale bar: 20 μm

Nowak, A. P. et al. Nature 2002, 417, 424−428

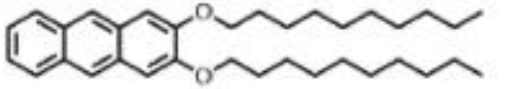

DDOA

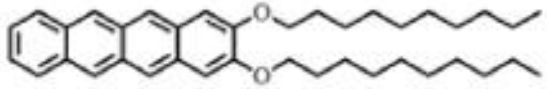

DDOT

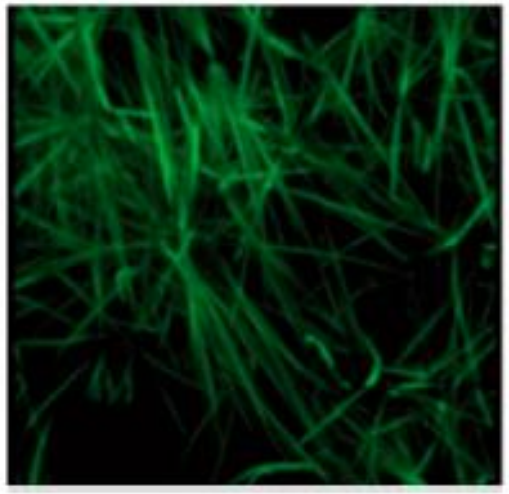

Del Guerzo, A. t al. J. Am. Chem. Soc. 2005, 127, 17984−17985

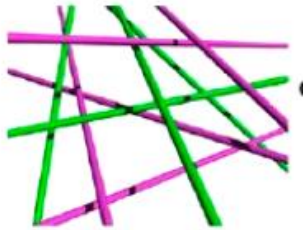

Interpenetrating self-sorting double network

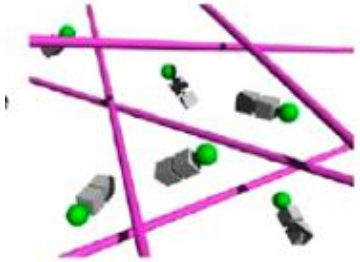

single network

Parallel self-sorting double network

Self-sorting composite hydrogel

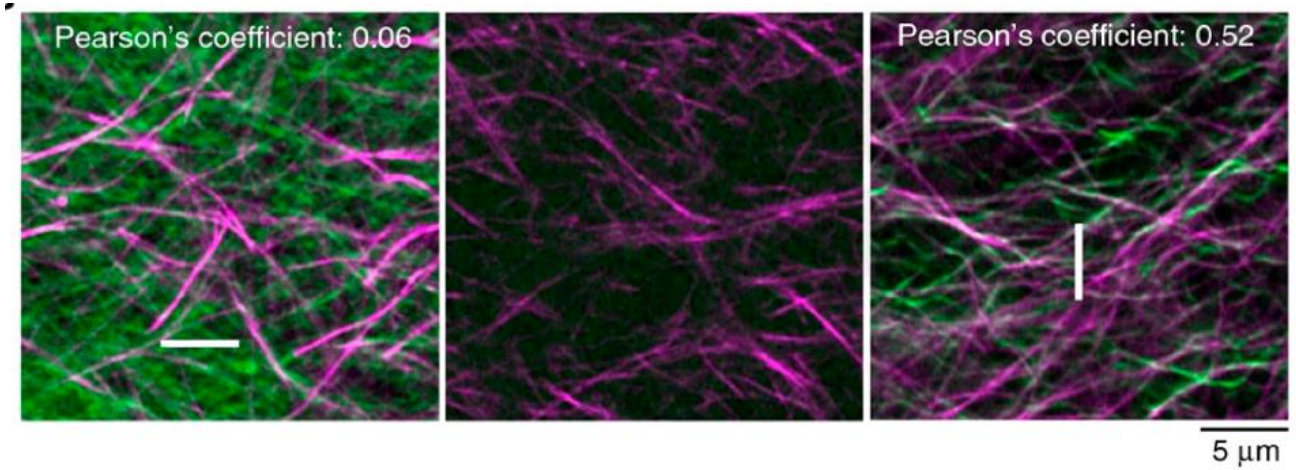

3D Airyscan CLSM (Confocal Laser Scanning Microscopy)
Green: peptide
Magenta: lipid

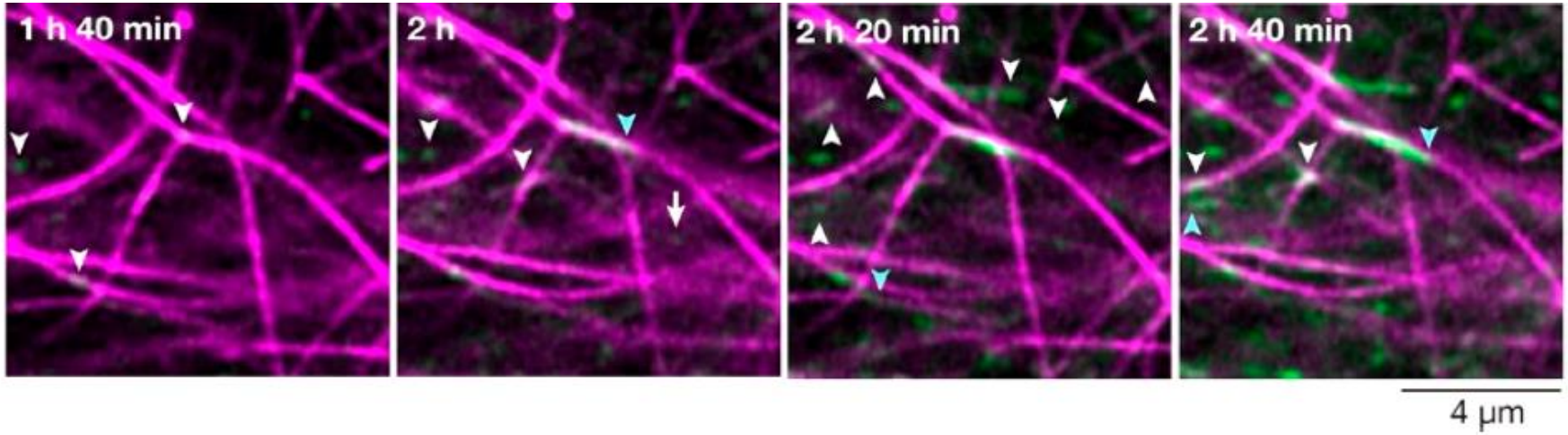

Time-lapse CLSM images of formation of nanofibers

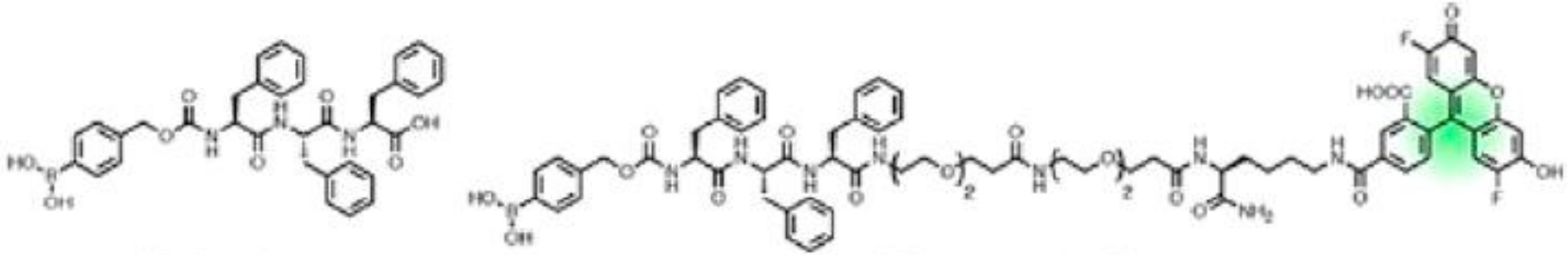

Hydrogelator

Fluorescent probe

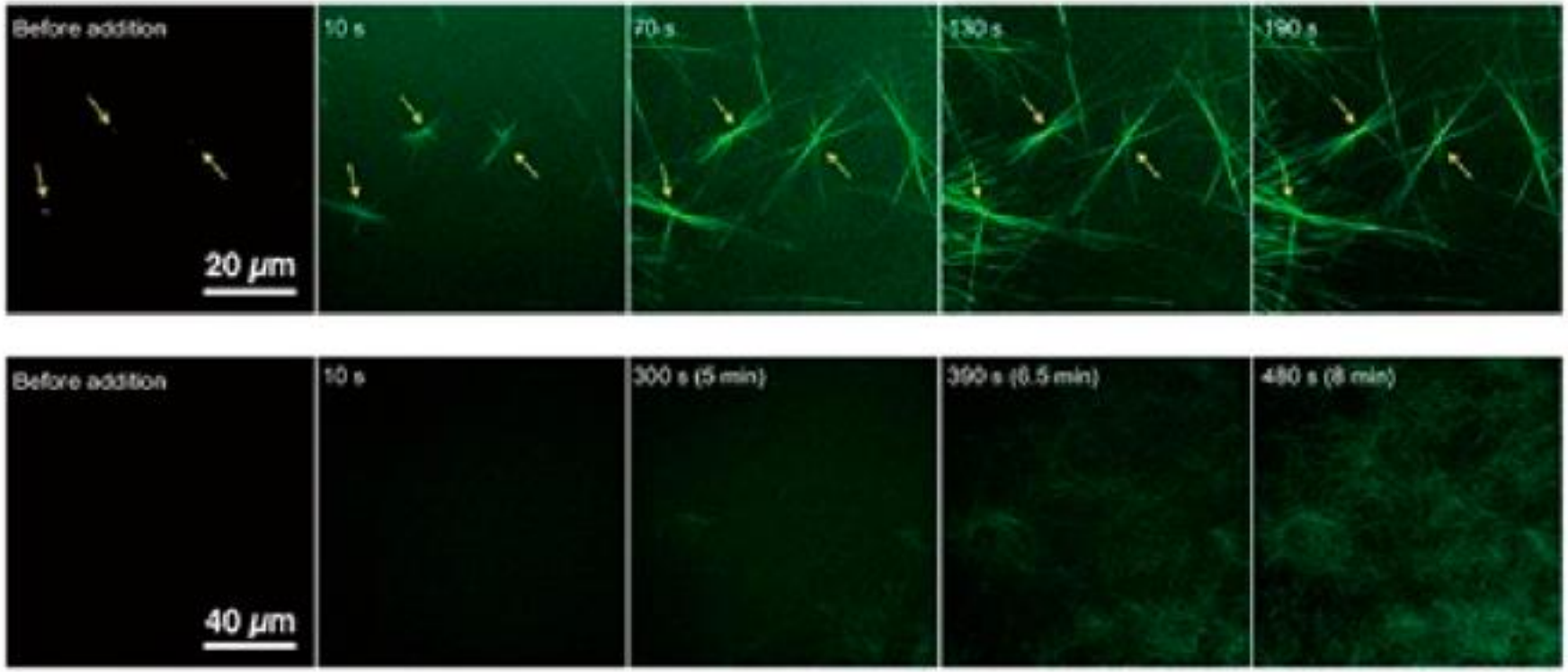

In the presence of seeds

No seeds

A nucleation-elongation mechanism

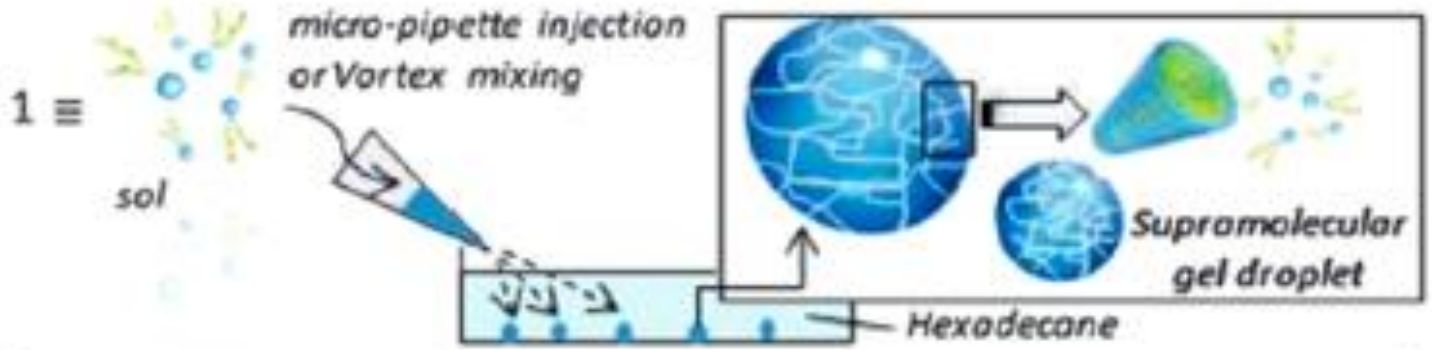

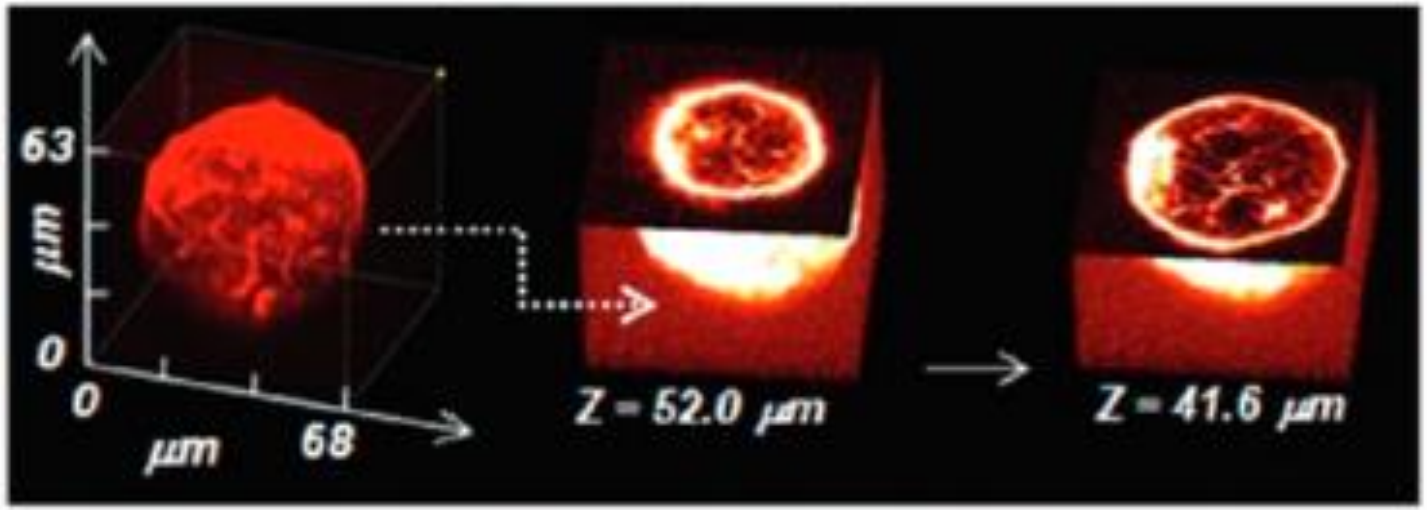

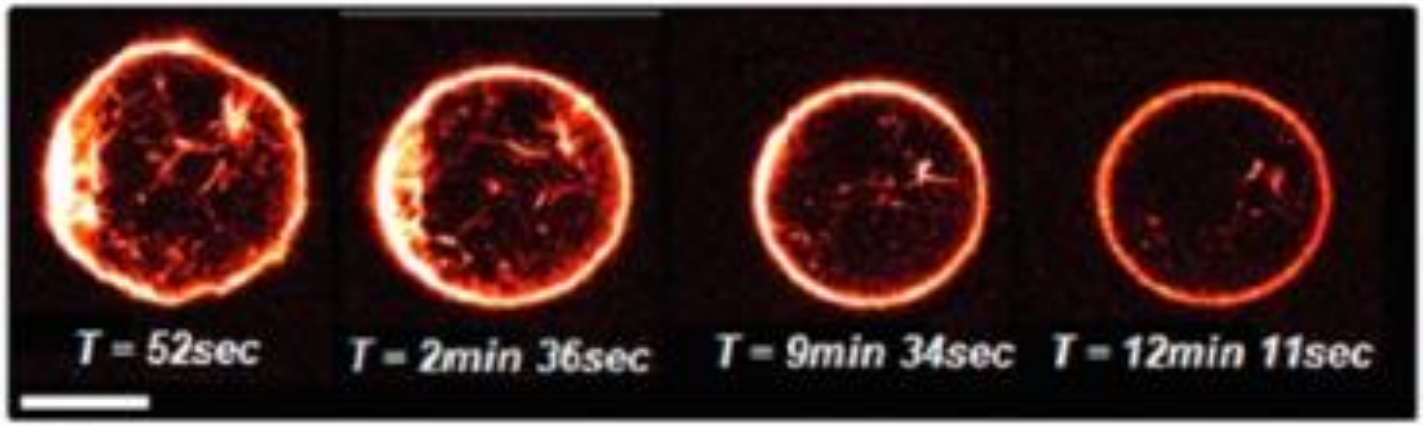

Schematic illustration of formation of supramolecular gel droplets.

Bottom: 3D CLSM images of the gel droplets.

Note the fibrous networks of the gelator within the droplets.

Self-assembly of block copolymers

$[PFS_{62}\text{-}b\text{-}(PDMS_{605}\text{-}r\text{-}PMVS_{21})]$

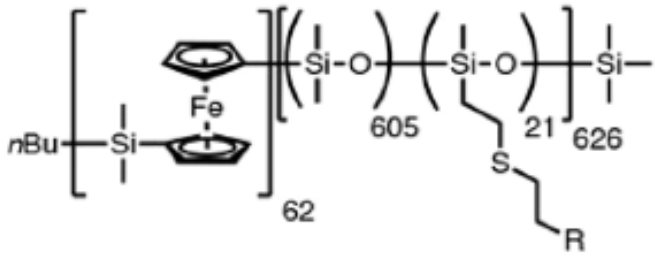

TEM and CLSM images of 11-block cylindrical RGB micelles (length: 5 µm).

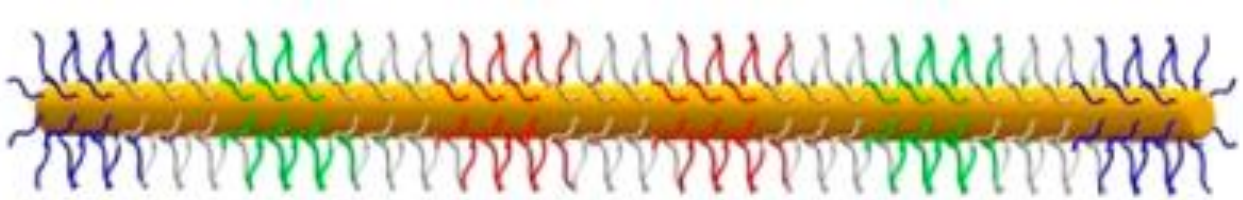

Scale bar: 5 µm (CLSM), 3 µm (TEM).

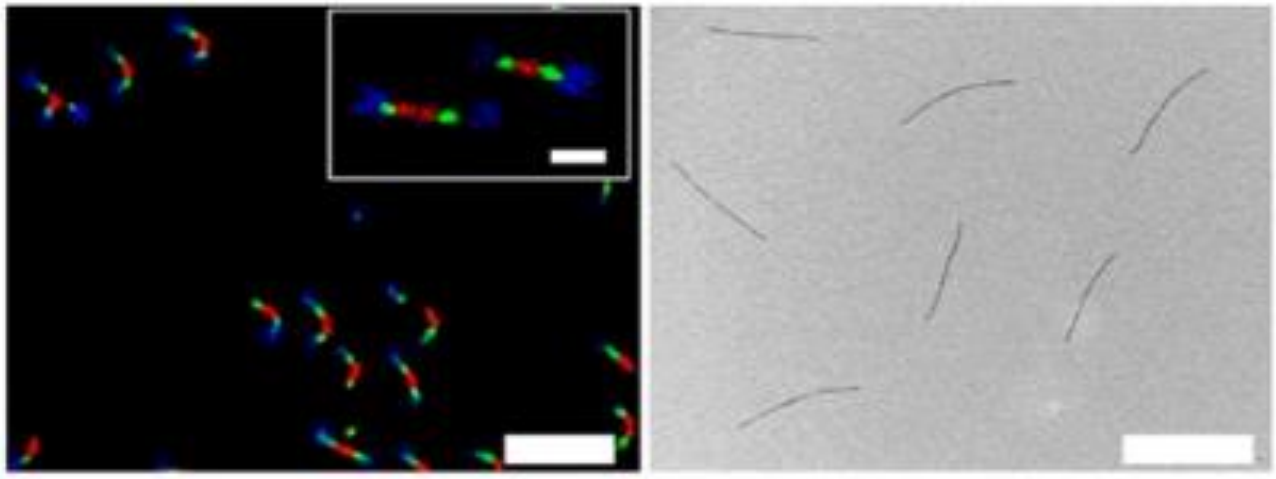

TEM and CLSM images of 7-block cylindrical RGB micelles.
Scale bar: 500 nm (TEM, left), 2 µm (TEM, right), 10 µm (CLSM, left), and 5 µm (CLSM, right)

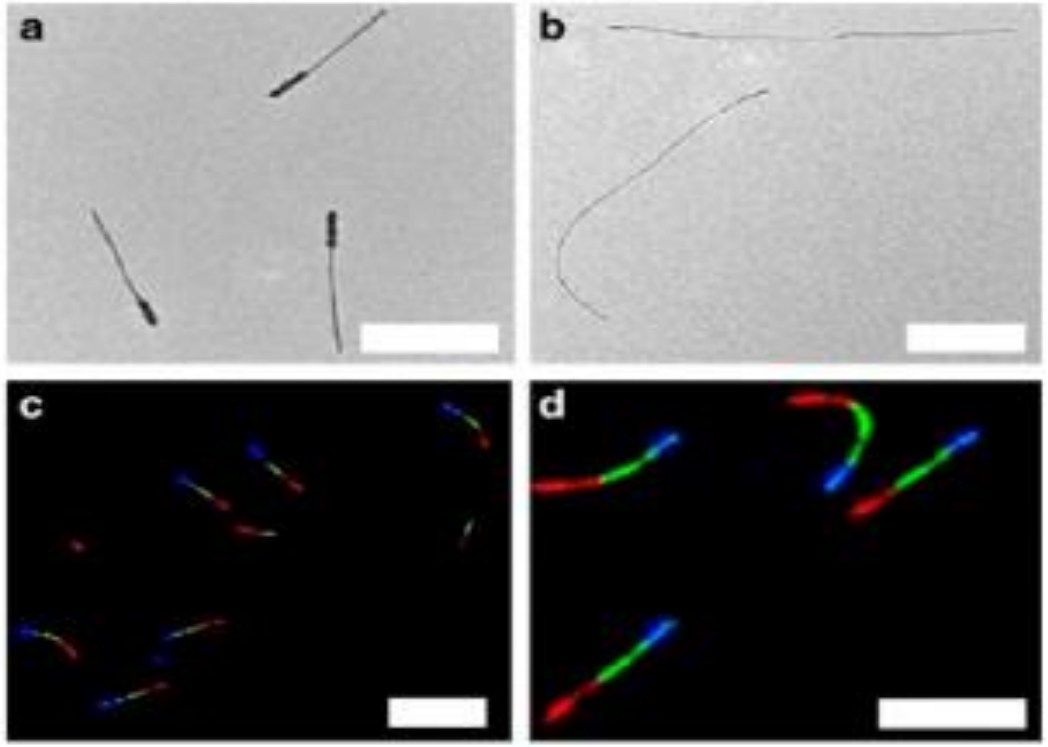

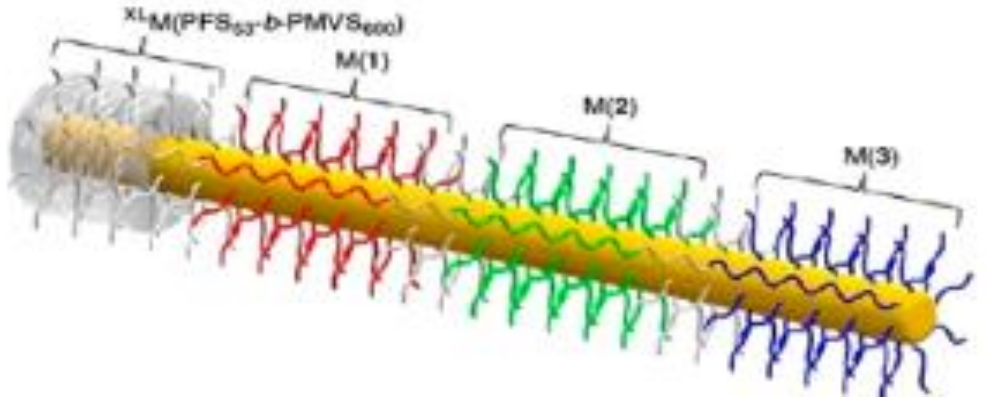

Conventional Confocal vs. Super-Resolution Microscopies

	conventional confocal microscopy	SIM	STED		SMLM (PALM/STORM/PAINT)
			2D STED	3D STED	
spatial resolution					
xy	~200 nm	~120 nm	~30 nm[a]	~100 nm[a]	~20 nm
z	~500 nm	~250 nm	~500 nm[a]	~200 nm[a]	~150 nm
imaging depth	~50 μm	~50 μm	~50 μm	~50 μm	~10 μm
acquisition speed (frame^{-1})	1 s–1 min	100 ms–10 s	1 s–1 min	1 s–1 min	>10 min
light intensity(W/cm^2)	10^2–10^3	1–10^2	>10^3	>10^3	10^3–10^4
disadvantages		prone to reconstruction artifacts	limited dye choice	limited dye choice	special buffers/dyes are required

[a]Depends on intensity of a depletion laser.

SIM: Structured Illumination Microscopy
STED: Stimulated Emission Depletion Microscopy
SMLM: Single Molecule Localization Microscopy
PALM: PhotoActivated Localization Microscopy
STORM: STochastic Optical Reconstruction Microscopy
PAINT: Point Accumulation for Imaging in Nanoscale Topography

Sauer, M.; Heilemann, M. Single Molecule Localization Microscopy in Eukaryotes. *Chem. Rev.* 2017, 117, 7244-7275.

The magic tetrahedron of Super Resolution Microscopy

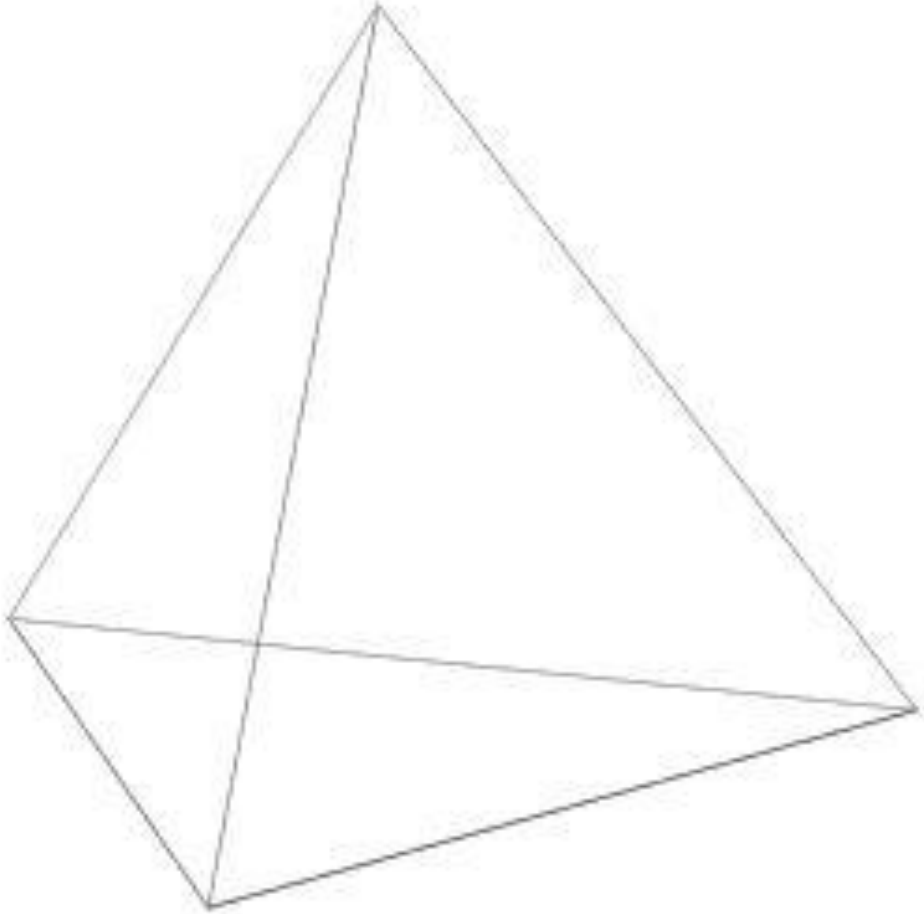

The resolution limit

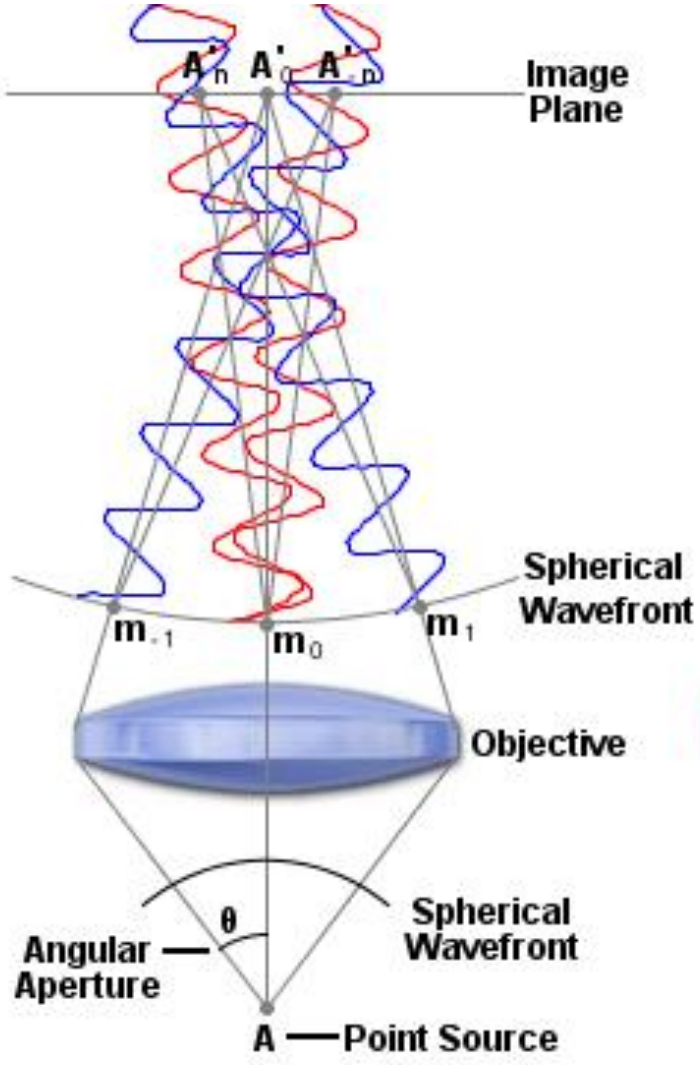

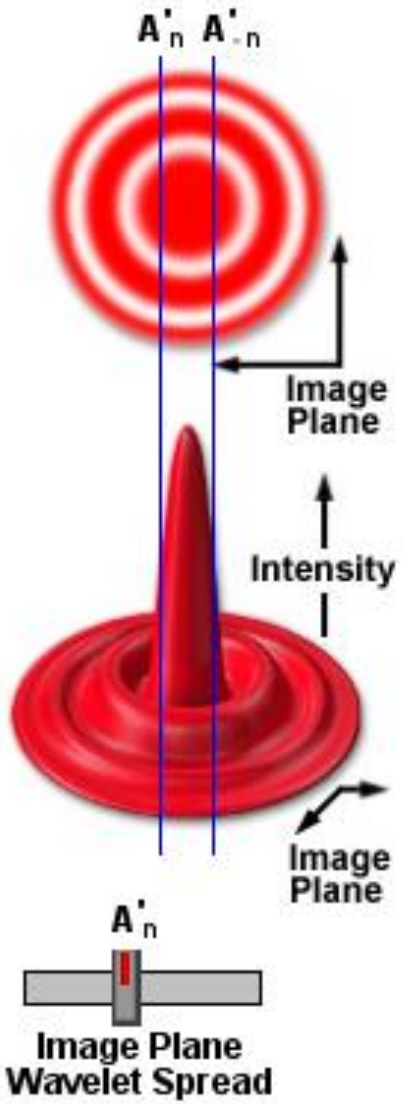

$$d_{\text{Abbe}} = \frac{\lambda}{2n \sin \alpha}$$

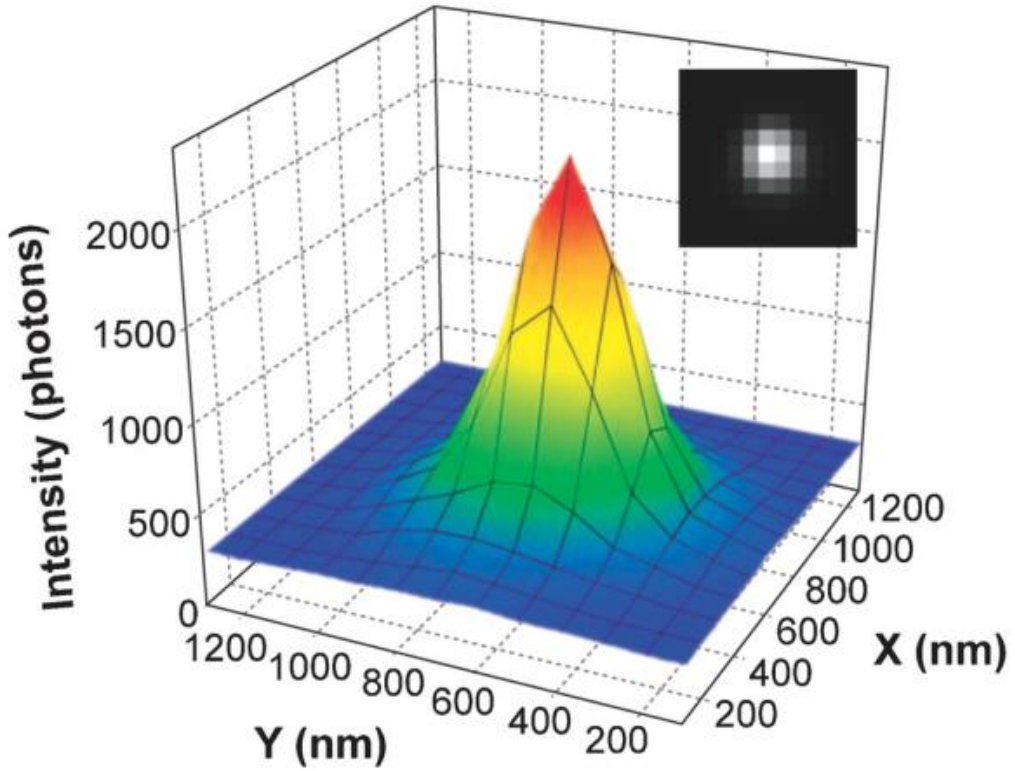

Point Spread Function

Pointillisme

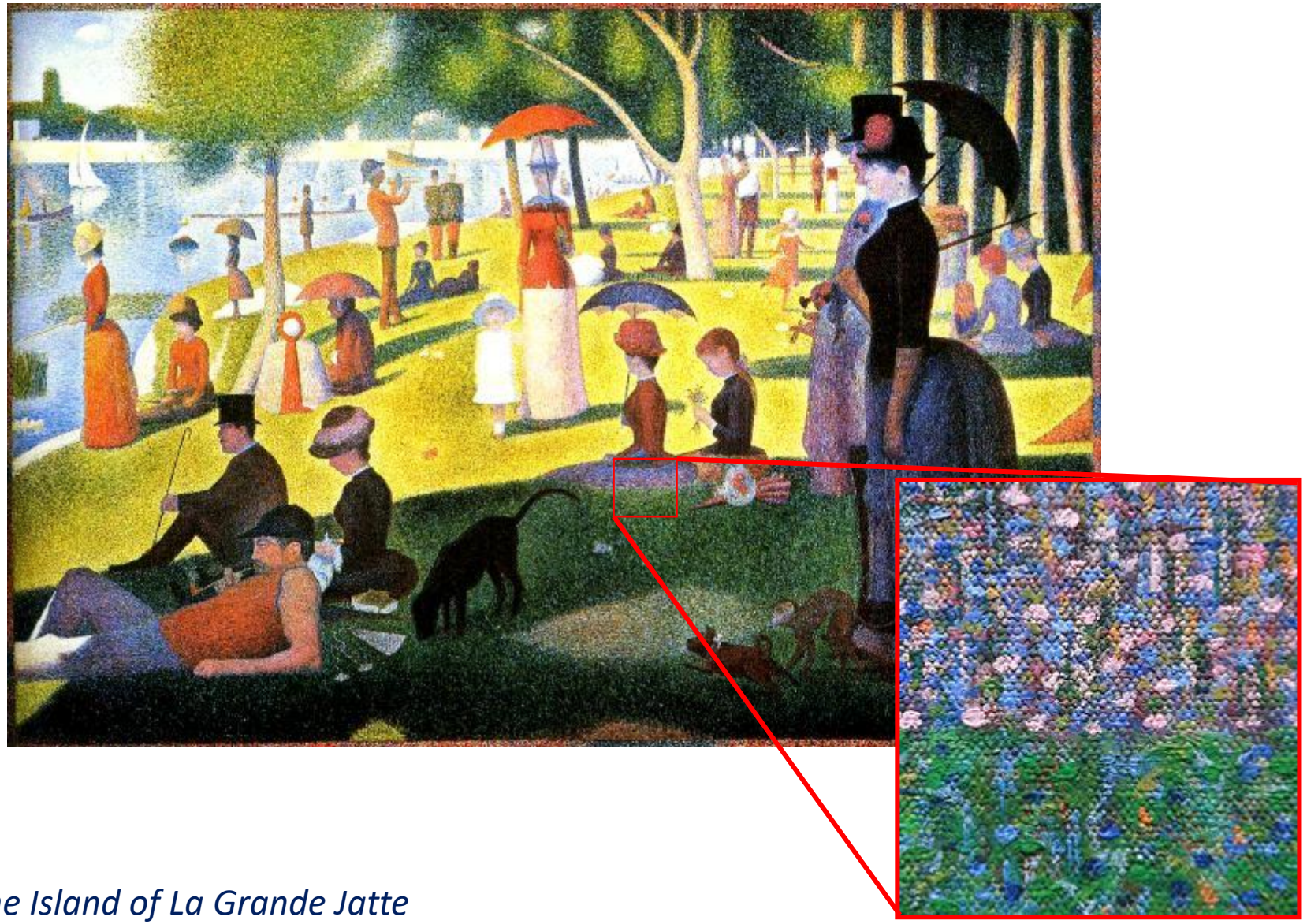

Georges-Pierre Seurat

Sunday Afternoon on the Island of La Grande Jatte

FIONA: Fluorescence Imaging with One Nanometer Accuracy

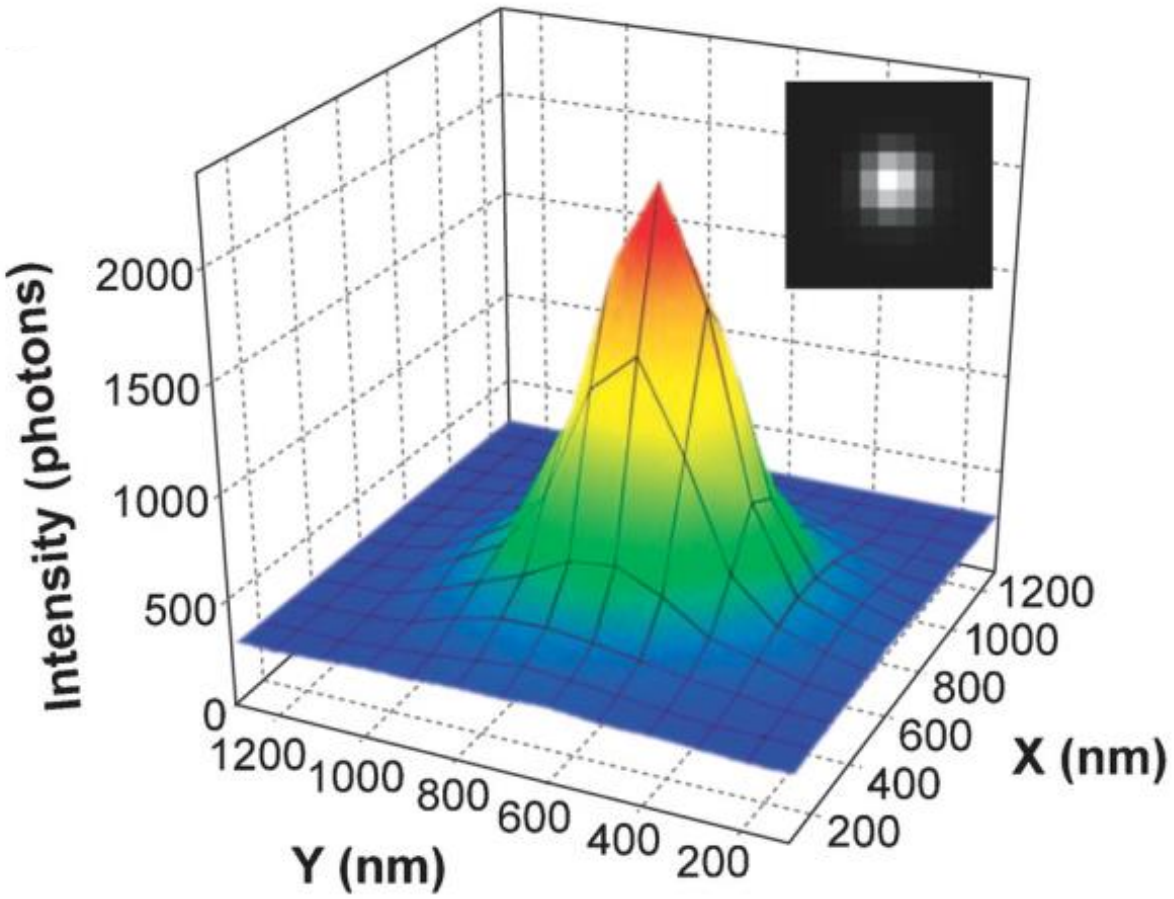

- **The light emitted by a single molecule is some hundreds of nanometers wide.**

- **However, the position of the molecule can be determined with 1 nm precision from a statistical analysis of the emission intensity.**

Single Molecule Fluorescence

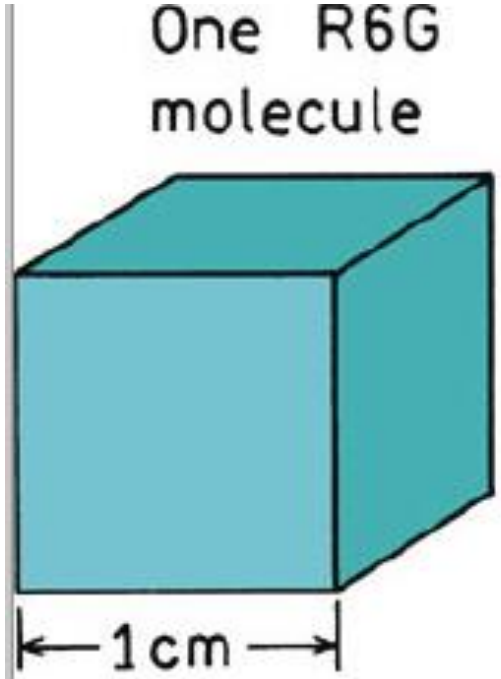

$I_F \approx 1.0$

$I_{RS} \approx 10^{10}$

V = 1 ml

$I_F \approx 1.0$

$I_{RS} \approx 1.0$

V = 97 fl

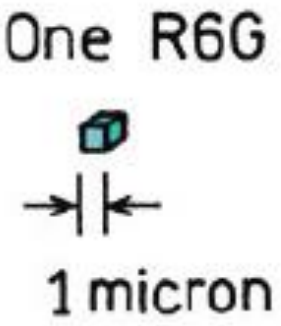

$I_F \approx 1.0$

$I_{RS} \approx 10^{-2}$

V = 1 fl

Two-photons excitation

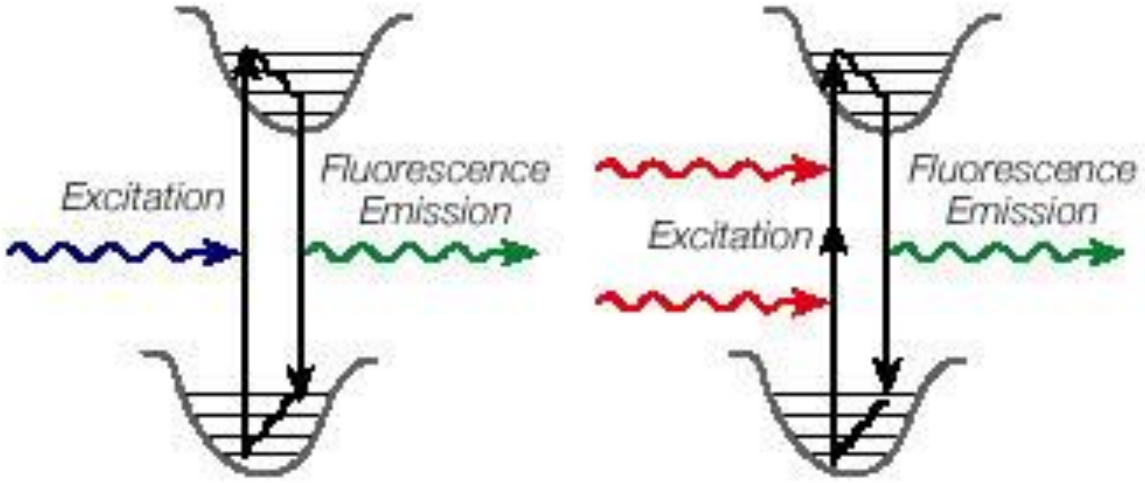

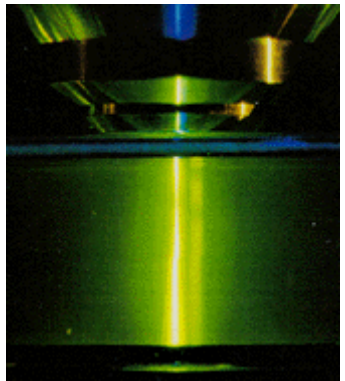

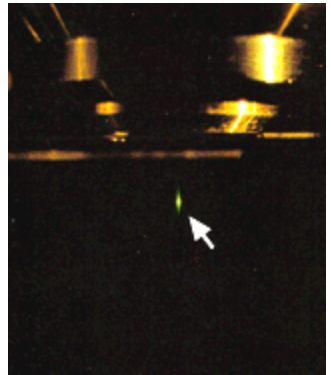

Pulsed laser (fs)!

3D patterning of supramolecular gels by two-photon excitation

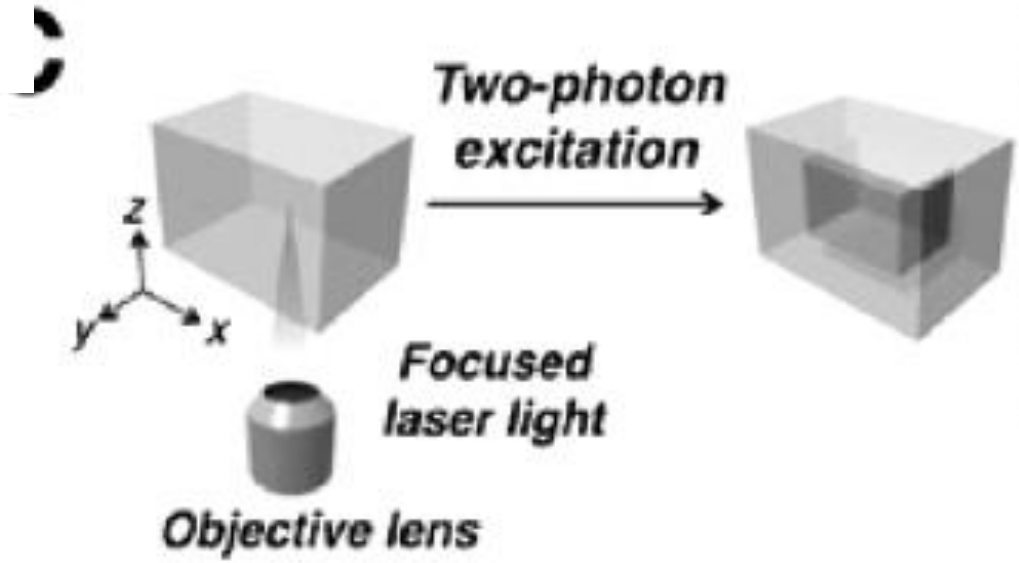

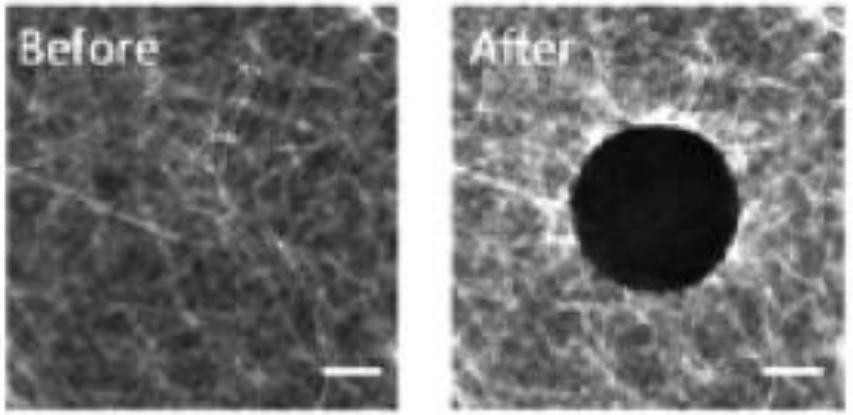

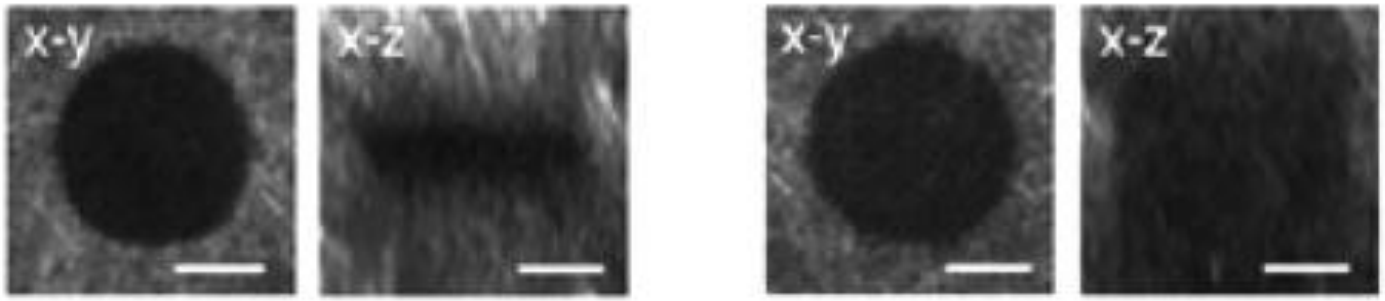

Scale bar: 10 µm

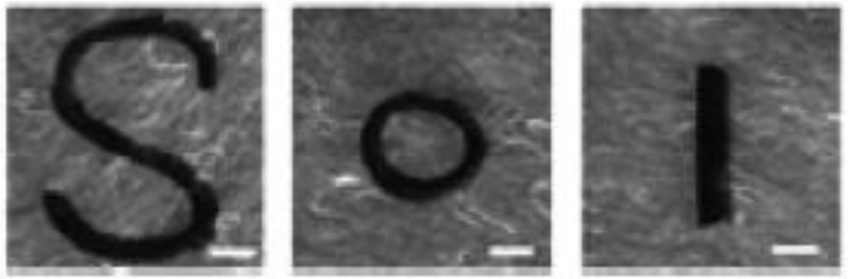

Scale bar: 20 µm

Yoshii, T. et al.
Angew. Chem., Int. Ed. 2014, 53, 7264−7267

Diffraction limit

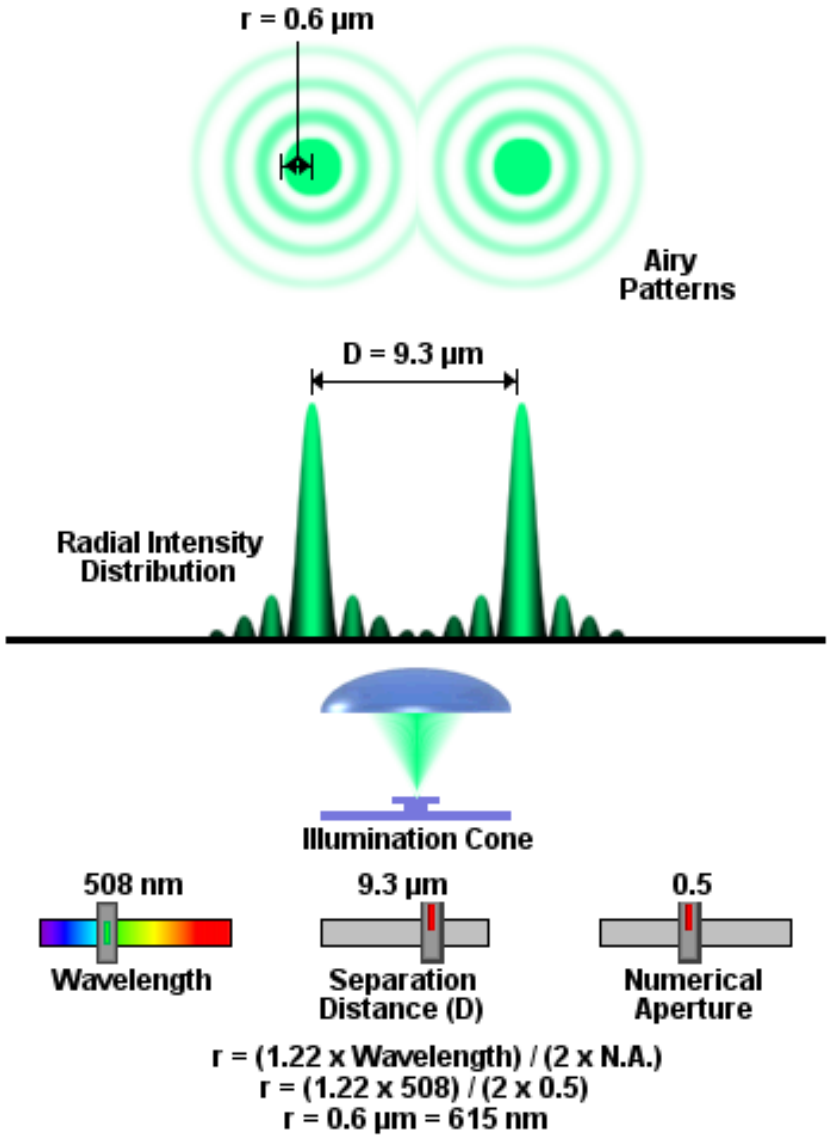

r = (1.22 x Wavelength) / (2 x N.A.)
r = (1.22 x 508) / (2 x 0.5)
r = 0.6 µm = 615 nm

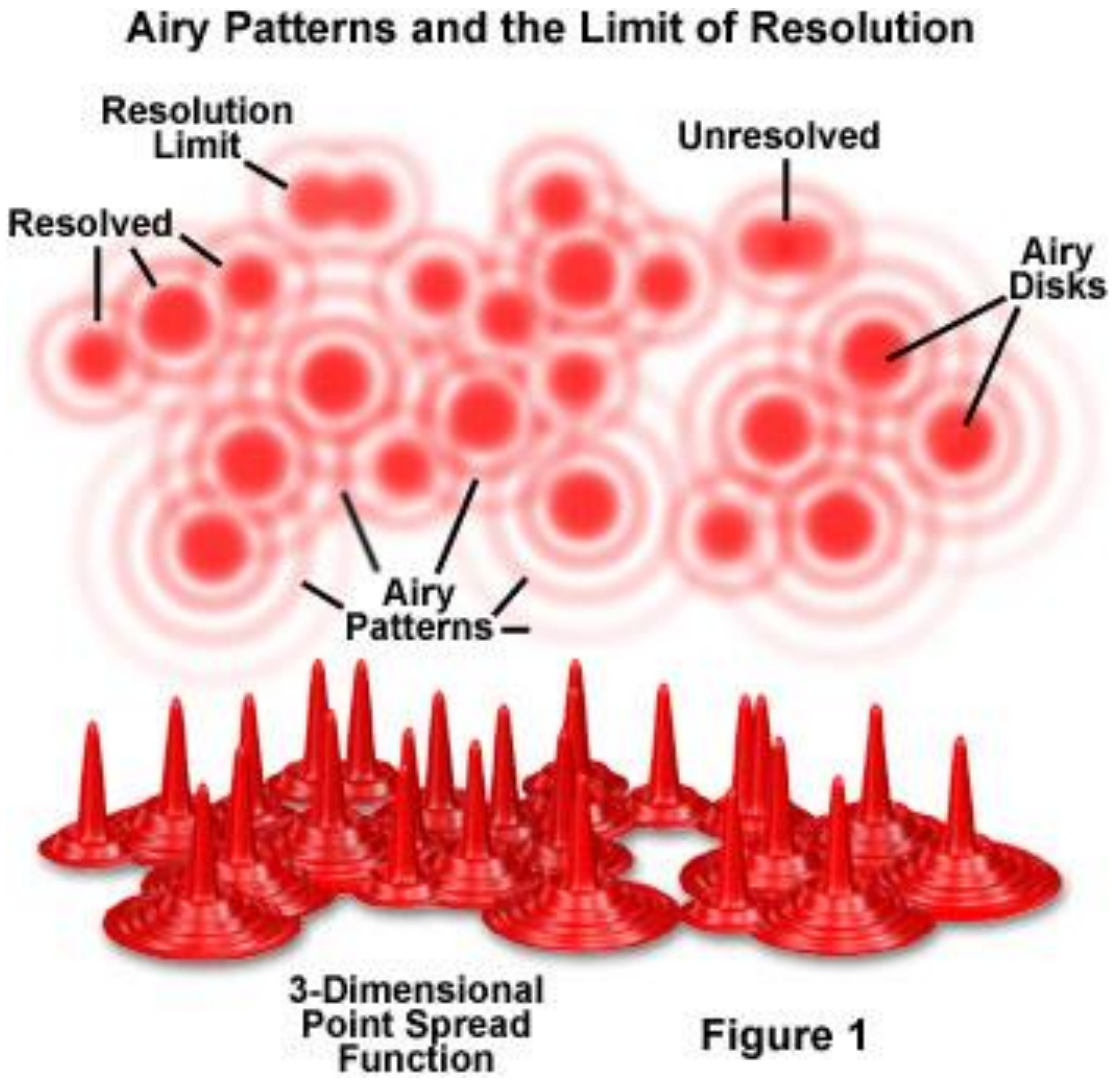

Figure 1

Overcoming the diffraction limit

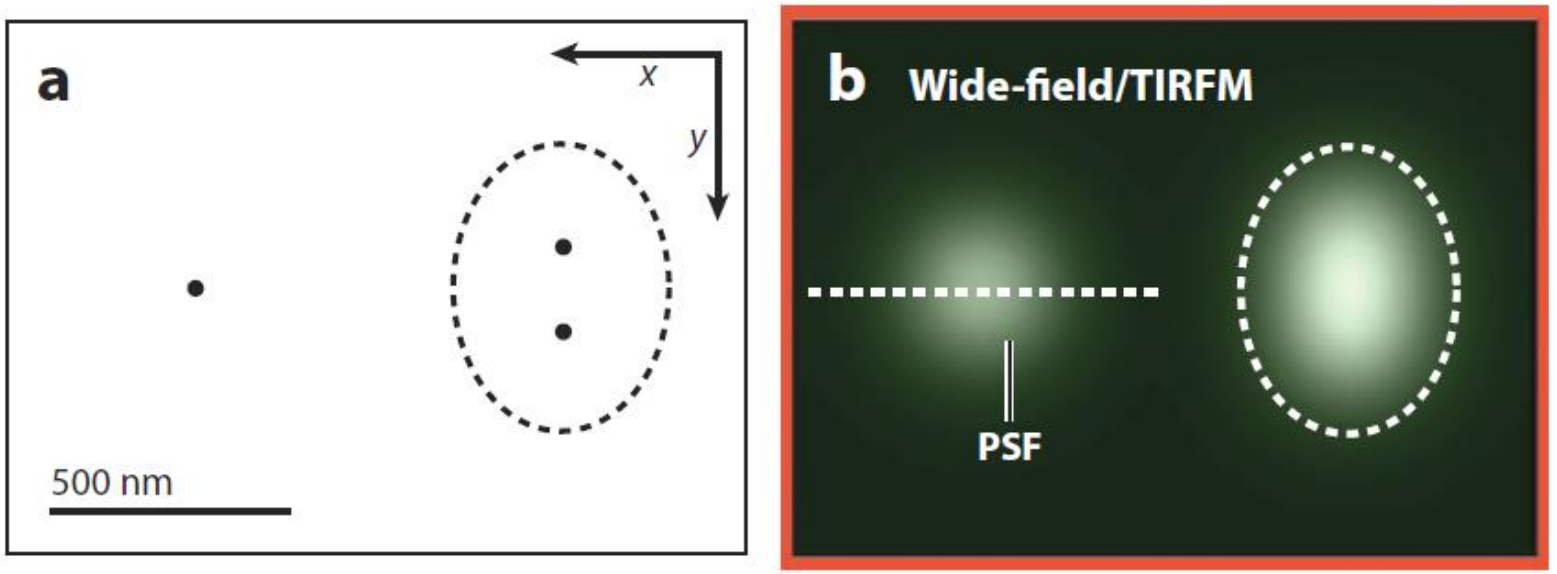

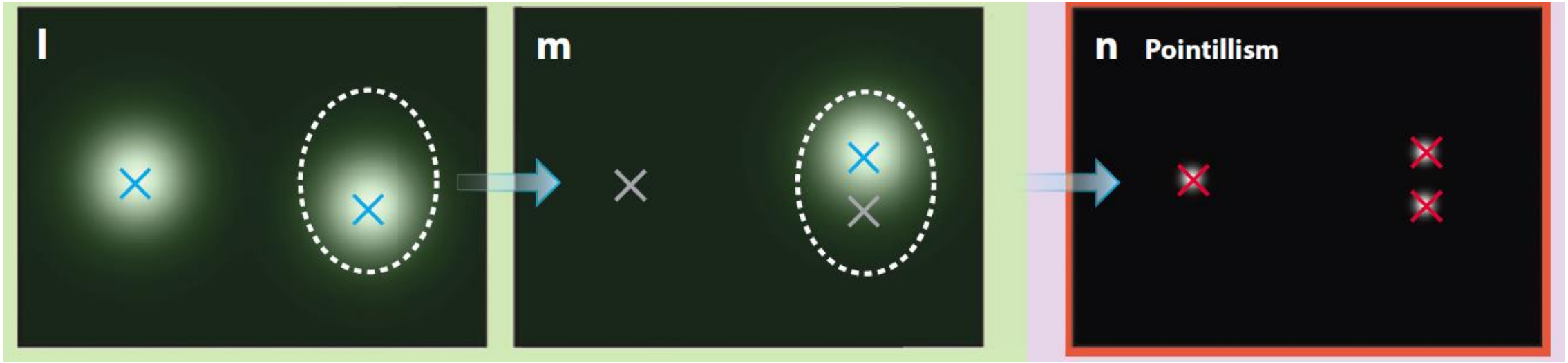

Overcoming the diffraction limit

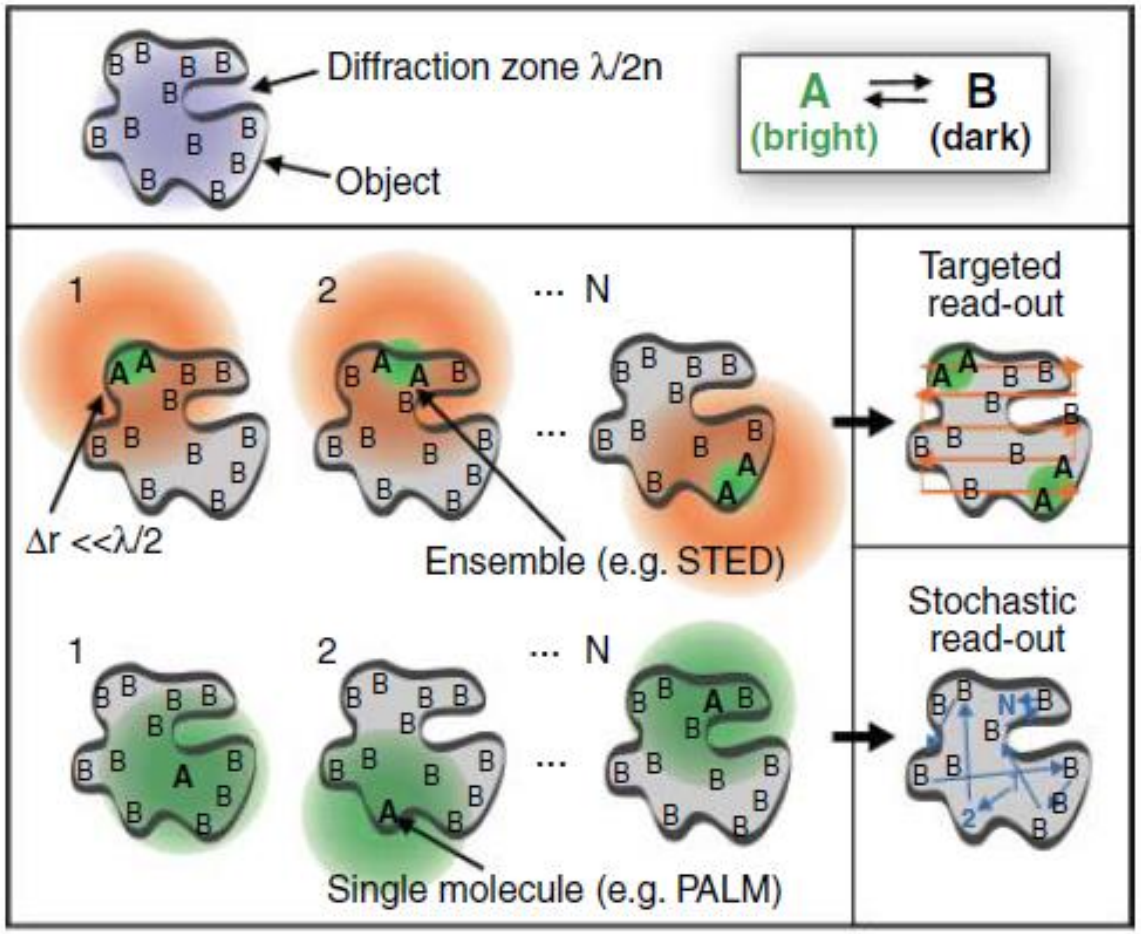

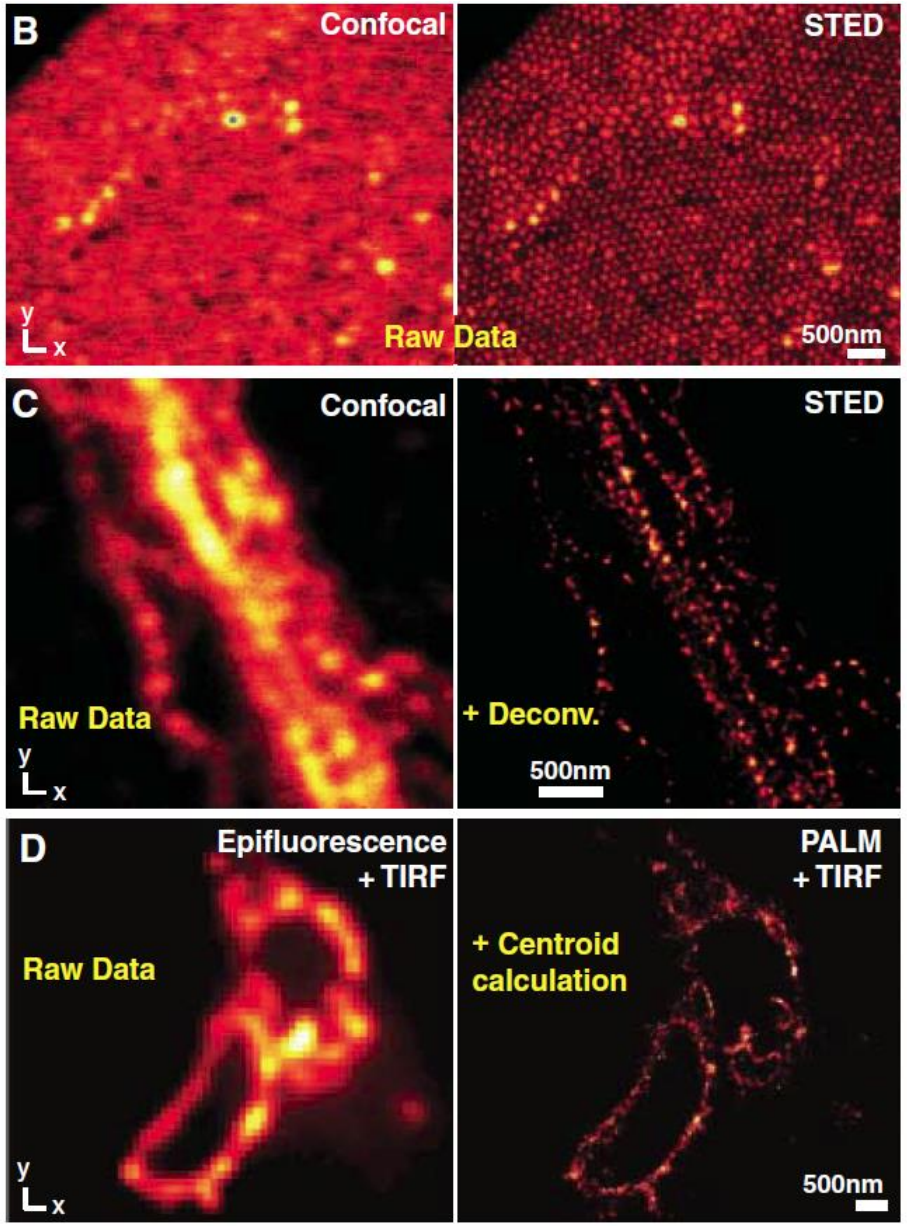

SMLM

Single Molecule Localization Microscopy

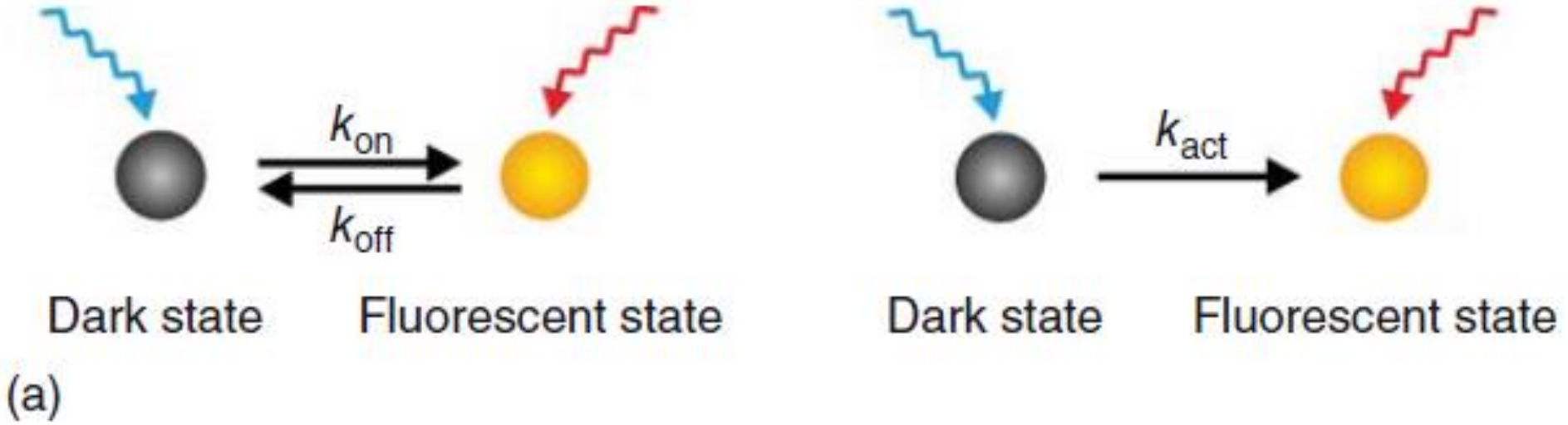

(a)

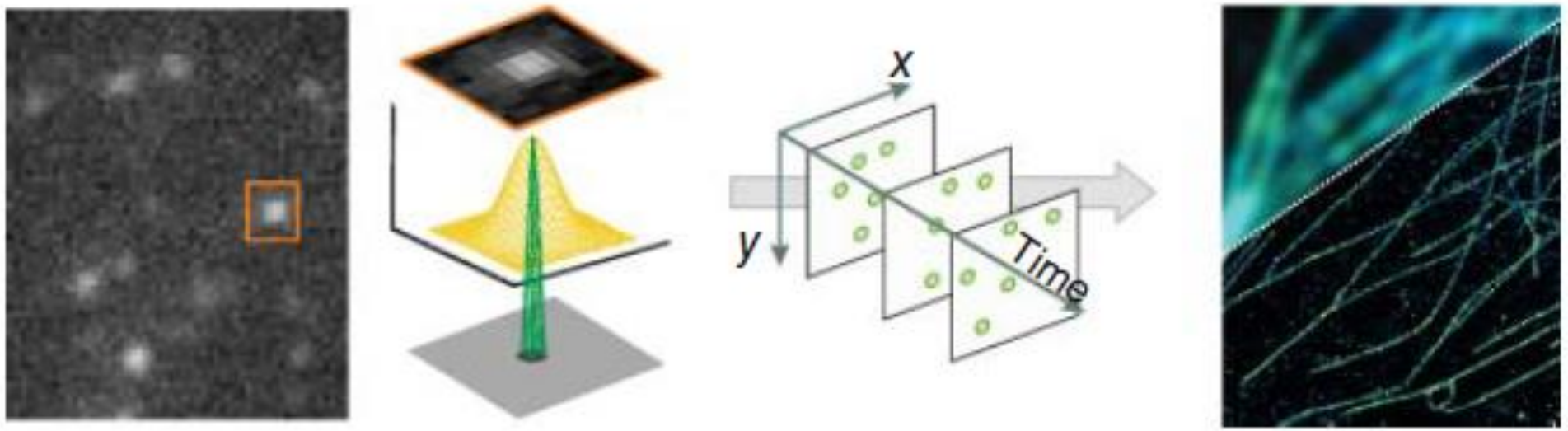

Localization of single fuorophore

Photoswitching between on/off states

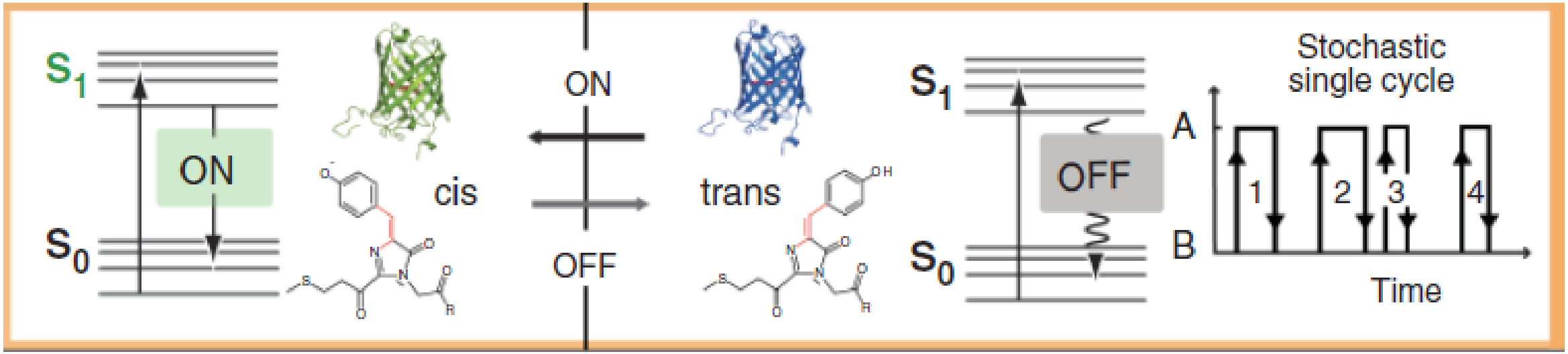

Photobleaching

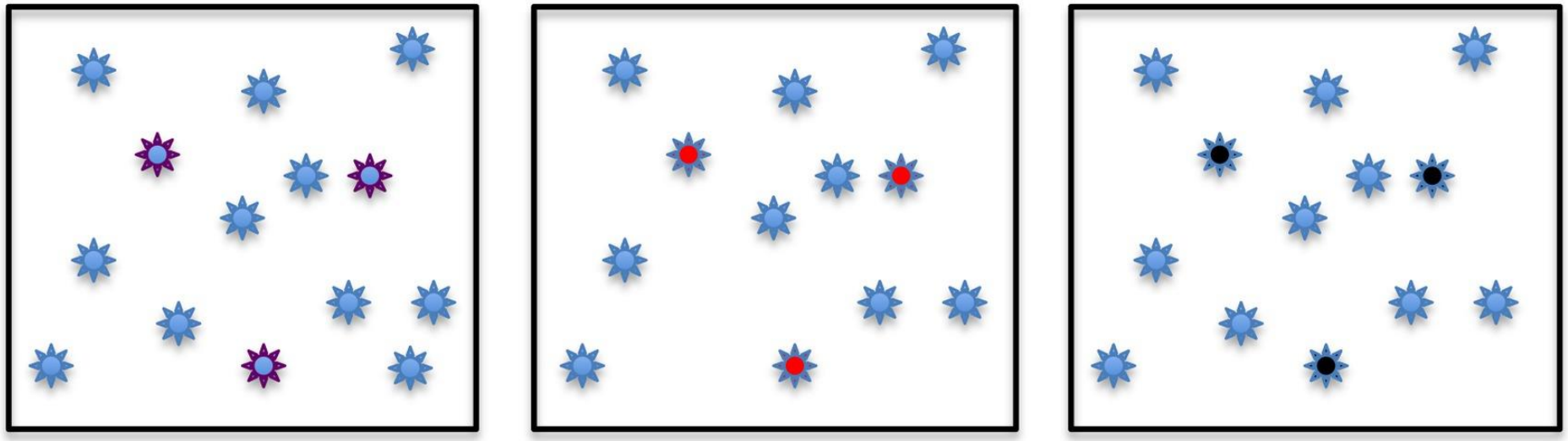

STED

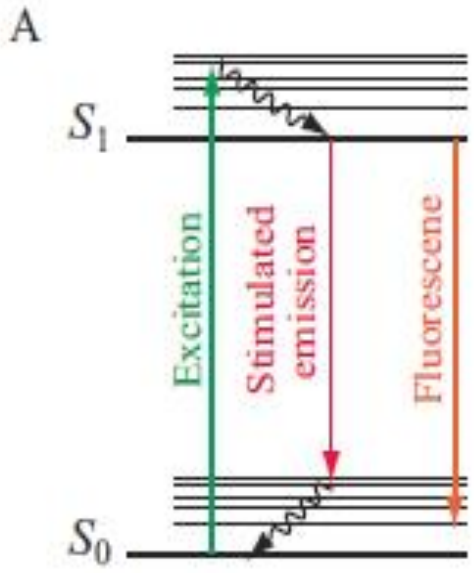
A
S_1
S_0
Excitation
Stimulated emission
Fluorescene

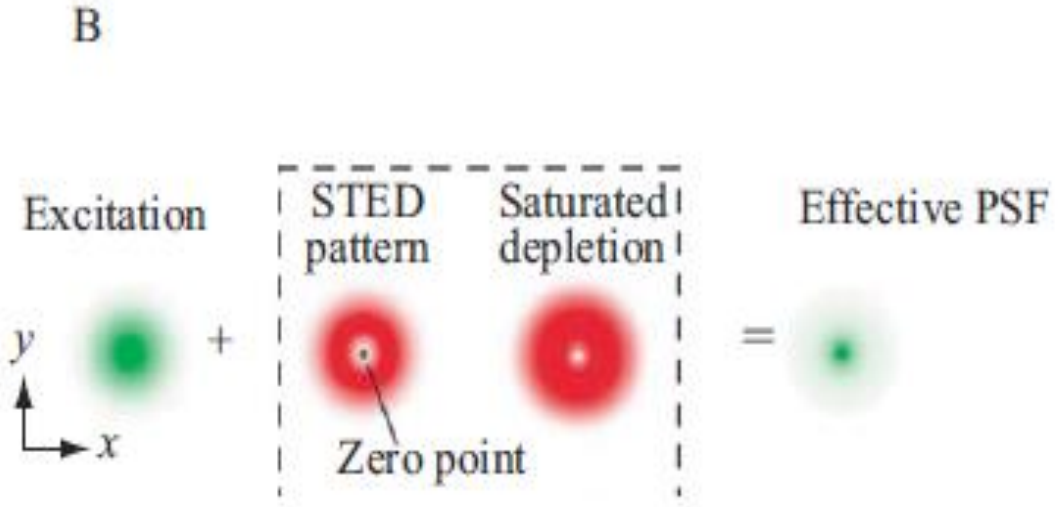
B
Excitation
STED pattern
Saturated depletion
Effective PSF
y
x
Zero point

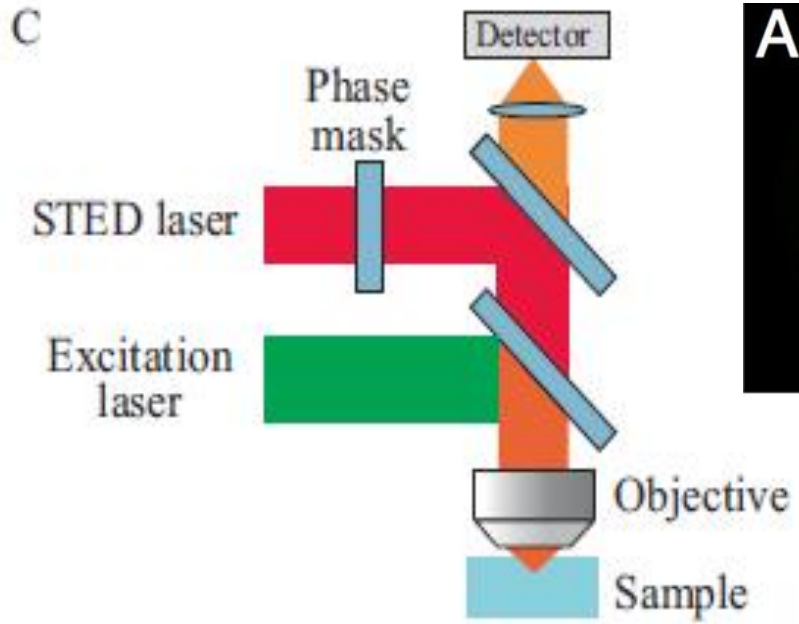
C
Detector
Phase mask
STED laser
Excitation laser
Objective
Sample

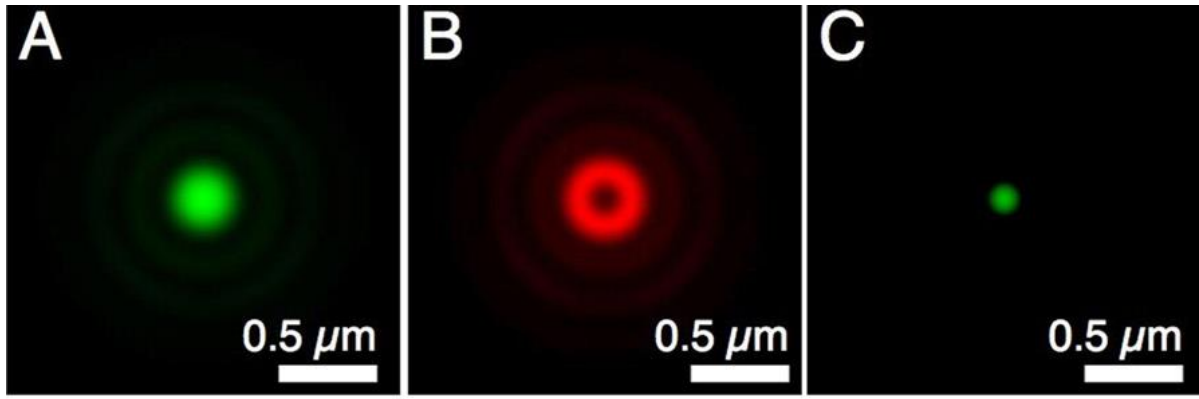
A
0.5 μm
B
0.5 μm
C
0.5 μm

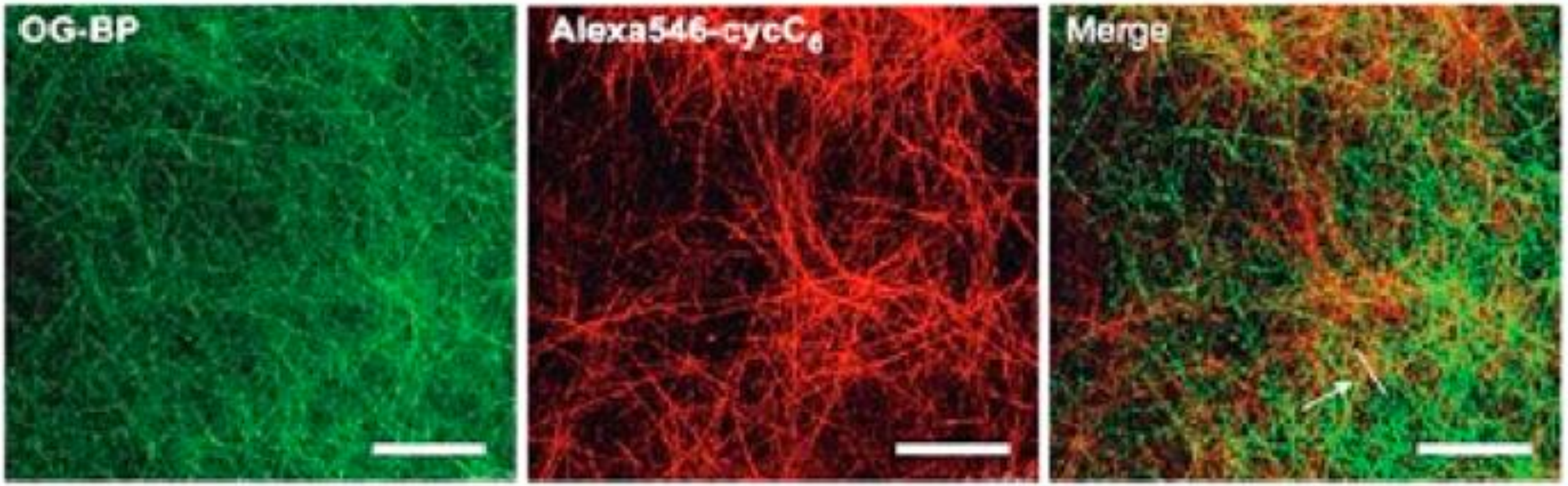

STED images of self-sorting supramolecular nanofibers comprising (green) peptide and (red) lipid-type hydrogelators. Scale bar: 5 μm.

STED and SMLM images of cylindrical micelles composed of PFS56-b-(PDMS775/DYE20)

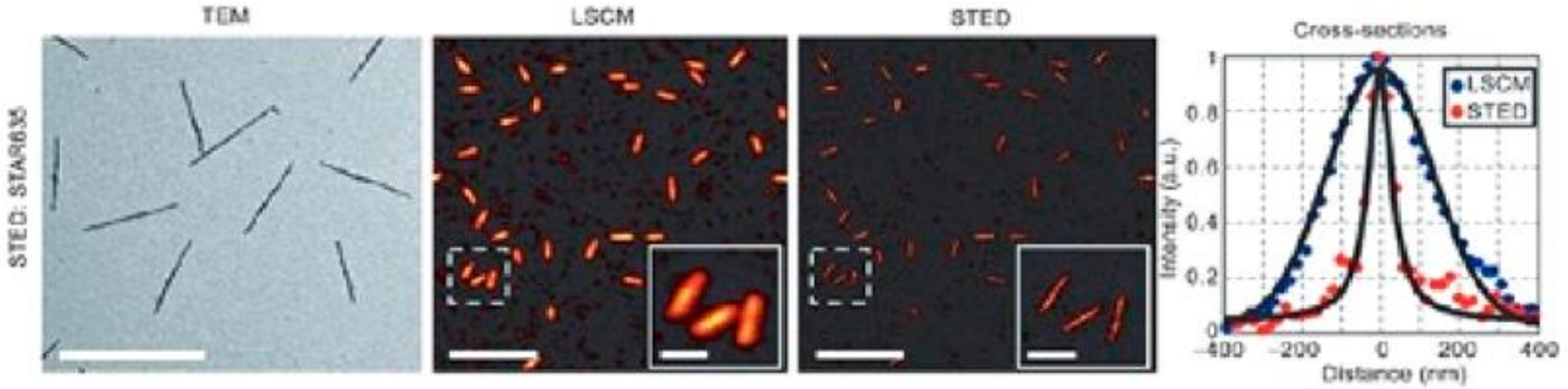

Scale bars: 2 µm (TEM), 5 µm (LSCM and STED), 1 µm (inset)

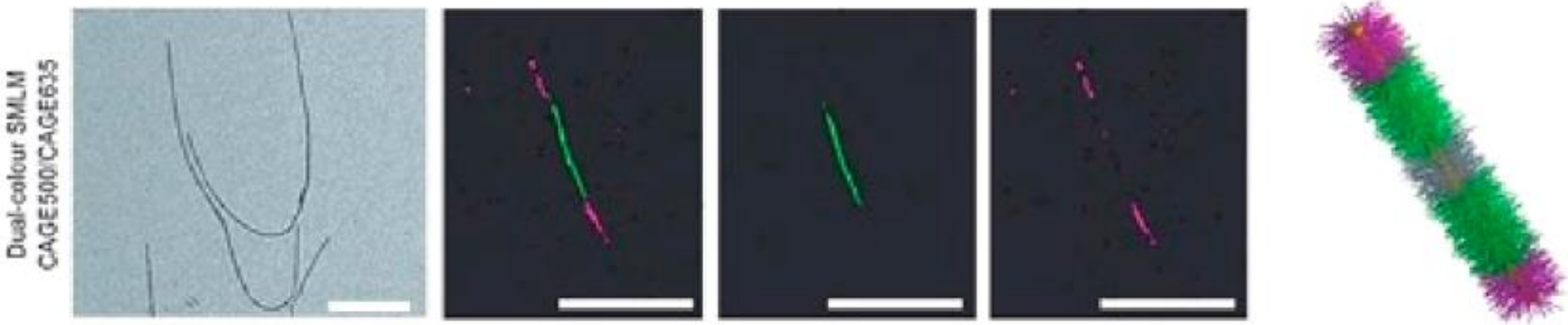

Scale bars: 1 µm (TEM), 2 µm (SMLM)

STORM

STochastic Optical Reconstruction Microscopy

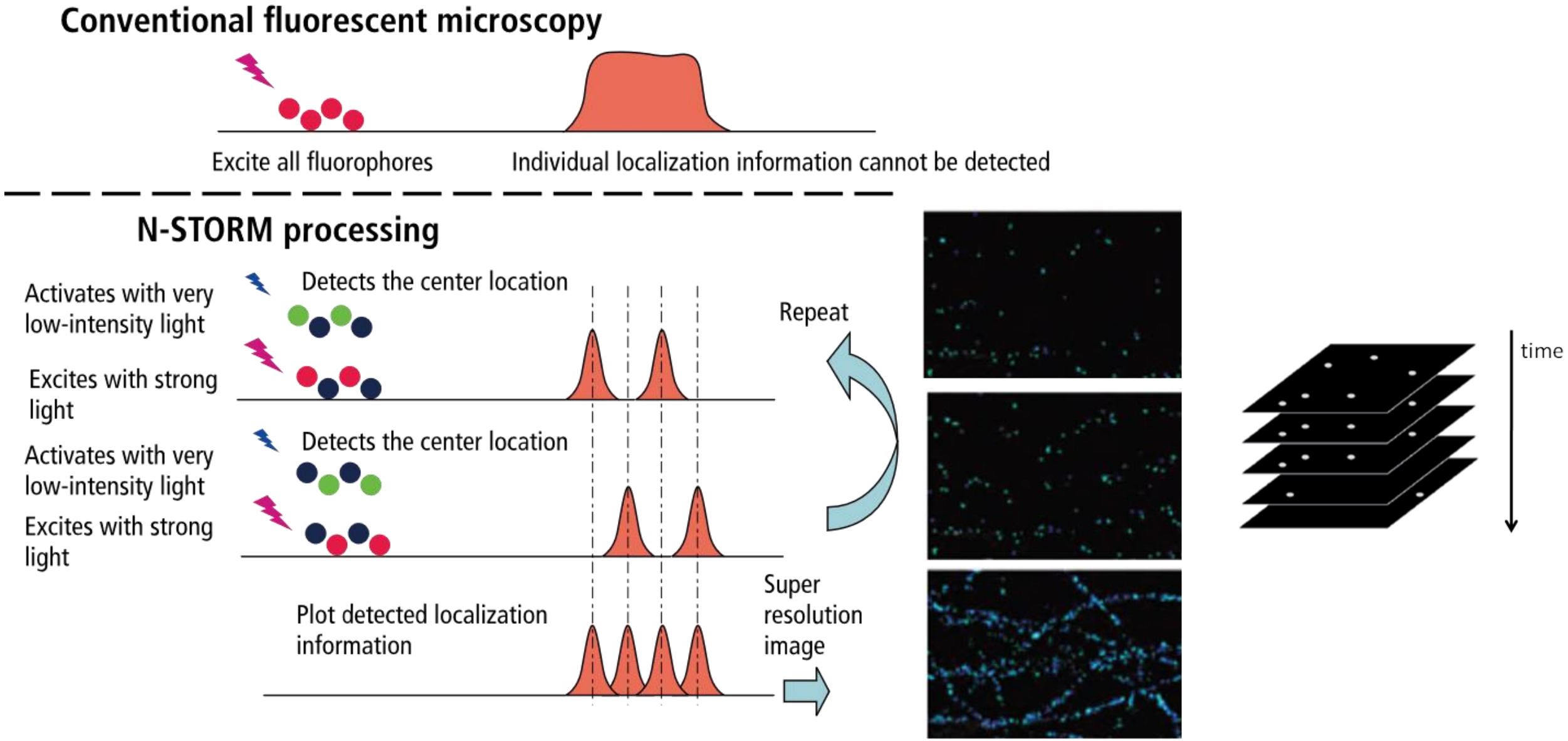

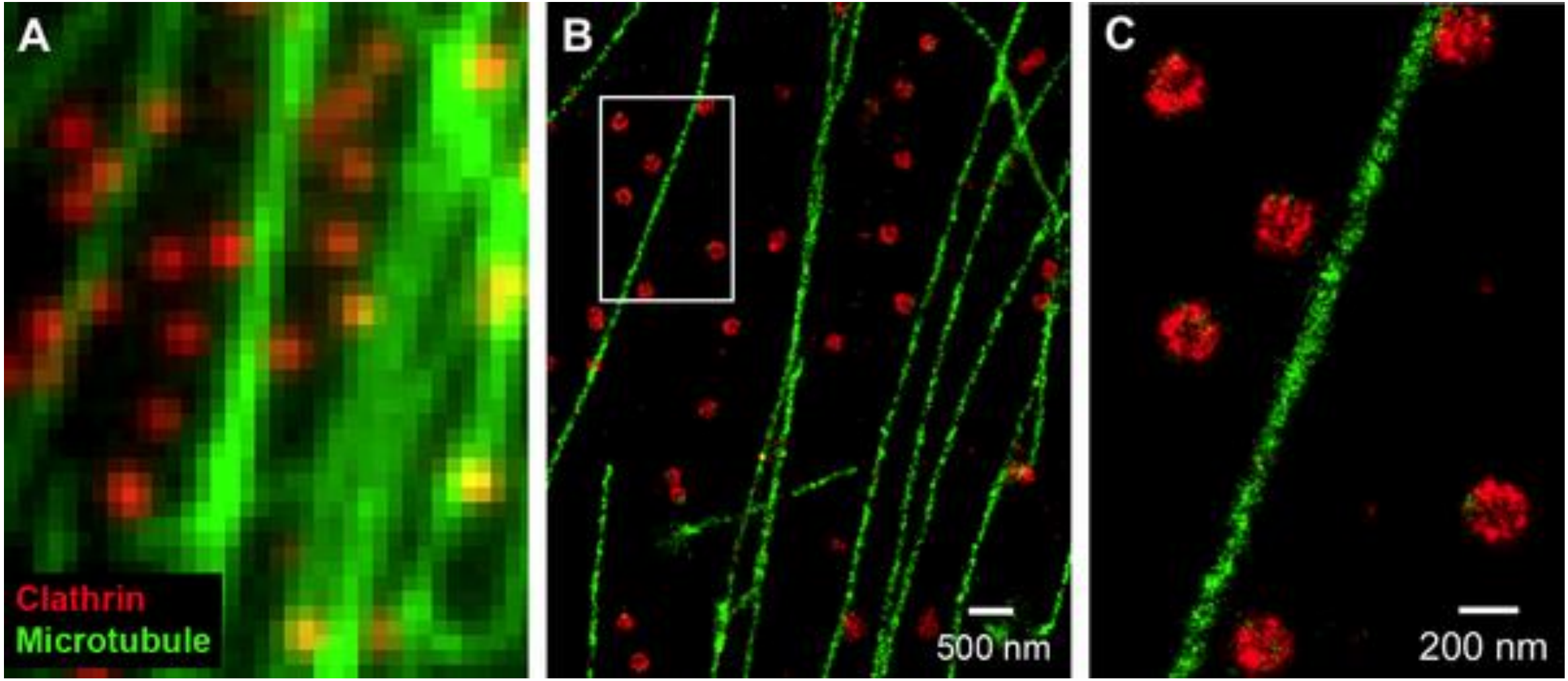

Comparison of conventional (A) and STORM (B,C) images of microtubules and clathrin-coated pits (CCPs) in a cell.
Science 317, 1749-1753 (2007).

Microtubules with STORM (red). Inset: STORM (red) vs. conventional fluorescence (grey).

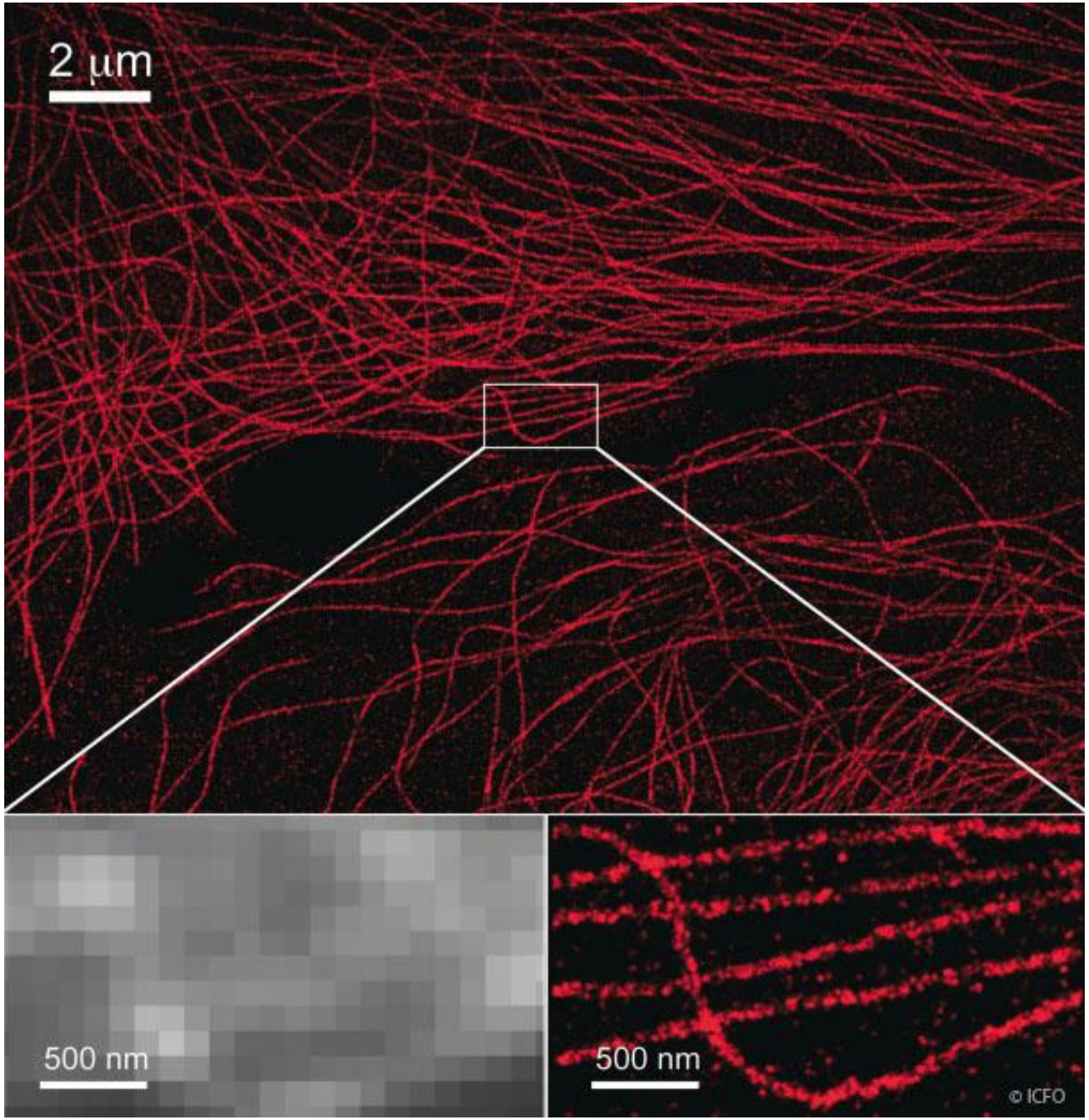

Time-dependent STORM imaging of polymers

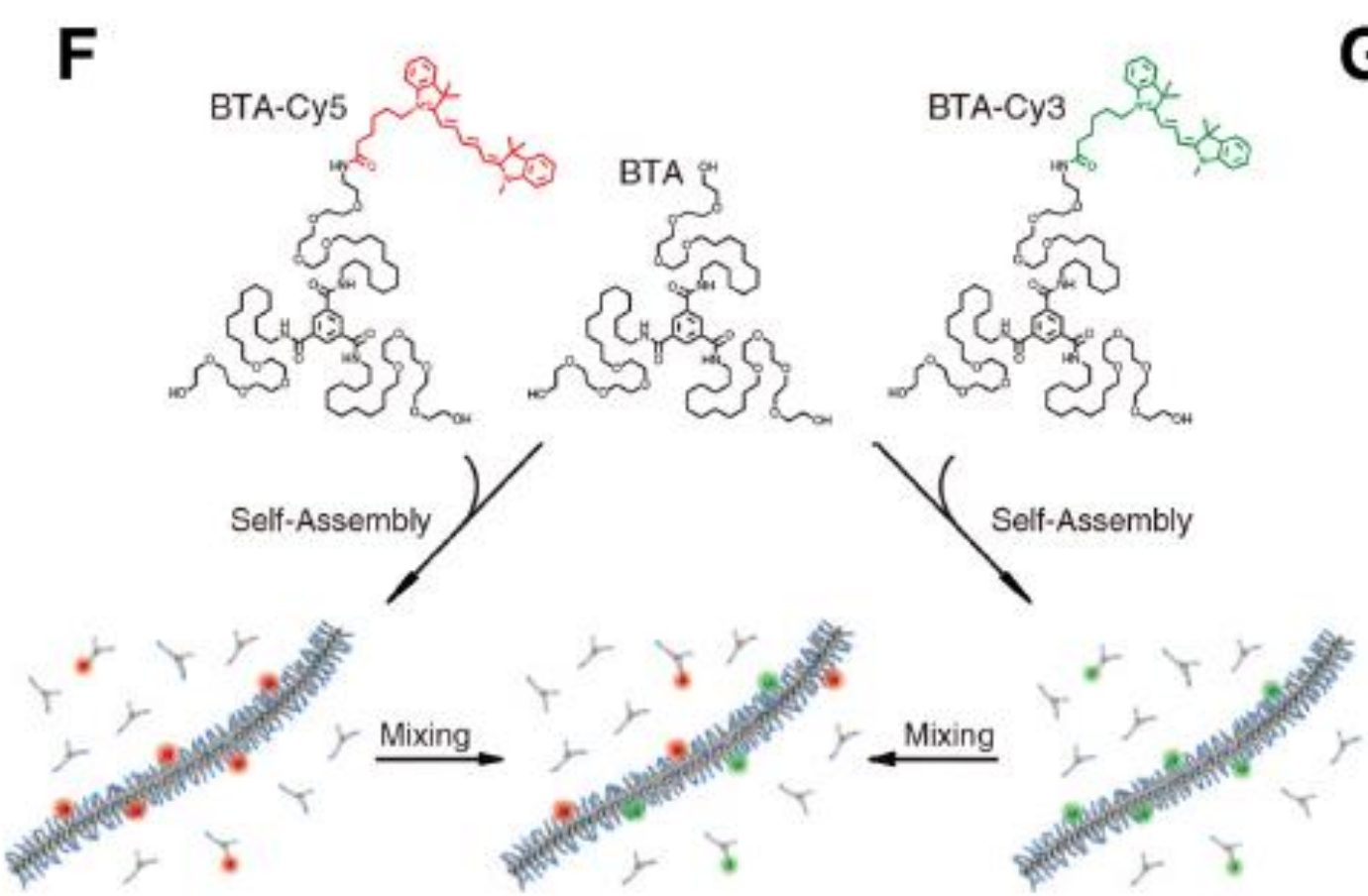

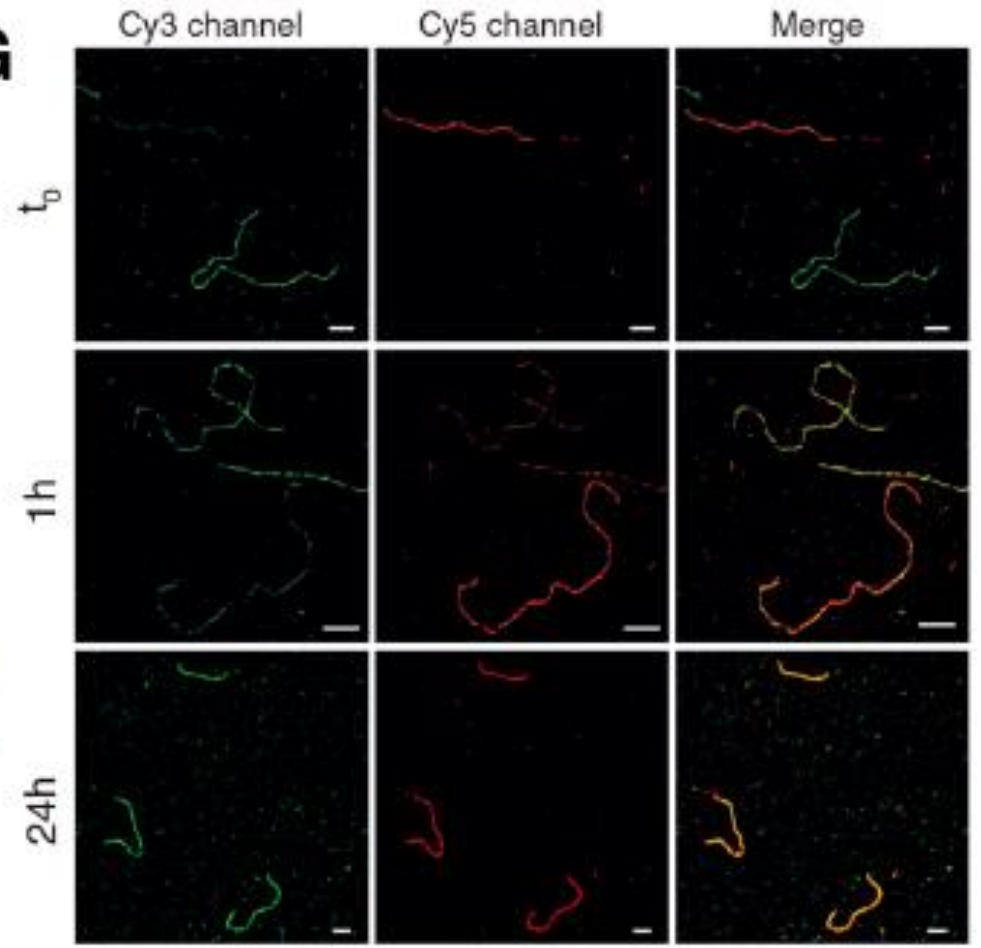

(F) Molecular structures of a monomer and fluorescent probes and schematic illustration of the monomer exchange between the supramolecular polymers.

(G) Spatial resolution: 25 nm. Scale bar: 1 μm

Albertazzi, L. et al. Science 2014, 344, 491−495

PALM: PhotoActivated Localization Microscopy

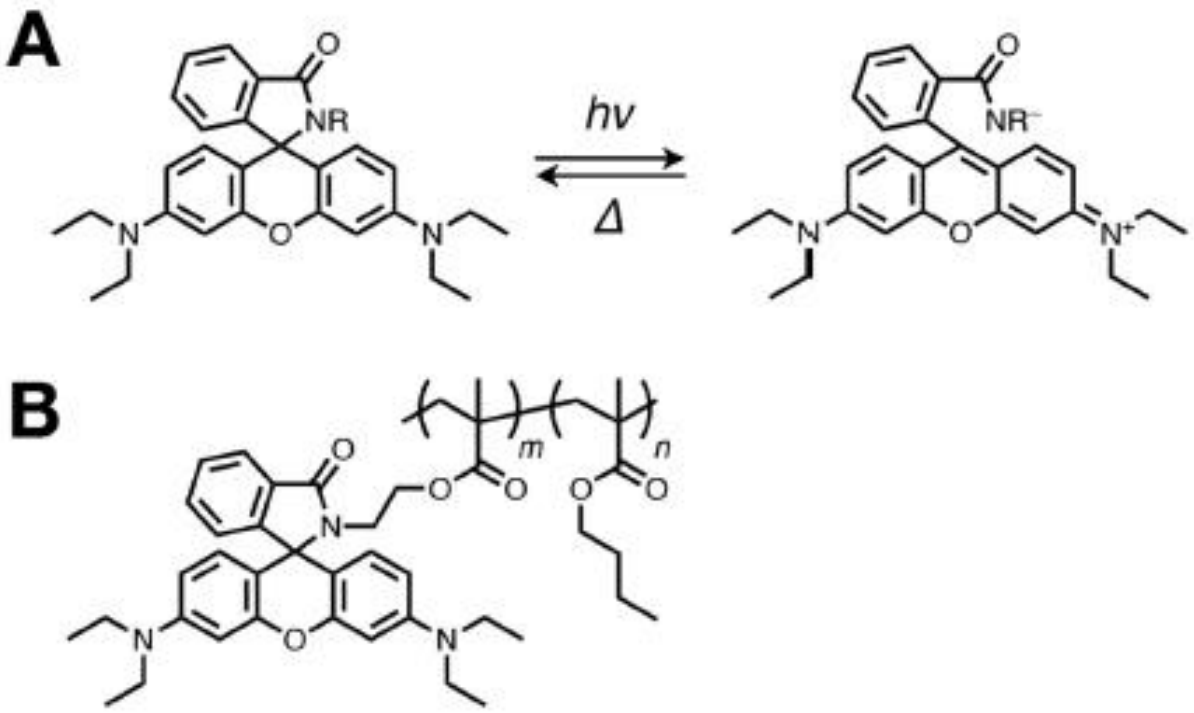

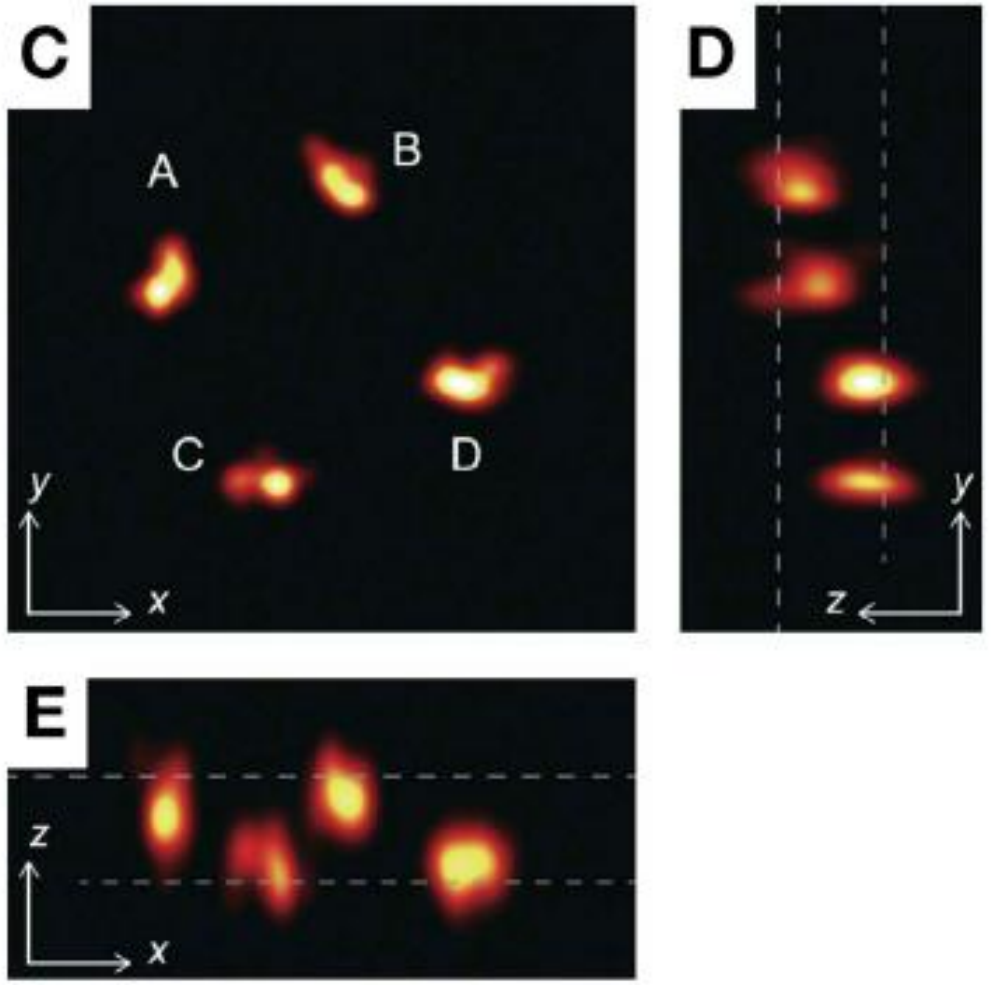

(A) ON/OFF switching of a tetraethylrhodamine derivative.
(B) Molecular structure and (C−E) 3D PALM images of a fluorescently modified polymer with a spatial resolution of 15 nm.

Aoki, H. et al. Soft Matter 2012, 8, 4390

PAINT (Point Accumulation for Imaging in Nanoscale Topography)

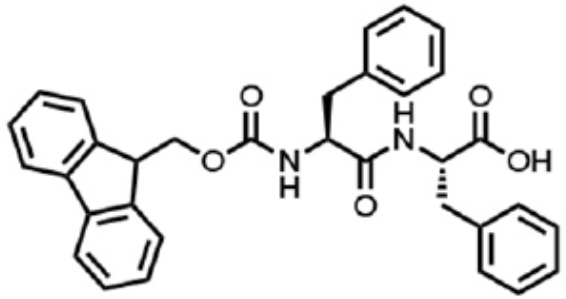

Fmoc-FF

peptide hydrogelator

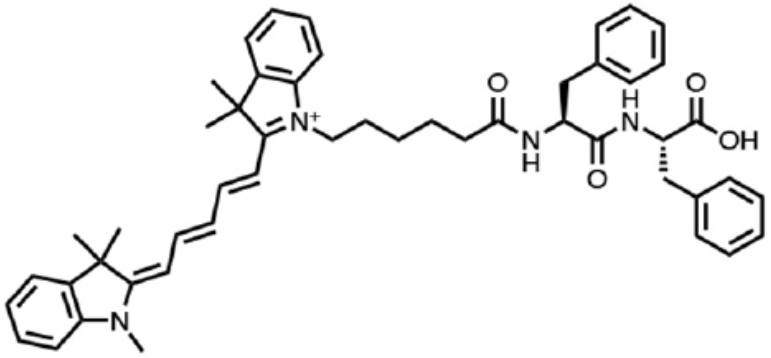

Cy5-FF

fluorescent probe

PAINT images of the Fmoc-FF gel with spatial resolution of ca. 50 nm.

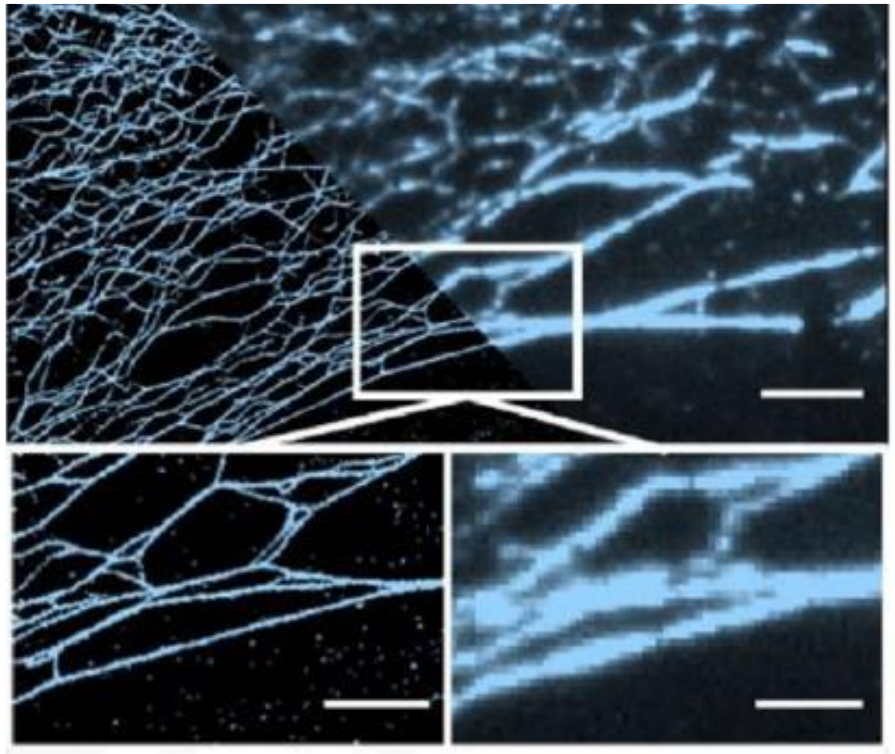

Scale bars: 2.5 µm

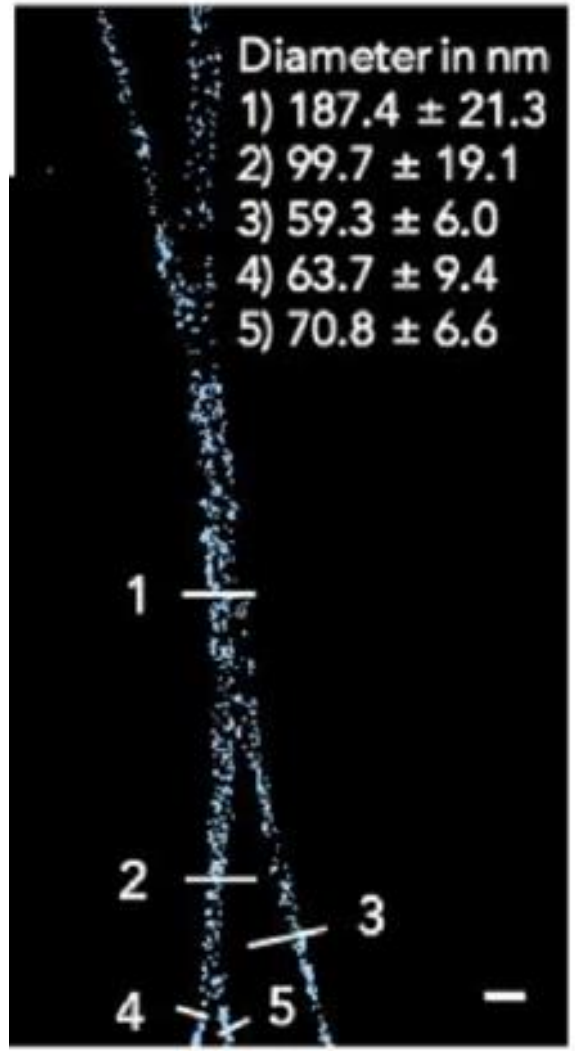

Scale bars: 200 nm

Fuentes, E. et al. Chem.- Eur. J. 2020, 26, 9869−9873

Microscopy *vs* Spectroscopy

Is vision reasoning?

Antonio, si vedono le molecole?